MEANDERING EFFECT FOR EVALUATION OF ROUGHNESS COEFFICIENTS AND BOUNDARY SHEAR DISTRIBUTION IN OPEN CHANNEL FLOW

A Thesis Submitted in Partial Fulfillment of the Requirements for the Degree of

Master of Technology
in
Civil Engineering

PINAKI PRASANNA NAYAK

DEPARTMENT OF CIVIL ENGINEERING

NATIONAL INSTITUTE OF TECHNOLOGY, ROURKELA

2010

MEANDERING EFFECT FOR EVALUATION OF ROUGHNESS COEFFICIENTS AND BOUNDARY SHEAR DISTRIBUTION IN OPEN CHANNEL FLOW

A Thesis Submitted in Partial Fulfillment of the Requirements for the Degree of

Master of Technology
in
Civil Engineering

Under the guidance and supervision of

Prof. K.C.Patra
&
Prof. K.K.Khatua

Submitted By:

PINAKI PRASANNA NAYAK

ROLL.NO: 607CE003

DEPARTMENT OF CIVIL ENGINEERING
NATIONAL INSTITUTE OF TECHNOLOGY, ROURKELA
2010

National Institute of Technology
Rourkela

CERTIFICATE

This is to certify that the thesis entitled "**Meandering Effect for Evaluation of Roughness Coefficients and Boundary Shear Distribution in Open Channel Flow**" being submitted by Pinaki Prasanna Nayak in partial fulfillment of the requirements for the award of **Master of Technology** in **Civil Engineering** at National Institute of Technology Rourkela, is a bonafide research carried out by her under our guidance and supervision.

The work incorporated in this thesis has not been, to the best of our knowledge, submitted to any other University or Institute for the award of any degree or diploma.

Prof. K.C. Patra
(Supervisor)

Prof. K. K. Khatua
(Co-Supervisor)

ACKNOWLEDGEMENTS

I sincerely express my deep sense of indebtedness and gratitude to Prof. K.C.Patra and Prof. K.K.Khatua for providing me an opportunity to work under their supervision and guidance. Their continuous encouragement, invaluable guidance and immense help have inspired me for the successful completion of the thesis work. I sincerely thank them for their intellectual support and creative criticism, which led me to generate my own ideas and made my work interesting as far as possible.

I would also like to express my sincere thanks to Prof. M. Panda, Head, Civil Engineering Department, Prof. A.K. Pradhan, Prof. P.K.Ray and Prof. R.Jha in providing me with all sorts of help and paving me with their precious comments and ideas. I am indebted to all of them.

I am also thankful to staff members and students associated with the Fluid Mechanics and Hydraulics Laboratory of Civil Engineering Department, especially Mr. P. Rout and Mr. K. M. Patra for their useful assistance and cooperation during the entire course of the experimentation and helping me in all possible ways.

Friendly environment and cooperative company made I had from my stay at NIT Rourkela, memorable and pleasant. The affection received from my batchmates and juniors will always remind me of my days as a student here. I wish to thank all of them heartily. Their support and suggestions were indeed of great help whenever needed.

I am thankful to my parents and my in-laws for their emotional support and being patient during the completion of my dissertation. Last but not the least; I thank the ALMIGHTY for blessing me and supporting me throughout.

Pinaki Prasanna Nayak

ABSTRACT

Almost all the natural channels meander. During uniform flow in an open channel the resistance is dependent on a number of flow and geometrical parameters. The usual practice in one dimensional flow analysis is to select an appropriate value of roughness coefficient for evaluating the carrying capacity of natural channel. This value of roughness is taken as uniform for the entire surface and for all depths of flow. The resistance coefficients for meandering channels are found to vary with flow depth, aspect ratio, slope and sinuosity and are all linked to the stage-discharge relationships. Although much research has been done on Manning's *n* for straight channels, less works are reported concerning the roughness values for meandering channels. An investigation concerning the variation of roughness coefficients for meandering channels with slope, sinuosity and geometry are presented. The loss of energy in terms of Manning's *n*, Chezy's *C*, and Darcy-Weisbach coefficient *f* are evaluated. A simple equation for roughness coefficient based on dimensional analysis is modeled and tested with the recent experimental data. The method gives discharge results that are comparable to that of the observed values as well as to other published data.

Knowledge on wall shear stress distribution in open channel flow is required to solve a variety of engineering and river hydraulic problems so as to understand the mechanism of sediment transport, and to design stable channels etc. The study on boundary shear and its distribution also give the basic idea on the resistance relationship. Good many works have been reported on the distribution of wall shear for straight channels, but only a few studies are reported on the works involving meandering channels. Experiments are conducted to evaluate wall shear from point to point along the wetted perimeter of the meandering open channel flow. The wall shear distributions in meandering channel is found to be dependent on the dimensionless parameters such as sinuosity, aspect ratio, and channel roughness. Equations are developed to predict the wall shear distribution in meandering channel which is adequate for the present data and other published data.

Key words: Aspect ratio(α), Bed slope(S), Boundary shear, Chezy's *C*, Darcy-Weisbach coefficient *f*, Manning's *n*, Dimensional analysis, Meandering channel, Open channel, Flow resistance, Sinuosity(S_r), Stage-discharge relationship, Wall shear distribution.

CONTENTS

LIST OF TABLES

LIST OF FIGURES AND PHOTOGRAPHS

LIST OF ACRONYMS AND SYMBOLS

Abbreviations

ADV	Acoustics Doppler Velocity Meter
ENU	East, North and Upward
LSCS	Linear Soil Conservation Services
W_{BF}	Bankfull channel width
WSD	West, South and Down ward
A	Area of channel cross section
b	Bottom width of channel
C	Chezy's channel coefficient
f	Darcy-Weisbach Friction factor
h	Height of channel
n	Manning's roughness coefficient

Symbols

$\%SF_B$	Percentage of shear force which is carried by the base
$\%SF_W$	Percentage of shear force which is carried by the walls
$A`$	Amplitude of a meander channel
b/h	Width depth ratio or aspect ratio
d`	The thickness of laminar sub-layer
ρ	Density of flowing fluid
f_a	Apparent friction factor
f_c	Composite friction
g	Acceleration due to gravity
$h`$	Distance from the channel wall
$h`_1$ and $h`_2$	Heights respectively from the wall
h_0	Distance from the channel bottom at which logarithmic law indicates zero velocity
k	Von Karman's constant
K_s	The equivalent sand grain roughness of the surface

M	Slope of the semi-log plot of velocity distributions
N_r	Reynolds number ratio
P	Wetted perimeter of the channel section
Q	Discharge
R	Hydraulic radius of the channel cross section
r_c	Least centerline radius of curvature
S	Bed Slope of the Channel
SF	Total shear force shear force
S_r	Sinuosity of the Channel
U	Primary longitudinal velocity
u^*	The velocity scale in the study of velocity distribution close to the walls in open channels
u_1 and u_2	The time averaged velocities
V	The secondary flow velocities
V_x	Longitudinal component of velocity in ADV
V_y	Radial component of velocity in ADV
V_z	Vertical component of velocity in ADV
W	The secondary flow velocities
μ	Dynamic viscosity of water
τ_0	Mean Wall shear stress by Energy Gradient Method
τ_w	Distribution of wall shear stress around wetted perimeter.
α	Aspect ratio
ν	Kinematic viscosity

CHAPTER 1

INTRODUCTION

1.1. GENERAL

Almost all the natural water resource conduits are open channel that meander. In fact straight river reaches longer than 10 to 12 times the channel widths are almost nonexistent in nature. Reliable estimates of discharge capacity are essential for the design, operation, and maintenance of open channels, more importantly for the prediction of flood, water level management, and flood protection measures.

River meandering is a complicated process involving a large number of channel and flow parameters. Inglis (1947) was probably the first to define meandering and it states "where however, banks are not tough enough to withstand the excess turbulent energy developed during floods, the banks erode and the river widens and shoals. In channels with widely fluctuating discharges and silt charges, there is a tendency for silt to deposit at one bank and for the river to move to the other bank. This is the origin of meandering…" Leliavsky (1955) summarizes the concept of river meandering in his book which quotes "The centrifugal effect, which causes the super elevation may possibly be visualised as the fundamental principles of the meandering theory, for it represents the main cause of the helicoidal cross currents which removes the soil from the concave banks, transport the eroded material across the channel, and deposit it on the convex banks, thus intensifying the tendency towards meandering. It follows therefore that the slightest accidental irregularity in channel formation, turning as it does, the stream lines from their straight course may, under certain circumstances constitute the focal point for the erosion process which leads ultimately to meander".

A river is the author of its own geometry. Distribution of flow and velocity in a meandering river is an important topic in river hydraulics to be investigated from a practical point of view in relation to the bank protection, navigation, water intakes, and sediment transport-depositional patterns. This further helps to determine the energy expenditure and bed shear stress distribution. The distribution of wall shear stress is influenced by many factors, notably the shape of the cross-section, the longitudinal variation in plan form geometry, the sediment concentration and the lateral and longitudinal distribution of wall roughness. Accurate assessment of the discharge capacity of meandering channels are

therefore essential in suggesting structures for flood control and in designing artificial waterways etc.

1.2. MEANDERING - ITS EFFECTS AND INFLUENCE

The term meandering derives its meaning from the river known to the ancient Greeks as Maiandros or Meander, characterised by a very convoluted path along the lower reach. As such, even in Classical Greece the name of the river had become a common noun meaning anything convoluted and winding, such as decorative patterns or speech and ideas, as well as the geomorphological feature. Strabo said: "... its course is so exceedingly winding that everything winding is called meandering." The Meander River is located in present-day Turkey, south of Izmir, eastward the ancient Greek town of Miletus, now Turkish Milet. It flows through a graben in the Menderes Massif, but has a flood plain much wider than the meander zone in its lower reach. In the Turkish name, the Büyük Menderes River, Menderes is from "Meander". Meanders are also formed as a result of deposition and erosion.

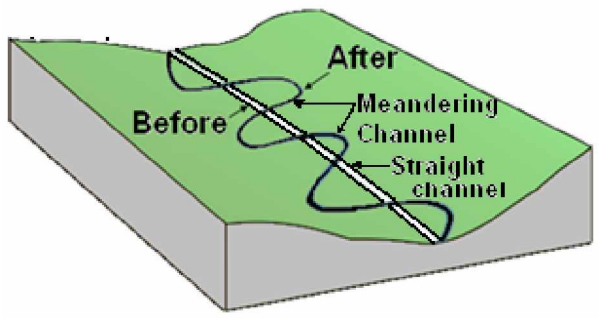

Fig. 1.1 Simple Illustration of Formation of Meandering Channel from Straight Reach

Meandering channels are equilibrium features that represent the most probable channel plan geometry, where single channels deviate from straightness (Fig. 1.1). A meander, in general, is a bend in a sinuous watercourse. It is formed when the moving water in a river erodes the outer banks and widens its valley. A stream of any volume of water may assume a meandering course, alternatively eroding sediments from the outside of a bend and depositing them on the inside. The result is a snaking pattern as the stream meanders back and forth across its down-valley axis. The degree of sinuosity required before a channel is called meandering. As bed width is related to discharge, meander wavelength also is related to discharge. The quasi-regular alternating bend of stream meanders are described in terms of their wavelength λ_m, their radius of curvature r_m, and their amplitude α_m and is bankfull

channel width W_{BF}. The radius of curvature of meander bends is not constant, so r_m is somewhat subjectively defined for the bend apex (Fig. 1.2).

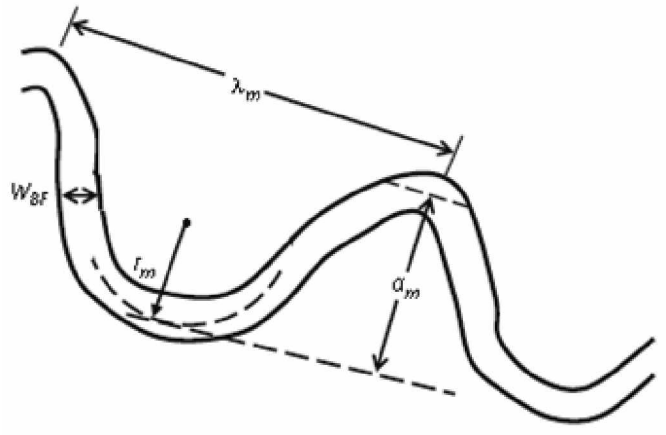

Fig. 1.2 Planform of a Meandering River Showing Meander Wavelength, Radius of Curvature, Amplitude and Bankfull Channel Width

It is an established fact that meandering represents a degree of adjustment of water and sediment laden river with its size, shape, and slope. The curvature develops and adjusts itself to transport the water and sediment load supplied from the watershed. The channel geometry, side slope, degree of meandering, roughness and other allied parameters are so adjusted that in course of time the river does the least work in turning, while carrying the loads. With the exception of straight rivers, for most of the natural rivers, the channel slope is usually less than the valley slope. The meander pattern represents a degree of channel adjustment so that a river with flatter slope can exist on a steeper valley slope.

Sinuosity is one of the channel types that a stream may assume overall or part of its course. All streams are sinuous at some time in their geologic history over some part of their length. The meander ratio or sinuosity index is a means of quantifying how much a river or stream meanders (how much its course deviates from the shortest possible path). It is calculated as the length of the stream divided by the length of the valley. A perfectly straight river would have a meander ratio of 1 (it would be the same length as its valley), while the higher this ratio, the more the river meanders. Sinuosity indices are calculated from the map or from an aerial photograph measured over a distance called the reach, which should be at least 20 times the average fullbank channel width. The length of the stream is measured by channel, or thalweg, length over the reach, while the bottom value of the ratio is the downvalley length or air distance of the stream between two points on it defining the reach. The sinuosity index plays a part in mathematical descriptions of streams (Fig. 1.3).

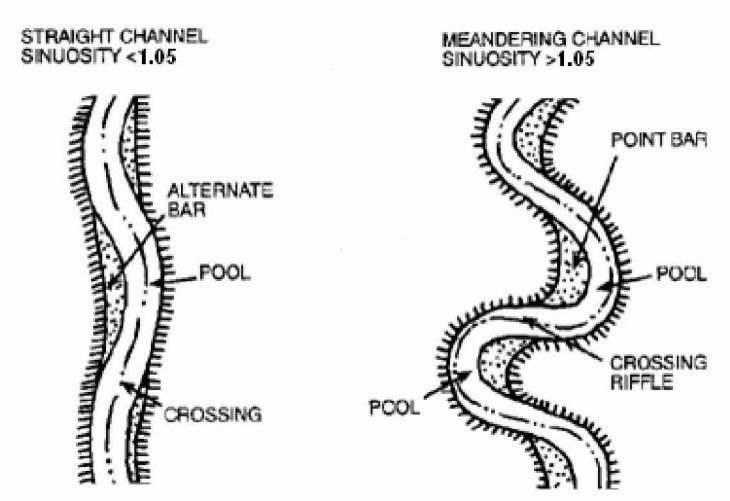

Fig. 1.3 Classification of Channels According to Sinuosity Ratio

Two parameters are used to classify meandering channels into its categories. Rivers with, is classified as straight when the sinuosity ratio is less than 1.05, and more are classified as sinuous and meandering. The other parameter defining meandering plan form is the ratio of the least centerline radius of curvature (r_c) to the channel width (b) given as (r_c/b). Meandering channels are also classified as shallow or deep depending on the ratio of the average channel width (b) to its depth (h). In shallow channels (b/h >5, Rozovskii, 1961) the wall effects are limited to a small zone near the wall which may be called as "wall zone". The central portion called "core zone" is free from the wall effects. In deep channels (b/h<5) the influence of walls are felt throughout the channel width. Meandering and the flow interaction between main channel and its adjoining floodplains are those natural processes that have not been fully understood.

1.3. ESSENCE OF PROPER VALUE OF ROUGHNESS COEFFICIENTS AND BOUNDARY SHEAR DISTRIBUTION IN MEANDERING CHANNEL FLOW

The usual practice in one dimensional flow analysis is to select an appropriate value of roughness coefficient for evaluating the actual stage-discharge relationship of natural channel. The energy loss in a meandering channel is influenced by the channel flow parameters and are assumed to be lumped into a single value manifested in the form of resistance coefficients in terms of Manning`s $n$, Chezy`s C and Darcy Weisbach f. An improper roughness value can either underestimates or overestimate the discharge. A number of researchers have studied the phenomenon of flow mostly in straight channels and

have proposed a number of methods for estimating the discharge. Sellin (1964) and Shino and Knight (1999), Patra and Kar (2000), Patra and Khatua (2006), etc. have shown that the structure of the flow is surprisingly complex, even for straight compound channels. It has velocity in all the three directions. Consequently, the use of design methods based on straight channels is inappropriate when applied to multiple stage meandering channels, results in large errors when estimating the discharge. Determination of suitable value of roughness coefficient for a given channel is therefore the most significant factor for evaluating the actual carrying capacity of a natural channel.

Knowledge on wall shear stress distribution in open channel flow is required to solve a variety of engineering and river hydraulics problems so as to give a basic idea on the resistance relationship, to understand the mechanism of sediment transport, and to design stable channels etc. The study also helps in the analysis of migration problems as well as bank erosion in river channel. It is a great challenge to the river engineers and researchers to predict the distribution of wall shear stress (τ_w) around the wetted perimeter of a given channel for a certain flow-rate. By integrating the wall shear stress along the surface, contribution to lift and drag on immersed objects can also be computed. Good many works have been reported on the distribution of wall shear for straight channels, but only a few studies are reported on the works involving meandering channels. The interaction between the primary longitudinal velocity *U*, the secondary flow velocities, *V* and *W* are responsible for non-uniform wall shear distribution in an open channel flow. So it is necessary for researchers and engineers to predict the distribution of wall shear in open channel flow both for straight and meandering reach in a sediment free condition.

1.4. SCOPE AND APPROACH OF PRESENT RESEARCH WORK

In general, the classical methods of discharge estimations are normally based on flow in a straight channel. These are essentially flawed when applied to meandering channels. The study undertaken in the present case is primarily a step in understanding the flow processes and distribution of boundary shear in an idealised meander channel. It is supported by data collected from three experimental channels of different geometry, slope, aspect ratio and sinuosity. Experiments are conducted using fabricated channels at the Fluid Mechanics and Hydraulics Engineering Laboratory at the National Institute of Technology, Rourkela, on straight and meandering channels under sediment-free condition. A rigid boundary channel

is considered to be more appropriate to study the basic nature of flow interaction and flow parameters than going for movable bed. Most of the discharge calculation for channel is based mainly on refined one dimensional (1D) method. However, both 2D and 3D approaches are more complex to use in practice.

An investigation of energy losses resulting from boundary friction, secondary flow, turbulence, and other factors in meandering channels has been presented. The energy loss is manifested in the form of variation of resistance coefficients of the channel with depth of flow. The variations of roughness coefficients with depths of flow are investigated. In the present study, it is attempted to formulate the models for predicting discharge by selecting a proper value of roughness coefficient in terms of Manning`s *n*, Chezy`s *C* and Darcy Weisbach *f*. The results of the present model are compared well with other established methods of Shino et al. (1999), LSCS method of James and Wark (1992), Toebes and Sooky (1967) method and the conventional method for discharge estimation. Also, a modified method has been proposed for evaluation of boundary shear in a meandering channel considering sinuosity and aspect ratio as basic influencing parameter.

1.5. ORGANISATION OF THE THESIS

The thesis comprises of five chapters. General introduction is given in Chapter 1, literature review is presented in Chapter 2, experimental work is outlined in Chapter 3, results and discussions of the present work is Chapter 4 and finally the conclusions are in Chapter 5.

The first chapter provides us a glance about the contents of the research work along with its related topics. It gives us an overview about the work done and presented in the dissertation.

The literature review presented in Chapter 2 relates us to the work done by other established authors in this field from the very beginning till date. The chapter emphasizes on the research carried out in straight and meandering channels based on stage-discharge relationships, roughness coefficients and boundary shear distribution.

Chapter 3 explains about the experimental work as a whole. This chapter discusses about the experimental set up and the adopted procedures of flow parameters, observations of channel. It also explains about the instruments used during the experimental processes.

The experimental results concerning boundary shear force, stage-discharge, and energy loss aspects in terms of Manning`s *n*, Chezy's *C* and Darcy-Weisbach *f* with the discussion of the results and theoretical considerations are depicted in Chapter 4.

Finally, Chapter 5 summarizes the important conclusions drawn from the present work. Scope of future work that can be further carried out is also discussed in this chapter.

References that have been made in the subsequent chapters are given at the end of the dissertation.

CHAPTER 2

LITERATURE REVIEW

2.1. GENERAL

A look into the plan form of all meandering channels show that there can be three distinct type of geometry. They are straight, curved or meandering. Almost all natural rivers meander. The name meander, which probably originated from the river Meanders in Turkey is so frequent in river that it has attracted the interest of investigators from many disciplines. Thomson (1876) was probably the first to point out the existence of spiral motion in curved open channel. Since then, a lot of laboratory and theoretical studies are reported, more so, in the last decade or so concerning the flow in straight or curved channel. It may be worth while to understand the nature of flow in straight channels before knowing about the meander channels. There are limited studies available concerning the flow in meandering channels.

Discharge estimation is based on the most suitable value of roughness coefficient. Knowledge on wall shear stress distribution in open channel flow is required to solve a variety of engineering and river hydraulic problems so as to understand the mechanism of sediment transport, and to design stable channels etc. The study on boundary shear and its distribution also give the basic idea on the resistance relationship.

2.2. PREVIOUS WORK ON ROUGHNESS COEFFICIENTS AND DISCHARGE ESTIMATION

The Meandering channel flow is considerably more complex than constant curvature bend flow. Due to continuous stream wise variation of radius of curvature flow geometry in meander channel is in the state of either development or decay or both. The following important studies are reported concerning the flow in meander channels.

Chezy was the first to investigate the flow in open the channel of the new Paris water supply. Chezy was the first to consider the wetted perimeter of channels as an analog of boundary resistance (Rouse and Ince, 1957). Chezy's equation has the form of $V = C\,R^{1/2}\,Sc^{1/2}$ that uses a resistance coefficient C, the hydraulic radius ($R=A/P$) and the slope of the channel (S_c).

The U.S. Army Corps of Engineers (Hydraulic 1956) conducted a series of stage-discharge experiments in meandering channels at the Waterways Experiments Station in Vicksburg. The main purpose of these experiments was to investigate the effect of the following geometric parameters on the conveyance capacity of compound meandering channels: radius of curvature of the bends, sinuosity of the main channel, depth of the floodplain flow, ratio of the floodplain area to the main channel area, and floodplain roughness. Although the study did not investigate the behaviour of the flow, its conclusions were of importance and were outlined as follows: (1) The effect of the main channel sinuosity on the channel conveyance was small when the main channel was narrow in comparison to the floodplain width; (2) the channel conveyance decreased as the sinuosity of the main channel increased; (3) the effect of the main channel sinuosity on the total channel conveyance was small when the floodplain width was more than three times the width of the meander belt; and (4) as the floodplain roughness increased, the conveyance decreased accordingly. Sinuosity is defined as the ratio of the length along the channel centre line between two points to the straight line distance between the points.

Cowan (1956) proposed an equation to evaluate n as

$$n = (n_b + n_1 + n_2 + n_3 + n_4)\, m$$

where, n_b = base n value; n_1 = addition for surface irregularities; n_2 = addition for variation in channel cross section; n_3 = addition for obstructions; n_4 = addition for vegetation; m = ratio for meandering. The above method was improved by Arcement and Schneider (1989). Suggested values for Manning's n are tabulated by Chow (1959).

The Soil Conservation Service (SCS) method for selecting roughness coefficient values for channels (Guide 1963) was found to be the best, giving a better stage prediction than the other methods. It proposed accounting for meander losses by adjusting the basic value of Manning's n on the basis of sinuosity (s), as follows:

$$\frac{n`}{n} = 1.0 \qquad \text{for } s < 1.2$$

$$\frac{n`}{n} = 1.15 \qquad \text{for } 1.2 \leq s < 1.5$$

$$\frac{n`}{n} = 1.15 \qquad \text{for } s \geq 1.5$$

where, n` = the adjusted value; and n = the basic value. Because n is proportional to $f^{1/2}$ the adjustment should be squared when using the Darcy-Weisbach equation.

Toebes and Sooky (1967) carried out several experiments in small-scale flumes to determine the overall conveyance of meandering channels as a function of stage for specific geometries and to study the redistribution of the erosive forces acting on the boundaries under overbank flow conditions. They concluded that the energy losses, caused partially by the main channel and floodplain interaction and the sinuosity of the main channel, depend on both the Reynolds and the Froude numbers. Velocity components were measured for the different geometries to investigate the secondary flows and the formation of helical currents in the main channel and floodplain. From experimental results in a small laboratory channel with a sinuosity of 1.09, they proposed an adjustment to Darcy Weisbach`s *f*.

Chang (1983) investigated energy expenditure and proposed an analytical model for obtaining the energy gradient, based on fully developed secondary circulation for wide rectangular sections. The method was for fully developed secondary circulation. In fact, the circulation took considerable distance to develop through a bend and begins to decay once the channel straightens out. For meanders there was also a tendency for the circulation to reverse between successive bends. The average energy gradient associated with secondary circulation along the channel was therefore substantially less than predicted assuming full development. Chang's approach was subsequently adapted to meandering channels by James and Wark (1992).

Later, Chang (1984) analysed the meander curvature and other geometric features of the channel using energy approach. It established the maximum curvature for which the river did the last work in turning, using the relations for flow continuity, sediment load, resistance to flow, bank stability and transverse circulation in channel bends. The analysis demonstrated how uniform utilisation of energy and continuity of sediment load was maintained through meanders. He accounted for applying his full circulation loss model together with non-uniform flow calculations and predicted the distribution of losses, boundary shear stresses, and water levels through bends.

Jarrett (1984) developed a model to determine Manning's *n* for natural high gradient channels having stable bed and in bank flow without meandering coefficient. He proposed, a

value for Manning`s *n* as $n = \frac{0.32\ S^{0.38}}{R^{0.16}}$ where, *S* is the channel gradient, *R* the hydraulic radius in meters. The equation was developed for natural main channels having stable bed and bank materials (boulders) without bed rock. It was intended for channel gradients from 0.002 – 0.04 and hydraulic radii from 0.15 – 2.1m, although Jarrett noted that extrapolation to large flows should not be too much.

Wormleaton and Hadjipanos (1985) measured the velocity in each subdivision of the channel, and found that even if the errors in the calculation of the overall discharge were small, the errors in the calculated discharges in the floodplain and main channel may be very large when treated separately. They also observed that, typically, underestimating the discharge on the floodplain was compensated by overestimating it for the main channel. The failure of most subdivision methods is due to the complicated interaction between the main channel and floodplain flows. The interaction phenomenon has been studied by many researchers [e.g., Myers (1978), Knight and Demetriou (1983), Knight and Shiono (1990), and Shiono and Knight (1991)] in an attempt to quantify the effect and hence to predict correctly the flow in compound channels.

Arcement and Schneider (1989) was basically modified Cowan method discussed above. It was designed specifically to account for selecting *n* values for natural channels and flood plains resistance. This work was performed for the U.S. Department of Transportation. In the modified equation the coefficients were taken as n_b = a base value *n* for the floodplain`s natural bare soil; n_1 = a correction factor for the effect of surface irregularities on floodplain (range0-0.02); n_2 = a value for variation in channel shape and size of the floodplain cross section; n_3 = a value for obstructions on the floodplain (range 0-0.03); n_4 = a value for vegetation on the floodplain (range 0.001-0.2); *m* = a correction factor for sinuosity of the floodplain=1.0. Each variable values were selected from tables in Arcement and Schneider (1989). The equation was verified for wooden floodplains with flow depths from 0.8-1.5 m.

James and Wark's comprehensive study (1992) compared different methods of estimating the conveyance in meandering compound channels, and was summarized in Wark and James (1994). The methods were compared with three sets of laboratory-based data.

The step nature of the SCS recommendation introduces discontinuities at the limits of the defined sinuosity ranges, with consequent ambiguity and uncertainty. To overcome the

problem the relationship was linearised, known as the Linearised SCS (LSCS) Method. He proposed the value of Manning`s *n* using two cases of sinuosity (S_r), i.e. $S_r < 1.7$ and $S_r \geq 1.7$.

Ervine et al. (1993) investigated the main parameters that affect the conveyance of compound meandering channels with different floodplain roughness using the Flood Channel Facility (FCF) at HR Wallingford, Oxfordshire, U.K. Three configurations were examined: (1) A 607 angle to the crossover with a regular trapezoidal main channel cross section; (2) a 607 angle to the crossover with a natural main channel cross section; and (3) a 1107 angle to the crossover with a natural main channel cross section. It was observed that the sinuosity has a large effect on both smooth and rough floodplain channels. The effect of the sinuosity decreases as the depth on the floodplain increases. The magnitude of this decrease is noticeably higher for channels with roughened floodplains. The aspect ratio of the main channel was also found to contribute significantly to the interaction between the floodplain and the main channel and, hence, also to the flow structure mechanisms. Higher meander belt ratios resulted in higher energy losses.

Greenhill and Sellin (1993) compared different subdivision methods applied to meandering channels, using FCF stage discharge data from smooth meandering channels with two sinuosities. It was found that the error in discharge prediction was drastically reduced when a refined division method was used. The refined method was based on dividing the channel into three sub-channels: the main river channel, using the main channel bed slope; the floodplain within the meander belt, using the valley slope; and the floodplain outside the meander belt, also using the valley slope. The refined method was found to predict discharges with a very low error margin when checked against the experimental smooth channel data, provided that the value of the Manning coefficient was accurately chosen.

Willets and Hardwick (1993) investigated flow in meandering channels using a small laboratory flume. Four sinuosities were examined with trapezoidal and natural cross sections for the channel. The conveyance of the overall channel was found to be affected inversely by the channel sinuosity. In other words, the flow resistance increases substantially with an increase in the main channel sinuosity. The main channel/floodplain flow interaction responsible for the flow resistance was also found to be dependent on the main channel cross section geometries.

James (1994) reviewed the various methods for bend loss in meandering channel proposed by different investigators. He tested the results of the methods using the data of FCF, trapezoidal channel of Willets, at the University of Aberdeen, and the trapezoidal channels measured by the US Army Corps of Engineers at the Waterways Experiment Station, Vicksburg. The results were found considerably different. He proposed some new methods accounting for additional resistance due to bend by suitable modifications of previous methods. His modified methods predicted well the stage discharge relationships for meandering channels.

Pang (1998) conducted experiments on compound channel in straight reaches under isolated and interacting conditions. It was found that the distribution of discharge between the main channel and floodplain was in accordance with the flow energy loss, which can be expressed in the form of flow resistance coefficient. In general, Manning's roughness coefficient *n* not only denoted the characteristics of channel roughness, but also influenced the energy loss in the flow. The value of *n* with the same surface in the main channel and floodplain possessed different values when the water depth in the section varied.

Shiono, Al-Romaih, and Knight (1999) reported the effect of bed slope and sinuosity on discharge of two stage meandering channel. Basing on dimensional analysis, an equation for the conveyance capacity was derived, which was subsequently used to obtain the stage-discharge relationship for meandering channel with over bank flow. It was found that the channel discharge increased with an increase in bed slope and it decreased with increase in sinuosity for the same channel. An error of 10% in discharge estimation was reported for relative depths exceeding 0.01.

Maria and Silva (1999) expressed the friction factor of rough turbulent meandering flows as the function of sinuosity and position (which is determined by, among other factors, the local channel curvature). They validated the expression by the laboratory data for two meandering channels of different sinuosity. The expression was found to yield the computed vertically averaged flows that were in agreement with the flow pictures measured for both large and small values of sinuosity.

Patra (1999), Patra and Kar (2000), Patra and Khatua (2006) and Khatua (2008) have shown that Manning's *n* not only denotes the roughness characteristics of a channel but also

the energy loss in the flow. Jana & Panda et.al (2006) have performed dimensional analysis and predicted the stage-discharge relationship in meandering channels of low sinuosity.

Lai Sat Hin et al. (2008) expressed that estimation of discharge capacity in river channels was complicated by variations in geometry and boundary roughness. Estimating flood flows was particularly difficult because of compound cross-sectional geometries and because of the difficulties of flow gauging. They presented results of a field study including the stage-discharge relationships and surface roughness in term of the Darcy-Weisbach friction factor, f_a for several frequently flooded equatorial natural rivers. Equations were presented giving the apparent shear force acting on the vertical interface between the main channel and floodplain. The resulted apparent friction factor, f_a was shown to increase rapidly for low relative depth. A method for predicting the discharge of overbank flow of natural rivers was then presented, by means of a composite friction, f_c, which represented the actual resistance to flow due to the averaged boundary shear force and the apparent shear force. Equations were also presented giving the composite friction factor from easily calculated parameters for overbank flow of natural rivers. The discharge obtained using the proposed methods showed a significant improvement over traditional methods, with an averaged error of 2.7%.

2.3. OVERVIEW OF THE RESEARCH WORK ON BOUNDARY SHEAR

Distribution of wall shear stress around the wetted perimeter of a channel is influenced by many factors notably, the shape of channel cross-section, the longitudinal variation in plan form geometry, the sediment concentration and the lateral-longitudinal distribution of wall roughness. It is important to appreciate the general three-dimensional flow structures that exist in open channels to understand the lateral distribution of boundary shear stress. The interaction between the primary longitudinal velocity U, and the secondary flow velocities, V and W are responsible for non-uniform wall shear distribution in an open channel flow. Researchers and engineers have predicted the distribution of wall shear in open channel flow for both straight and meandering reach.

Einstein's (1942) hydraulic radius separation method is still widely used in laboratory studies and engineering practice. Einstein divided a cross-sectional area into two areas and assumed that the down-stream component of the fluid weight was balanced by the resistance of the bed. Likewise, the downstream component of the fluid weight in area A_w was balanced

by the resistance of the two side-walls. There was no friction at the interface between the two areas A_b and A_w. In terms of energy, the potential energy provided by area A_b was dissipated by the channels bed, and the potential energy provided by area A_w was dissipated by the two side-walls.

Since 1960s, several experimental studies related to boundary shear and its distribution in open channel flow has been reported by many eminent researchers. Lundgren and Jonsson (1964) extended the logarithmic law to a parabolic cross-sectional open-channel and proposed a method to determine the shear stress.

Ghosh and Roy (1970) presented that the boundary shear distribution in both rough and smooth open channels of rectangular and trapezoidal sections was obtained by direct measurement of shear drag on an isolated length of the test channel utilizing the technique of three point suspension system suggested by Bagnold. Existing shear measurement techniques were reviewed critically. Comparisons were made of the measured distribution with other indirect estimates, from isovels, and Preston tube measurements, based on Keulegan's resistance laws. The discrepancies between the direct and indirect estimates were explained and out of the two indirect estimates the surface Pitot tube technique was found to be more reliable. The influence of secondary flow on the boundary shear distribution was not accurately defined in the absence of a dependable theory on secondary flow.

Kartha and Leutheusser (1970) expressed that the designs of alluvial channels by the tractive force method requires information on the distribution of wall shear stress over the wetted perimeter of the cross-section. The study was undertaken in order to provide some details on actually measured shear distributions and, hence, to check the validity of available design information. The latter was entirely analytical in origin and was based either on the assumption of laminar flow or on over-simplified models of turbulent channel flow. The experiments were carried out in a smooth-walled laboratory flume at various aspect ratios of the rectangular cross-section. Wall shear stress was determined with Preston tubes which were calibrated by a method exploiting the logarithmic form of the inner law of velocity distribution. Results were presented which clearly suggested that none of then present analytical techniques could be counted upon to provide any precise details on tractive force distributions in turbulent channel flow.

Ghosh and Kar (1975) reported the evaluation of interaction effect and the distribution of boundary shear stress in meander channel with floodplain. Using the relationship proposed by Toebes and Sooky (1967) they evaluated the interaction effect by a parameter (*W*). The interaction loss increased up to a certain floodplain depth and there after it decreased. They concluded that the channel geometry and roughness distribution did not have any influence on the interaction loss.

Myers (1978) carried out the experimentation using Preston tube to measure shear stress distributions around the periphery of a complex channel, consisting of a deep section and one flood plain. Measurements were made with full cross section flow and with flow confined to the deep, or channel, section. The results were used to quantify the momentum transfer due to interaction between the channel flow and that over its flood plain, demonstrating the danger of neglecting this phenomenon in complex channel analysis. Lateral momentum transfer throughout the channel and flood plain was compared under isolated and interacting conditions.

Knight and Macdonald (1979) studied that the resistance of the channel bed was varied by means of artificial strip roughness elements, and measurements made of the wall and bed shear stresses. The distribution of velocity and boundary shear stress in a rectangular flume was examined experimentally, and the influence of varying the bed roughness and aspect ratio were accessed. Dimensionless plots of both shear stress and shear force parameters were presented for different bed roughness and aspect ratios, and those illustrated the complex way in which such parameters varied. The definition of a wide channel was also examined, and a graph giving the limiting aspect ratio for different roughness conditions was presented. The boundary shear stress distributions and isovel patterns were used to examine one of the standard side-wall correction procedures. One of the basic assumptions underlying the procedure was found to be untenable due to the cross channel transfer of linear momentum.

Knight (1981) proposed an empirically derived equation that presented the percentage of the shear force carried by the walls as a function of the breadth/depth ratio and the ratio between the Nikuradse equivalent roughness sizes for the bed and the walls. A series of flume experiments were reported in which the walls and bed were differentially roughened,

normal depth flow was set, and measurements were made of the boundary shear stress distribution. The results were compared with other available data for the smooth channel case and some disagreements noted. The systematic reduction in the shear force carried by the walls with increasing breadth/depth ratio and bed roughness was illustrated. Further equations were presented giving the mean wall and bed shear stress variation with aspect ratio and roughness parameters. Although the experimental data was somewhat limited, the equations were novel and indicated the general behavior of open channel flows with success. This idea was further discussed by Noutsopoulos and Hadjipanos (1982).

Knight et al. (1984), Hu (1985) and Knight and his associates collected a great deal of experimental data about the effect of the side walls at different width–depth ratios. With these data, they proposed several empirical relations which are very helpful in the studies of open-channel flow and sediment transport.

Knight and Patel (1985) reported some of the laboratory experiments results concerning the distribution of boundary shear stresses in smooth closed ducts of a rectangular cross section for aspect ratios between 1 and 10. The distributions were shown to be influenced by the number and shape of the secondary flow cells, which, in turn, depended primarily upon the aspect ratio. For a square cross section with 8 symmetrically disposed secondary flow cells, a double peak in the distribution of the boundary shear stress along each wall was shown to displace the maximum shear stress away from the center position towards each corner. For rectangular cross sections, the number of secondary flow cells increased from 8 by increments of 4 as the aspect ratio increased, causing alternate perturbations in the boundary shear stress distributions at positions where there were adjacent contra-rotating flow cells. Equations were presented for the maximum, centerline, and mean boundary shear stresses on the duct walls in terms of the aspect ratio.

Chiu and Chiou (1986) extended the logarithmic law to rectangular cross-sections and provided an analytical method to compute the wall shear stress. A parameter estimation method was developed for a system of three-dimensional mathematical models of flow in open channels, which did not require (primary flow) velocity data. It broadened the applicability and effectiveness of the model in scientific investigations into the complex interaction among the primary and secondary flows, shear stress distribution, channel characteristics (roughness, slope, and geometry), and other related variables governing all transport processes in open channels. The results were answered quantitatively many

questions that aroused in open channel hydraulics. The difficulty was that the calculation of boundary shear stress required the knowledge of velocity profile.

Knight and co-workers (1978—92), has led to an improved understanding of the lateral distributions of wall shear stress in prismatic channels and ducts. Nezu and Nakagawa (1993) pointed out that the results calculated by Chiu and Chiou revealed large errors.

Rhodes and Knight (1994) deduced results of laboratory experiments on wide smooth rectangular ducts which were reported in terms of the relationship between duct aspect ratio b/h and the shear force on the walls expressed as a proportion of the total boundary shear force, $\%SF_w$. The data set (range $0.02 \leq b/h \leq 50$) overlapped and extended the work of Knight and Patel (1985) that had range $0.1 \leq b/h \leq 10$. A new form of empirical model was proposed for the $\%SF_w$—b/h relationship. When compared with the $\%SF_w$ predicted by assuming the shear force on an element of the boundary to be simply proportional to its length, the model results deviated from it, with definite maximum and minimum deviations.

Following Einstein`s idea, Yang and Lim (1997) proposed an analytical method to delineate the two areas as given and determine the boundary shear stress distribution. An analytical approach for the partitioning of the flow cross-sectional area in steady and uniform three-dimensional channels was presented. The mechanism and direction of energy transport from the main flow were analyzed first. Based on the availability of surplus energy from the main flow, a concept of energy transportation through a minimum relative distance toward a unit area on the wetted perimeter was proposed. This led to a novel method to analytically divide the flow area into various parts corresponding to the channel shape and roughness composition of its wetted perimeter. The demarcated boundary or “division line” was evaluated using the presented equation. The existence of the division lines, which were lines of zero Reynolds shear stress within the flow region, had been proved through comparison with turbulence characteristics measurements. The method was illustrated in a study of the shear stress distribution in smooth rectangular open channels. Analytical solutions, valid for all aspect ratios, were derived for the mean side wall and bed shear stresses, and they compared well with existing experimental data from various researchers. However, their method was inconvenient for applications because of its implicit and segmental form except without considering the effect of secondary currents.

Patra and Kar (2000) reported the test results concerning the boundary shear stress, shear force, and discharge characteristics of compound meandering river sections composed of a rectangular main channel and one or two floodplains disposed off to its sides. They used five dimensionless channel parameters to form equations representing the total shear force percentage carried by floodplains. A set of smooth and rough sections were studied with aspect ratio varying from 2 to 5. Apparent shear forces on the assumed vertical, diagonal, and horizontal interface plains were found to be different from zero at low depths of flow and changed sign with increase in depth over floodplain. They proposed a variable-inclined interface for which apparent shear force was calculated as zero. They presented empirical equations predicting proportion of discharge carried by the main channel and floodplain.

Yang and McCorquodale (2004) developed a method for computing three-dimensional Reynolds shear stresses and boundary shear stress distribution in smooth rectangular channels by applying an order of magnitude analysis to integrate the Reynolds equations. A simplified relationship between the lateral and vertical terms was hypothesized for which the Reynolds equations become solvable. This relationship was in the form of a power law with an exponent of n = 1, 2, or infinity. The semi-empirical equations for the boundary shear distribution and the distribution of Reynolds shear stresses were compared with measured data in open channels. The power-law exponent of 2 gave the best overall results while n = infinity gave good results near the boundary.

Guo and Julien (2005) determined the average bed and sidewall shear stresses in smooth rectangular open-channel flows after solving the continuity and momentum equations. The analysis showed that the shear stresses were functions of three components: (1) gravitational; (2) secondary flows; and (3) interfacial shear stress. An analytical solution in terms of series expansion was obtained for the case of constant eddy viscosity without secondary currents. In comparison with laboratory measurements, it slightly overestimated the average bed shear stress measurements but underestimated the average sidewall shear stress by 17% when the width–depth ratio becomes large. A second approximation was formulated after introducing two empirical correction factors. The second approximation agreed very well (R^2 > 0.99 and average relative error less than 6%) with experimental measurements over a wide range of width–depth ratios.

Dey and Cheng (2005) and Dey and Lambert (2005) developed the expressions for the Reynolds stress and bed shear stress, assuming a modified logarithmic law of velocity

profile due to upward seepage and with stream wise sloping beds. The computed Reynolds stress profiles were in agreement with the experimental data.

Khatua (2008) and Khatua et al. (2009) undertook a series of laboratory tests for smooth and rigid meandering channels and developed numerical equations to evaluate and predict the boundary shear distribution.

2.4. OBJECTIVES OF THE PRESENT RESEARCH WORK

The present research work is intended to study the variations of stage-discharge relationship with channel roughness, geometry and sinuosity in straight and meandering channels. The review shows the effect of the parameters such as the bed slope, aspect ratio, sinuosity, roughness coefficients, flow depth, etc. on the discharge estimation. Using dimensional analysis, a model for roughness coefficients is planned on which a method of calculation of discharge carried by meandering channel can be proposed. Again, the boundary shear distribution for meandering channels can be improved. This should be useful in the solution of many practical problems and for better understanding of the mechanism of flow. The present work is also directed towards understanding the underlying mechanism of flow resistance and flow distribution in the straight and meander channel rather than simulating a prototype situation. The experimental channel dimensions are small due to space and other limitations in the laboratory. In view of the above, the research program is taken up with the following objectives:

- To investigate the loss of energy with flow depth for meandering and straight channels in terms of variation of Manning's n, Chezy`s C, Darcy-Weisbach f from the experimental runs.

- To propose equations to estimate the percentage of shear carried by the wall of the meandering channel and to extend the models to the channels of high width ratio and sinuosity.

- To study the flow parameters of meandering channel on the basis of which a simple but accurate method of calculation of discharge carried by a meandering channel can be proposed.

- To validate the developed models using the available experimental channel data from other investigators.

CHAPTER 3

EXPERIMENTAL WORK

3.1. GENERAL

The experiments have been conducted in the Fluid Mechanics and Hydraulics Laboratory of the Civil Engineering Department at the National Institute of Technology, Rourkela, India. In the laboratory, four types of flumes are fabricated in which channels of varying sinuosity; geometry and slope are cast inside. Experiments have been conducted in the channels by changing the geometrical parameters. This chapter discusses in detail the experimental procedure along with the apparatus required during the present work.

3.2. EXPERIMENTAL SETUP

The present research uses both meandering and straight experimental channels fabricated inside the tilting flumes separately in the Fluid Mechanics and Hydraulics Engineering Laboratory of the Civil Engineering Department, at the National Institute of Technology, Rourkela. The present work is mainly based on the observation taken inside two straight channels, one of rectangular cross section (Type-I) and another of trapezoidal cross section (Type-II). The other two channels are Type-III and Type-IV respectively, consisting of meandering channel. The tilting flumes are made out of metal frame with glass walls at the test reach. The flumes are made tilting by hydraulic jack arrangement. Inside each flume, separate meandering/straight channels are cast using 5mm thick Perspex sheets. To facilitate fabrication, the whole channel length has been made in blocks of 1.20 m length each. The photo graphs of Type-II, III and IV experimental channels with measuring equipments taken from the down stream side are shown in Photos 3.1, 3.2, and 3.3 respectively. The detailed geometrical features of the experimental channels are given in Table 3.1.

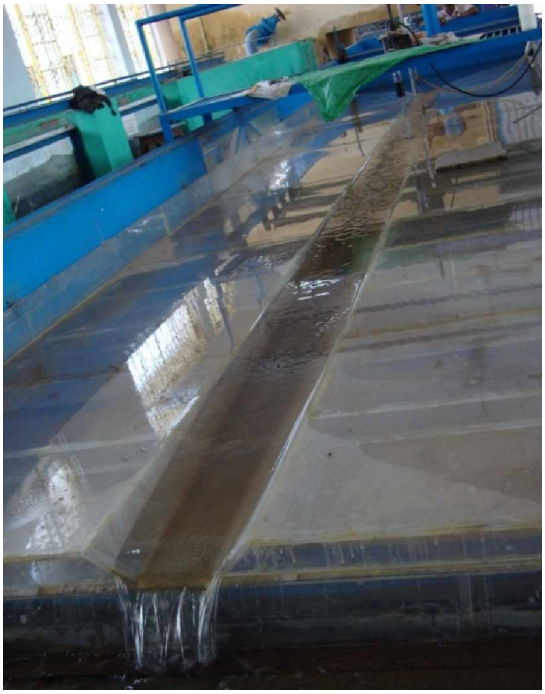

Photo 3.1

Photo 3.2

Photo 3.3

Table 3.1 Details of Geometrical Parameters of the Experimental Channels

Sl no.	Item description	Type-I	Type-II	Type-III	Type-IV
1	Channel Type	Straight	Straight	Meandering	Meandering
2	Wave length in down valley direction	-	-	400 mm	2185 mm
3	Amplitude	-	-	162	685 mm
4	Geometry of Main channel section	Rectangular	Trapezoidal (side slope 1:1)	Rectangular	Trapezoidal (side slope 1:1)
5	Nature of surface of bed	Smooth and rigid bed	Smooth and rigid bed	Smooth and rigid bed	Smooth and rigid bed
6	Channel width (b)	120 mm	120 mm at bottom and 280 mm at top	120 mm	120 mm at bottom and 280 mm at top
7	Bank full depth of channel	120 mm	80 mm	120 mm	80 mm
8	Bed Slope of the channel	0.0019	0.003	0.0031	Varying
9	Meander belt width	-	-	443 mm	1650 mm
10	Minimum radius of curvature of channel centerline at bend apex	-	-	140 mm	420 mm
11	Sinuosity	1.00	1.00	1.44	1.91
12	Cross over angle in degree	-	-	104	102
13	Flume size	0.45mx0.4m x12m long	2.0m×0.6m×12m long	0.6mx0.6mx 12m long	2.0m×0.6m×12 m long

The fabricated channels have the following details.

1. **Type-I channel**: The straight channel section has the dimension of 120 mm×120 mm. The channel is cast inside a tilting flume of 12 m long, 450 mm wide, and 400 mm deep. The bed slope of the channel is kept at 0.0019. The plan view and details of the geometrical parameters of the Type-I channel are shown in Fig. 3.1 (a) and (b), respectively.

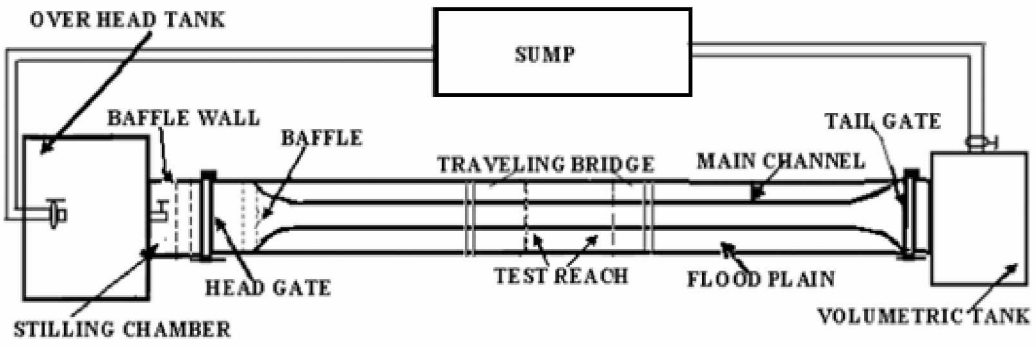

Fig. 3.1(a) - Plan View of Type-I Channel inside the Experimental Flume

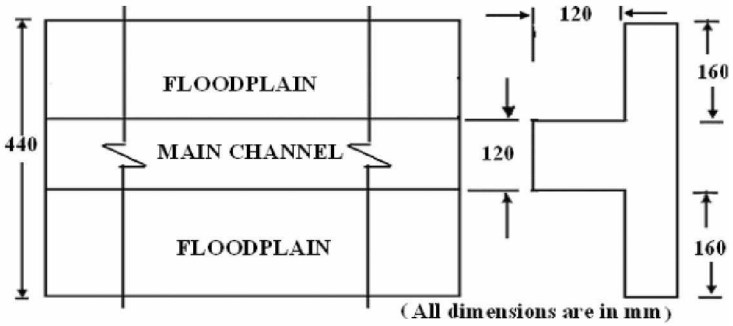

Fig. 3.1(b) Details of Geometrical Parameter of Type- I Channel

2. **Type-II channel**: The straight channel section is trapezoidal in cross section. The channel is of 120 mm wide at bottom, 280 mm wide at top having depth of 80 mm, and side slopes of 1:1 (Photo 3.1). The channel is cast inside a tilting flume of 12m long, 200 mm wide, and 600 mm deep. The bed slope of the channel is kept at 0.0033. The plan view and details of the geometrical parameters of the Type-II channel are shown in Fig. 3.2 (a) and (b), respectively.

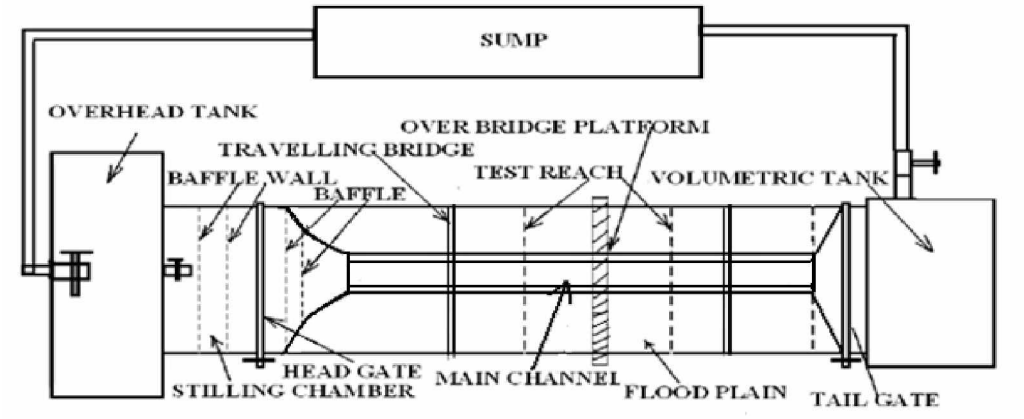

Fig. 3.2(a) Plan View of Type-II Channel inside the Experimental Flume

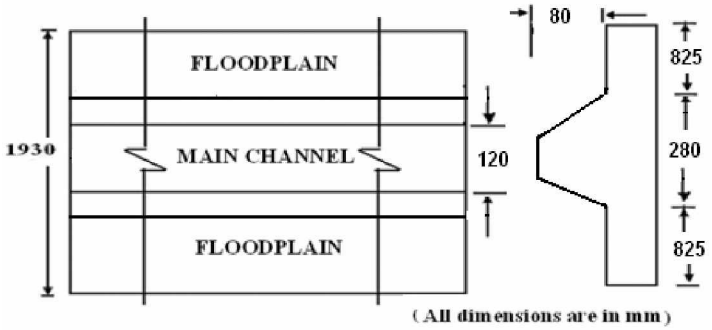

Fig. 3.2(b) Details of Geometrical Parameter of Type- II Channel

3. **Type-III channel**: The rectangular meandering channel has dimensions of 120 mm×120 mm in cross section. It has wavelength L = 400 mm, double amplitude $2A'$ = 323 mm giving rise to sinuosity of 1.44 (Photo 3.2). This mildly meandering channel is placed inside a tilting flume of 12 m long, 600 mm wide, and 600 mm deep. The plan view and details of the geometrical parameters of the Type-III channel are shown in Fig. 3.3 (a) and (b), respectively.

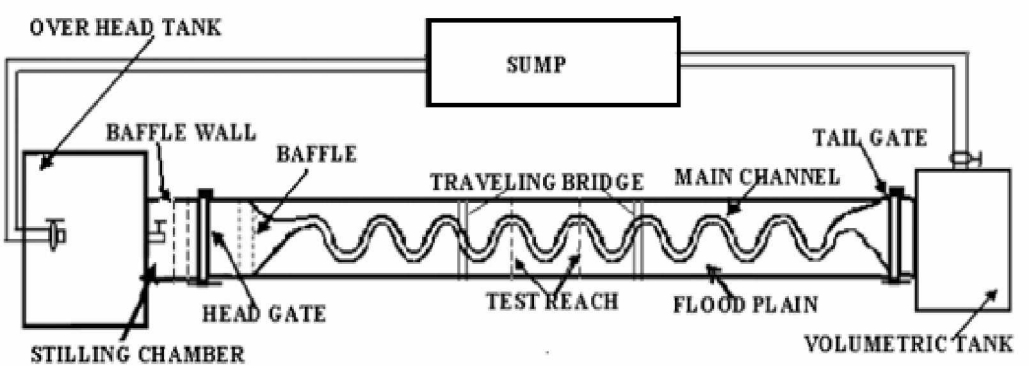

Fig. 3.3(a) Plan View of Type-III Channel inside the Experimental Flume

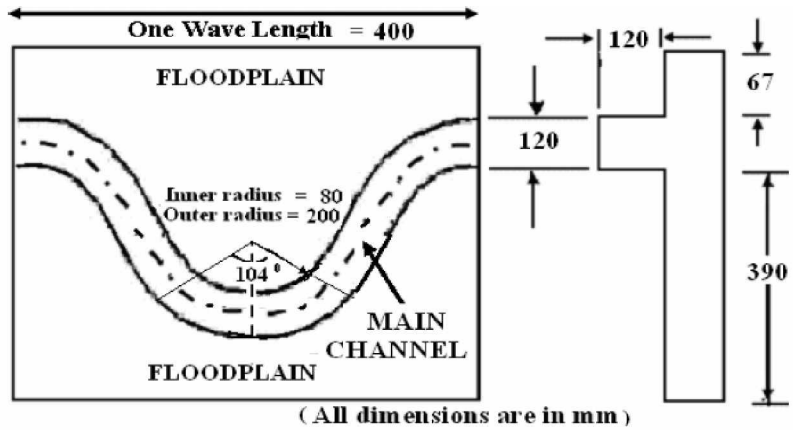

Fig. 3.3(b) Details of One Wavelength of Type- III Channel

4. **Type-IV channel**: This meandering channel is trapezoidal in cross section. The channel is 120 mm wide at bottom, 280 mm at top having full depth of 80 mm, and side slopes of 1:1. The channel has wavelength L = 2185 mm and double amplitude $2A'$ = 1370 mm. Sinuosity for this channel is scaled as 1.91 (Photo 3.3). The plan view and details of the geometrical parameters of the Type-IV channel are shown in Fig. 3.4 (a) and (b), respectively.

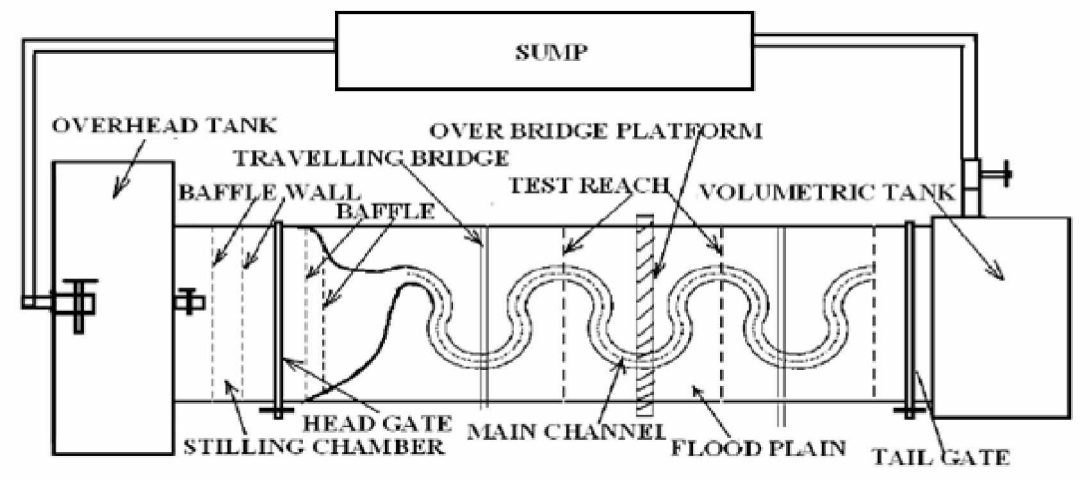

Fig. 3.4(a) Plan View of Type-IV Channel inside the Experimental Flume

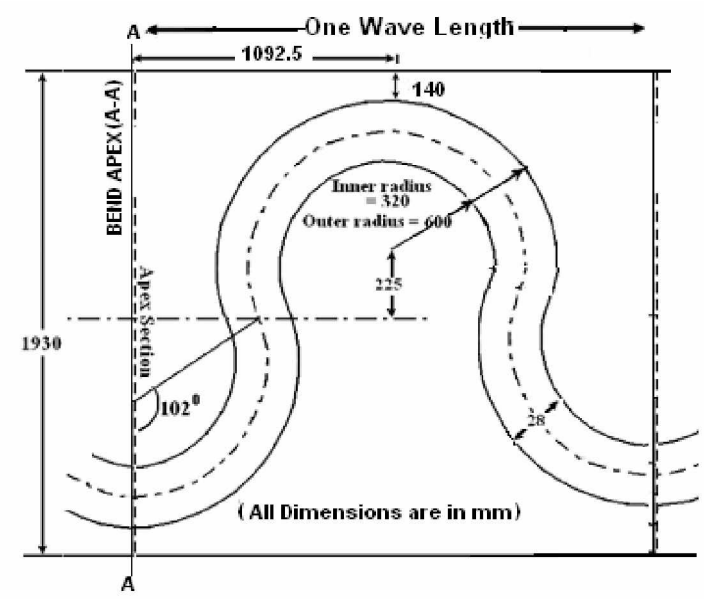

Fig. 3.4(b) Details of One Wavelength of Type- IV Channel

3.3. EXPERIMENTAL PROCEDURE

3.3.1. Apparatus and Methodology

Water is supplied to the experimental setup by a recirculating system of water supply (Photo 3.4). Two parallel pumps are used to pump water from an underground sump to the overhead tank (Photo 3.4a). The overhead tank (Photo 3.4b) has an over flow arrangement to spill

excess water to the sump and thus maintain a constant head. From the over head tank, water is led to a stilling tank (Photo 3.4 c) located at the upstream of the channel. A series of baffle walls between the stilling tank and channels are kept to reduce turbulence of the incoming water. At the end of the experimental channel, water is allowed to flow through a tailgate and is collected in a masonry volumetric tank (Photo 3.4f) from where it is allowed to flow back to the underground sump. From the sump, water is pumped back to the overhead tank, thus setting a complete re-circulating system of water supply for the experimental channel. The tailgate (Photo 3.4e) helps to establish uniform flow in the channel. It should be noted that the establishment of a flow that has its water surface parallel to the valley slope (where the energy losses are equal to potential energy input) may become a standard whereby the conveyance capacity of a meandering channel configuration is assessed.

Water surface slope measurement is carried out using a pointer gauge (Photo 3.5) fitted to the travelling bridge operated manually having least count of 0.1 mm. Point velocities are measured using a 16-Mhz Micro ADV (Acoustic Doppler Velocity-meter) at a number of locations across the predefined channel section. Guide rails are provided at the top of the experimental flume on which a travelling bridge is moved in the longitudinal direction of the entire experimental channel. The point gauge and the micro-ADV attached to the travelling bridge can also move in both longitudinal and the transverse direction of the experimental channel at the bridge position (Photo 3.6). The micro-ADV readings are recorded in a computer placed besides the bridge (Photo 3.7 a, b). As the ADV is unable to read the data of upper most layer (up to 5cm from free surface), a micro -Pitot tube (Photo 3.8, Photo 3.9 a, b, c) of 4 mm external diameter in conjunction with suitable inclined manometer are used to measure velocity and its direction of flow at the pre defined points of the flow-grid. A flow direction finder is also used to get the direction of maximum velocity with respect to the longitudinal flow direction. The Pitot tube is physically rotated normal to the main stream direction till it gives maximum deflection of manometer reading. The angle of limb of Pitot tube with longitudinal direction of the channel is noted by the circular scale and pointer arrangements attached to the flow direction meter.

Discharge in the channel is measured by the time rise method. The water flowing out at the down stream end of the experimental channel is led to a rectangular measuring tank of 1690 mm long x 1030 mm wide for Type-I channel, 1985 mm long xl900 mm wide for the Type-III channel and 2112 mm long x 3939 mm wide tank for Type-II and Type-IV channel.

The change in the depth of water with time is measured by stopwatch in a glass tube indicator with a scale having least count of 0.01mm.

A hand-operated tailgate weir is constructed at the downstream end of the channel to regulate and maintain the desired depth of flow in the flume. The bed slope is set by adjusting the whole structure, tilting it upwards or downwards with the help of a leaver, which is termed as slope changing leaver (Photo 3.12). Readings are taken for the different slopes, sinuosity and aspect ratio.

3.3.2. Determination of Channel Slope

At the tail end, the impounded water in the channel is allowed to remain standstill by blocking the tail end. For Type-I and Type-II channel, the mean slope is obtained by dividing the level difference between the two end points of the test reach of 1 m along the centerline. The level difference between channel bed and water surface are recorded at a distance of one wavelength along its centerline for Type-III and Type-IV channels. For meandering channels, the mean slopes for Type-III and Type-IV channels is obtained by dividing the level difference between these two points by the length of meander wave along the centerline.

3.3.3. Measurement of Discharge and Water Surface Elevation

A point gauge with least count of 0.1 mm is used to measure the water surface elevation above the bed of the channel. A measuring tank located at the end of each test channel receives water flowing through the channels. Depending on the flow rate, the time of collection of water in the measuring tanks vary between 50 to 262 seconds; lower one for higher rate of discharge. The time is recorded using a stopwatch. Change in the mean water level in the tank over the time interval is recorded. From the knowledge of the volume of water collected in the measuring tank and the corresponding time of collection, the discharge flowing in the experimental channel for each run of each channel is obtained.

Start →

Photo 3.4(a)

Photo 3.4(b)

Photo 3.4(c)

Photo 3.4(d)

Photo 3.4(e)

Photo 3.4(f)

Photo 3.4 Recirculating Water System

Photo 3.5

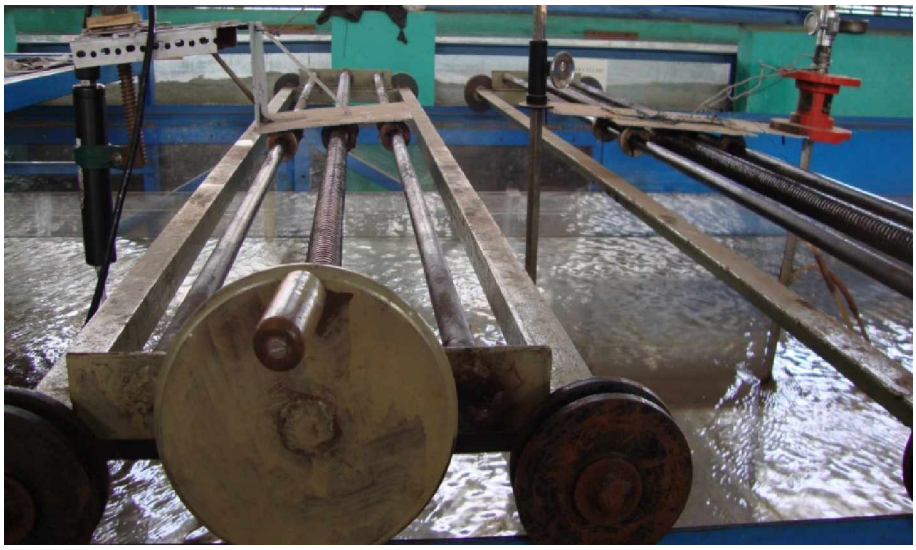

Photo 3.6

Photo 3.7(a)

Photo 3.7(b)

Photo 3.8

Photo 3.9(a)

Photo 3.9(b)

Photo 3.9 (c)

Photo 3.10

Photo 3.11

Photo 3.12

3.3.4. Measurement of Velocity and Its Direction

A 16-MHz Micro ADV (Acoustic Doppler Velocity-meter) manufactured by M/s SonTek, San Diego, Canada is used for 3-axis (3D) velocity measurement at each grid point of the channel sections (Photo 3.7a). The higher acoustical frequency of 16 MHz makes the Micro-ADV the optimal instrument for laboratory study. The Micro ADV with the software package is used for taking high-quality three dimensional velocity data at different points. The data is received at the ADV-processor. A computer attached with the processor (Photo 3.7b) shows the 3-dimensional velocity data after compiling with the software package. At every point, the instrument records a number of velocity data per minute. With the statistical analysis using the installed software, mean values of 3D point velocities are recorded for each flow depth. The Micro-ADV uses the Doppler shift principle to measure the velocity of small particles, assuming to be moving at velocities similar to the fluid (Fig. 3.5 a). Velocities is resolved into three orthogonal components (tangential, radial, and vertical) and are measured at 5 cm below the sensor head, minimizing interference of the flow field, and allowing measurements to be made close to the bed.

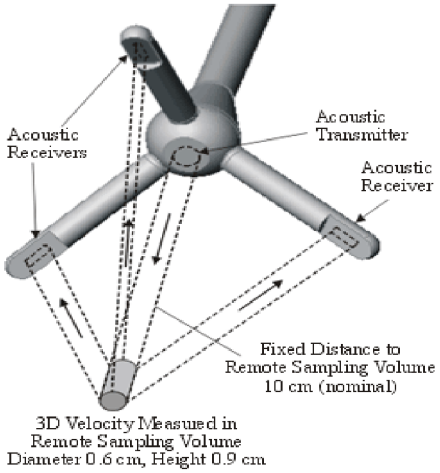

Fig. 3.5 (a) - Standard Features of a MicroADV

The Micro ADV has excellent features (Fig. 3.5 b) such as

- Three-axis velocity measurement
- High sampling rates - up to 50 Hz
- Small sampling volume - less than 0.1 cm^3
- Distance to Sampling Volume-5 cm
- Small optimal scatterer - excellent for low flows
- High accuracy upto1% of measured range
- Large velocity ranges between 1 mm/s to 2.5 m/s
- Excellent low-flow performance
- No recalibration needed
- Comprehensive software

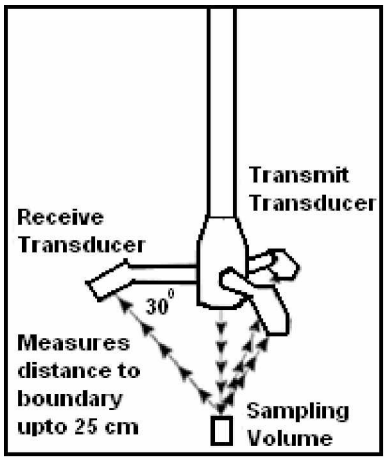

Fig. 3.5 (b) - Details of Probe of a MicroADV

Boasting a sampling volume of less than 0.09 cc and sampling rates up to 50 Hz, the 16-MHz MicroADV is an ideal laboratory instrument for low flow and turbulence studies. Though the ADV has proven its versatility and reliability in a wide variety of applications, yet it is unable to read the upper layer velocity, that is, up to 50 mm from free surface. To overcome the short, a standard Prandtl type micro-Pitot tube in conjunction with a manometer of accuracy 0.12 mm is used for the measurement of point velocity readings at the specified location for the upper 50 mm region from free surface across the channel. The results from the observations have been discussed in the next chapter.

A flow direction meter is used to find the direction of the velocity readings taken by micro Pitot tube in the experimental channel. It essentially consists of a copper tube at lower end of which a metal pointer rod tied with a thread is attached, while another pointer at the upper end of the tube moves over a circular metallic protractor. The copper tube is fixed with the protractor through a ball bearing arrangement. The thread tied to the pointer rod is lowered into water that moves along the resultant direction of flow. The copper tube with the metal pointer rod at upper end is made to rotate till the pointer and thread are in a vertical straight line parallel to each other. The angle of rotation by upper pointer with the metallic protractor gives the direction of flow. The deviation of the angle of flow shown by the pointer with respect to the zero position of the metallic protractor (tangential direction) is taken as the local direction of the total velocity vector in the channel.

When flow is confined to meander channel, velocity measurements are taken at the bend apex so as to get a broad picture of flow parameters covering half the meander wave length. For straight channels, the measurement is taken at the section in the central test reach. While taking velocity readings using Pitot tube, the tube is placed facing the direction of flow and then is rotated along a plane parallel to the bed and till it registers relatively a maximum head difference in the attached manometer. The deviation angle between the reference axis and the total velocity vector is considered positive, when the velocity vector is directed away from the outer bank. The total head h reading by the Pitot tube at the location in the channel is used to give the magnitude of the total velocity vector as $U = 2gh$, where g is the acceleration due to gravity. Resolving U into the tangential and radial directions, the local velocity components are determined. While doing so, the tube coefficient is taken as unit and the error due to turbulence in the computation of U is considered negligible. Using the data of velocities by Pitot tube and micro-ADV close to the

surface of the channels, the boundary shear at various points on the channel bed at the predefined channel sections are evaluated from the logarithmic velocity distribution relationship which is described in the next chapter.

All measurements are carried out under quasi-uniform flow condition by maintaining the out flow through downstream tailgate. Using the downstream tailgate, uniform flow is maintained for each experimental run and for each channel by maintaining the water surface slope parallel to the valley bed slope. Experimental results are accessed concerning stage-discharge-resistance relationships for meandering channels with rigid and smooth boundaries. All observations are recorded in the central test reach for straight channel of type-I and type-II and at the bend apex of Type-III and type-IV (Photo 3.10 and Photo 3.11) meandering channels. Details of flow parameter of the experimental channels and the associated runs are given in Table-3.2**.**

Table- 3.2 Hydraulic Details of the Experimental Runs

Sl no	Item description	Type-I	Type-II	Type-III	Type-IV
1	Channel Type	Straight	Straight	Meandering	Meandering
2	Number of runs for stage-discharge data	11	5	15	55 (Slopes - 0.003, 0.0042, 0.0053, 0.008, 0.013, 0.015, 0.021)
3	Discharge (cm^3/s)	1061, 1280, 2148, 2307, 2902, 3249, 4117, 4548, 5058, 5947, 6312	4766, 6961, 8147, 8961, 9739	316, 426, 1347 1669, 2200, 2357, 2619, 2757, 2946, 3338, 3698, 4191, 4656, 5596, 5680	Slope-0.003 (1479, 2605, 3101, 3717, 4097, 4563, 5994) Slope-0.0042 (4798, 5329, 5899, 7210, 7809, 8636) Slope-0.0053 (294, 484, 987, 1742, 2048, 2757, 3224, 3338, 3698, 4191, 4656, 5515, 6396, 7545) Slope-0.008 (904, 1416, 2165, 4863, 5492, 6768, 8473) Slope-0.013 (2357, 4877, 5410, 5991, 7181, 8157, 9480) Slope-0.015 (1319, 2742, 4497, 4884, 6209, 8112, 8397) Slope-0.021 (1286, 2150, 3346, 4070, 5451, 6123, 9223)
	Depth of flow (cm) corresponding to flow discharge of runs	3.02, 3.44, 4.98, 5.24, 6.21, 6.80, 8.15, 8.82, 9.55, 10.92, 11.48	5.2, 6.4, 7.0, 7.4, 7.8	1.29, 1.57, 3.44, 4.05, 4.98, 5.31, 5.78, 6.08, 6.41, 7.11, 7.7, 8.55, 9.34, 10.9,11.01	Slope-0.003 (3.1, 4.5, 5.0, 5.6, 5.9, 6.3, 7.4) Slope-0.0042 (5.7, 6.1, 6.5, 7.2, 7.5, 7.8) Slope-0.0053 (1.1, 1.4, 2.2, 3.1, 3.4, 4.1, 4.6, 4.7, 4.9, 5.3, 5.6, 6.2, 6.7, 7.3) Slope-0.008 (1.9, 2.5, 3.3, 5.1, 5.6, 6.2, 7.0) Slope-0.013 (3.1, 4.8, 5.1, 5.4, 6.0, 6.4, 7.0) Slope-0.015 (2.1, 3.3, 4.4, 4.6, 5.3, 6.2, 6.3) Slope-0.021 (1.9, 2.6, 3.4, 3.9, 4.6, 4.9, 6.3)
5	Nature of surface of bed	smooth and rigid bed	smooth and rigid bed	smooth and rigid bed	smooth and rigid bed
6	No. of runs for detailed measurement of 3 dimensional point using Micro ADV	6	5	6	12

CHAPTER 4

RESULTS AND DISCUSSIONS

4.1. GENERAL

The results of experiments concerning the distribution of velocity, flow, and boundary shear stress of meandering channels are presented in this chapter. Analysis of results is done for roughness coefficients and distribution of boundary shear in a meandering channel. The overall summary of experimental runs for straight channel (Type-I and Type-II) are given in Table 4.1 (a) and for meandering channels of Type-III and Type-IV it is given in Table 4.1 (b) and Fig. 4.1 (c), respectively. The detailed skeleton of the probe limits are shown in Fig. 4.1.

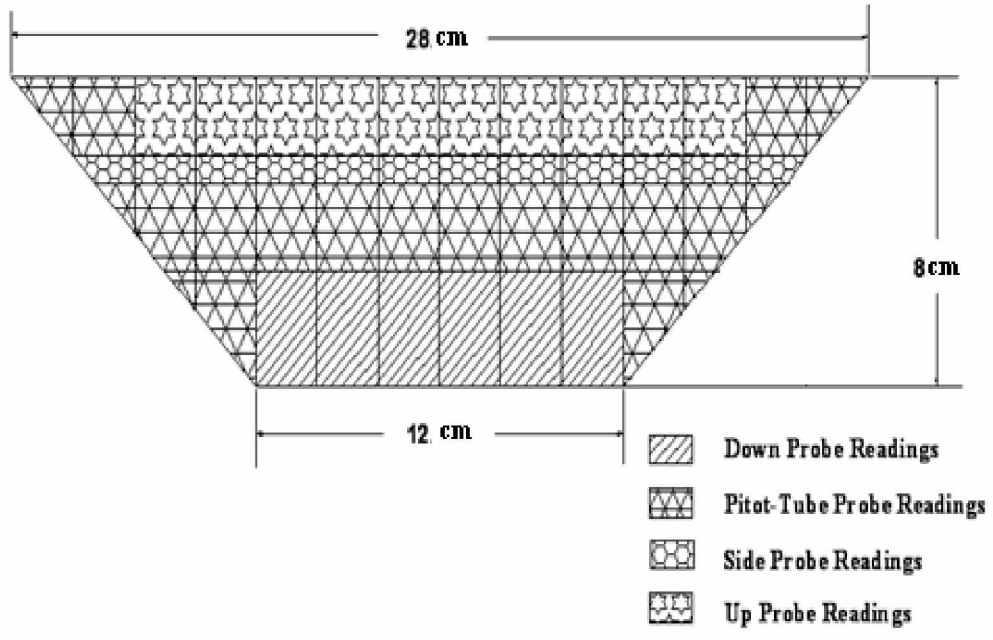

Fig. 4.1 Cross Section of Channel for Experimentation

Despite the use of three types of probes (up probe, down probe and side probe) there is a fringe zone for which the data could not be recorded due to the inherent limitations of the ADV as discussed in the previous chapter. The division of the channel section is done for the convenience to take the readings at maximum possible points as shown in Fig. 4.1. Therefore, the Pitot tube has been used to record the velocity of the fringe zone.

Table 4.1(a) Experimental Runs for Type-I and Type-II Straight Channels

Channel Type	Run No	Discharge Q (m^3/sec)	Flow Depth h (m)	Channel Width b (m)	Cross Section Area A(m^2)	Wetted Perimeter P(m)	Hydraulic Radius R= (A/P)	Average Velocity (Q/A) (m/sec)	Aspect Ratio(α)
(1)	(2)	(3)	(4)	(5)	(6)	(7)	(8)	(9)	(10)
Type-I Straight Rectangular Channel Sinuosity=1 Slope=0.0019	SR1	0.00106	0.030	0.12	0.0036	0.18	0.020	0.293	3.974
	SR2	0.00128	0.034	0.12	0.0041	0.19	0.022	0.310	3.488
	SR3	0.00215	0.050	0.12	0.0060	0.22	0.027	0.359	2.410
	SR4	0.00231	0.052	0.12	0.0063	0.22	0.028	0.367	2.290
	SR5	0.00290	0.062	0.12	0.0075	0.24	0.031	0.389	1.932
	SR6	0.00325	0.068	0.12	0.0082	0.26	0.032	0.398	1.765
	SR7	0.00412	0.082	0.12	0.0098	0.28	0.035	0.421	1.472
	SR8	0.00455	0.088	0.12	0.0106	0.30	0.036	0.430	1.361
	SR9	0.00506	0.096	0.12	0.0115	0.31	0.037	0.441	1.257
	SR10	0.00595	0.109	0.12	0.0131	0.34	0.039	0.454	1.099
	SR11	0.00631	0.115	0.12	0.0138	0.35	0.039	0.458	1.045
Type-II Straight Trapezoidal Channel Sinuosity=1 Slope=0.0033	ST1	0.00477	0.052	0.12	0.0089	0.27	0.033	0.533	2.308
	ST2	0.00696	0.064	0.12	0.0118	0.30	0.039	0.591	1.875
	ST3	0.00815	0.070	0.12	0.0133	0.32	0.042	0.613	1.714
	ST4	0.00896	0.074	0.12	0.0144	0.33	0.044	0.624	1.622
	ST5	0.00974	0.078	0.12	0.0154	0.34	0.045	0.634	1.544

Table 4.1(b) Experimental Runs for Type-III Meandering Channel

Channel Type	Run No	Discharge Q (m^3/sec)	Flow Depth h (m)	Channel Width b (m)	Cross Section Area A(m^2)	Wetted Perimeter P(m)	Hydraulic Radius R= (A/P)	Average Velocity (Q/A) (m/sec)	Aspect Ratio(α)
(1)	(2)	(3)	(4)	(5)	(6)	(7)	(8)	(9)	(10)
Type-III Meandering Rectangular Channel Sinuosity=1.44 Slope= 0.0031	MR1	0.00032	0.013	0.12	0.0015	0.15	0.011	0.207	9.302
	MR 2	0.00043	0.016	0.12	0.0019	0.15	0.012	0.229	7.643
	MR 3	0.00135	0.034	0.12	0.0041	0.19	0.022	0.326	3.488
	MR 4	0.00167	0.041	0.12	0.0049	0.20	0.024	0.343	2.963
	MR 5	0.00220	0.050	0.12	0.0060	0.22	0.027	0.368	2.410
	MR 6	0.00236	0.053	0.12	0.0064	0.23	0.028	0.370	2.260
	MR 7	0.00262	0.058	0.12	0.0069	0.24	0.029	0.378	2.076
	MR 8	0.00276	0.061	0.12	0.0073	0.24	0.030	0.378	1.974
	MR 9	0.00295	0.064	0.12	0.0077	0.25	0.031	0.383	1.872
	MR 10	0.00334	0.071	0.12	0.0085	0.26	0.033	0.391	1.688
	MR 11	0.00370	0.077	0.12	0.0092	0.27	0.034	0.400	1.558
	MR 12	0.00419	0.086	0.12	0.0103	0.29	0.035	0.408	1.404
	MR 13	0.00466	0.093	0.12	0.0112	0.31	0.037	0.415	1.285
	MR 14	0.00560	0.109	0.12	0.0130	0.34	0.039	0.429	1.105
	MR 15	0.00568	0.110	0.12	0.0132	0.34	0.039	0.430	1.090

Table 4.1(c) Experimental Runs for Type-I V Meandering Channels

Channel Type	Run No	Discharge Q (m^3/sec)	Flow Depth h (m)	Channel Width b (m)	Cross Section Area A(m^2)	Wetted Perimeter P(m)	Hydraulic Radius R= (A/P)	Average Velocity (Q/A) (m/sec)	Aspect Ratio(α)
(1)	(2)	(3)	(4)	(5)	(6)	(7)	(8)	(9)	(10)
Meandering Trapezoidal Channel Sinuosity=1.91 Slope=0.003	MT1	0.00148	0.031	0.12	0.0047	0.21	0.023	0.316	3.871
	MT2	0.00261	0.045	0.12	0.0074	0.25	0.030	0.351	2.667
	MT3	0.00310	0.050	0.12	0.0085	0.26	0.033	0.364	2.398
	MT4	0.00372	0.056	0.12	0.0099	0.28	0.035	0.377	2.143
	MT5	0.00410	0.059	0.12	0.0106	0.29	0.037	0.388	2.034
	MT6	0.00456	0.063	0.12	0.0115	0.30	0.039	0.396	1.905
	MT7	0.00599	0.074	0.12	0.0144	0.33	0.044	0.418	1.622
Meandering Trapezoidal Channel Sinuosity=1.91 Slope=0.0042	MT8	0.00480	0.057	0.12	0.0101	0.28	0.036	0.476	2.105
	MT9	0.00533	0.061	0.12	0.0110	0.29	0.038	0.483	1.967
	MT10	0.00590	0.065	0.12	0.0120	0.30	0.040	0.491	1.846
	MT11	0.00721	0.072	0.12	0.0138	0.32	0.043	0.522	1.667
	MT12	0.00781	0.075	0.12	0.0146	0.33	0.044	0.534	1.600
	MT13	0.00864	0.078	0.12	0.0154	0.34	0.045	0.559	1.538
Meandering Trapezoidal Channel Sinuosity=1.91 Slope=0.0053	MT14	0.00029	0.011	0.12	0.0014	0.15	0.009	0.215	11.429
	MT15	0.00048	0.014	0.12	0.0019	0.16	0.012	0.250	8.333
	MT16	0.00099	0.022	0.12	0.0032	0.18	0.017	0.313	5.405
	MT17	0.00174	0.031	0.12	0.0047	0.21	0.023	0.368	3.834
	MT18	0.00205	0.034	0.12	0.0053	0.22	0.024	0.386	3.488
	MT19	0.00276	0.041	0.12	0.0066	0.24	0.028	0.418	2.927
	MT20	0.00322	0.046	0.12	0.0075	0.25	0.030	0.428	2.637
	MT21	0.00334	0.047	0.12	0.0077	0.25	0.031	0.431	2.581
	MT22	0.00370	0.049	0.12	0.0083	0.26	0.032	0.443	2.434
	MT23	0.00419	0.053	0.12	0.0092	0.27	0.034	0.457	2.264
	MT24	0.00466	0.056	0.12	0.0099	0.28	0.036	0.470	2.135
	MT25	0.00552	0.062	0.12	0.0112	0.29	0.038	0.491	1.942
	MT26	0.00640	0.067	0.12	0.0126	0.31	0.041	0.509	1.788
	MT27	0.00755	0.073	0.12	0.0142	0.33	0.043	0.533	1.637
Meandering Trapezoidal Channel Sinuosity=1.91 Slope=0.008	MT28	0.00090	0.019	0.12	0.0026	0.17	0.015	0.342	6.316
	MT29	0.00142	0.025	0.12	0.0036	0.19	0.019	0.391	4.800
	MT30	0.00217	0.033	0.12	0.0050	0.21	0.023	0.437	3.692
	MT31	0.00486	0.051	0.12	0.0087	0.26	0.033	0.558	2.353
	MT32	0.00549	0.056	0.12	0.0097	0.28	0.035	0.564	2.162
	MT33	0.00677	0.062	0.12	0.0113	0.30	0.038	0.600	1.935
	MT34	0.00847	0.070	0.12	0.0133	0.32	0.042	0.637	1.714
Meandering Trapezoidal Channel Sinuosity=1.91 Slope=0.013	MT35	0.00236	0.031	0.12	0.0047	0.21	0.023	0.504	3.871
	MT36	0.00488	0.048	0.12	0.0080	0.25	0.031	0.613	2.526
	MT37	0.00541	0.051	0.12	0.0087	0.26	0.033	0.620	2.353
	MT38	0.00599	0.054	0.12	0.0094	0.27	0.034	0.638	2.222
	MT39	0.00718	0.060	0.12	0.0108	0.29	0.037	0.665	2.000
	MT40	0.00816	0.064	0.12	0.0118	0.30	0.039	0.693	1.875
	MT41	0.00948	0.070	0.12	0.0133	0.32	0.042	0.713	1.714
Meandering Trapezoidal Channel Sinuosity=1.91 Slope=0.015	MT42	0.00132	0.021	0.12	0.0030	0.18	0.017	0.445	5.714
	MT43	0.00274	0.033	0.12	0.0050	0.21	0.024	0.543	3.636
	MT44	0.00450	0.044	0.12	0.0072	0.24	0.030	0.623	2.727
	MT45	0.00488	0.046	0.12	0.0076	0.25	0.031	0.640	2.609
	MT46	0.00621	0.053	0.12	0.0092	0.27	0.034	0.677	2.264
	MT47	0.00811	0.062	0.12	0.0112	0.29	0.038	0.727	1.951
	MT48	0.00840	0.063	0.12	0.0115	0.30	0.039	0.728	1.905
Meandering Trapezoidal Channel Sinuosity=1.91 Slope=0.021	MT49	0.00129	0.019	0.12	0.0026	0.17	0.015	0.487	3.558
	MT50	0.00215	0.026	0.12	0.0038	0.19	0.020	0.566	4.558
	MT51	0.00335	0.034	0.12	0.0052	0.22	0.024	0.639	3.082
	MT52	0.00407	0.039	0.12	0.0062	0.23	0.027	0.656	2.975
	MT53	0.00545	0.046	0.12	0.0076	0.25	0.031	0.714	2.553
	MT54	0.00612	0.049	0.12	0.0083	0.26	0.032	0.739	2.553
	MT55	0.00922	0.063	0.12	0.0114	0.30	0.038	0.809	3.553

4.2. STAGE-DISCHARGE VARIATION FOR MEANDERING CHANNELS

In the present investigation involving the flow in straight and meandering channels, achieving steady and uniform flow has been difficult due to the effect of curvature and the influence of a number of geometrical parameters. However, for the purpose of present work, an overall uniform flow is tried to be achieved in the channels. Flow depths in the experimental channel runs are so maintained that the water surface slope becomes parallel to the valley slope. At this stage, the energy losses are taken as equal to potential energy input. This has become a standard whereby the conveyance capacity of a meandering channel configuration can be assessed (Shiono, Al- Romaih, and Knight, 1999). Under such conditions, the depths of flow at the channel centerline separated by one wavelength distance must be the same. In all the experimental runs this simplified approach has been tried to achieve. This stage of flow is taken as normal depth, which can carry a particular flow only under steady and uniform conditions. The stage discharge curves plotted for different bed slopes for particular sinuosities of channel are shown in Fig. 4.2. The discharge increases with an increase in bed slope for the same stage.

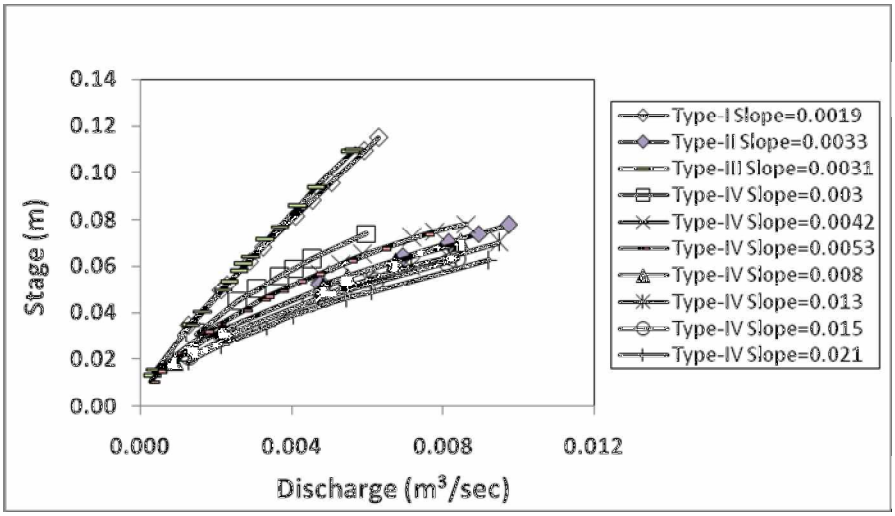

Fig. 4.2 Stage Discharge Variations in Open Channel Flow

4.3. VARIATION OF REACH AVERAGED LONGITUDINAL VELOCITY *U* WITH DEPTH OF FLOW

Plots between the reach averaged velocity *U* and non-dimensional flow depth for all the experimental channels for the four types of channels are shown in Fig. 4.3. From the figure it

can be seen that for all the channels, the increase in reach averaged longitudinal velocity of flow is nearly in accordance with the increase in depth of flow.

The drop in the reach averaged velocity is higher for Type-IV channel. This may be due to spreading of water to a wider section for Type-IV channel than Type-I and Type-III channel sections, (Sinuosity S_r= 1 for Type-I and Type-II, S_r= 1.44 for Type-III, and S_r= 1.91 for Type-IV), resulting additional resistance to flow. For all flow conditions, the rate of increase of velocity with flow depth is higher for the sinus channel of Type-IV and lower for straight channel of Type-I. This is mainly due to their large differences in the longitudinal bed slopes. The slope of the channel is an important parameter influencing the desired driving force. As for higher slopes (Type-IV, slope=0.021, 0.015, 0.013) in a particular channel there is increase in the rate of velocity with flow depth.

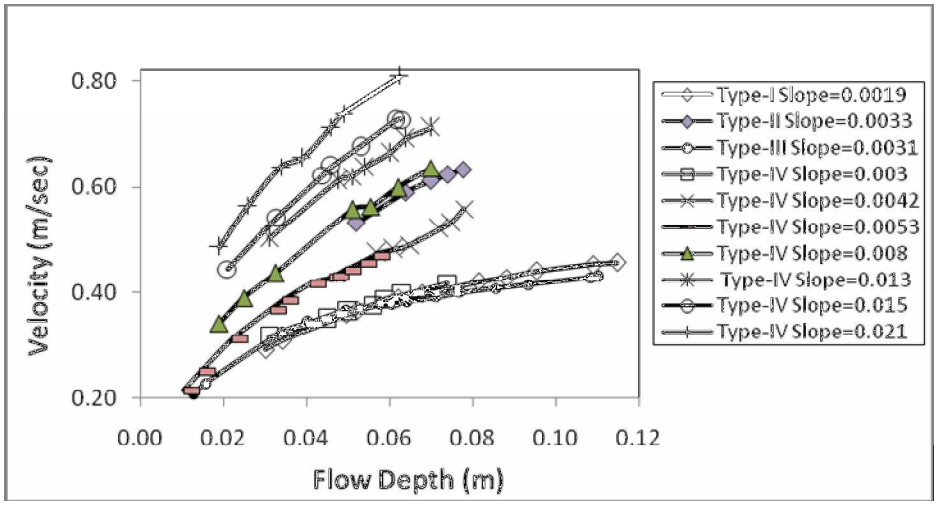

Fig. 4.3 Variations of Velocity with Flow Depth in Open Channel Flow

4.4. DISTRIBUTION OF TANGENTIAL (LONGITUDINAL) VELOCITY

Measurement of velocity for the experimental channels is mostly recorded by a micro-ADV. The instrument uses the sign convention for 3-dimensional velocity as positive for ENU (east, north and upward) and negative for WSD (west, south and down ward) directions respectively for the longitudinal (V_x), radial (V_y) and vertical components (V_z). For the experimental channel position, east refers to the direction of longitudinal velocity. The east probe of ADV is kept in the longitudinal flow direction. Accordingly the other two flow directions are referred. In the experiments for meandering channels, the readings are taken at the bend apex with tangential velocity direction taken as east. For radial velocity, positive

stands for outward and negative stands for inward radial velocity direction. Similarly, for vertical component of velocity when the ADV readings shows positive, then the velocity component is upward and if negative, it is in the down-ward direction. The detailed velocity and boundary shear distribution are carried out for three channels of Type-II, Type-III and Type-IV of sinuosity 1.00, 1.44 and 1.91, respectively. As the sinuosity of Type-I is similar as Type-II so, the detailed velocity distribution and evaluation of boundary shear has not been done. The measurements are taken at any cross section of the channel reach for straight channels of Type-II and at the bend apex for meandering channels of Type-III (Fig. 4.4a) and Type-IV (Fig. 4.4b).

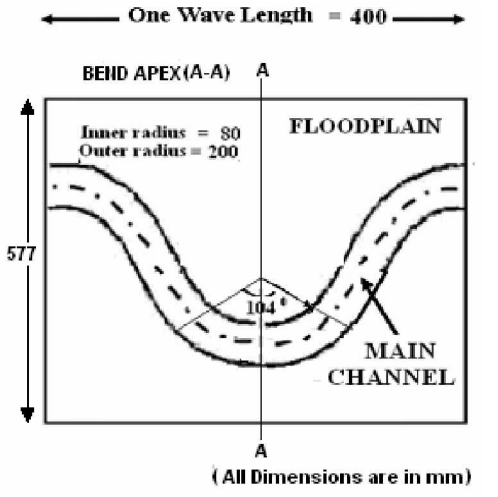

Fig. 4.4 (a) Location of Bend Apex (A-A) of Type-III Meandering Channel

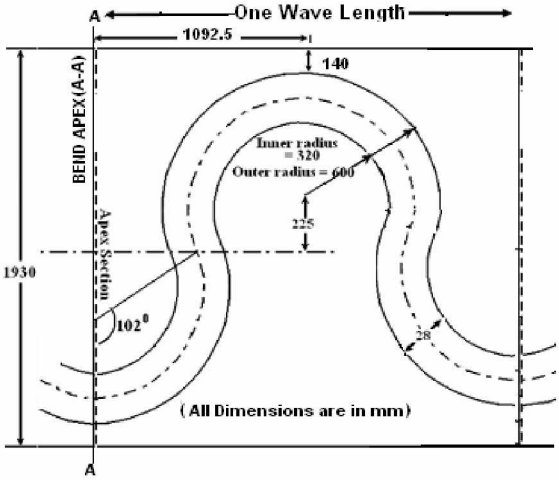

Fig. 4.4 (b) Location of Bend Apex (A-A) of Type-IV Meandering Channel

For the straight channels of Type-II the radial distribution of tangential velocity with the boundary shear distribution are shown in Figs.4.5.1-4.5.4. For meander channels, the radial distribution of tangential velocity in contour form for the runs of meandering channels of Type-III at bend apex are shown in Fig. 4.6.1 through Fig. 4.6.6. Similarly for Type-IV channels the radial distributions of tangential velocity at bend apex are shown in Fig. 4.7.1-4.7.6. The Fig. 4.5.1 - 4.5.4, Fig. 4.6.1- 4.6.6 and Fig.4.7.1-4.7.6 also show the boundary shear distribution for straight channel of Type-II and meandering channels of Type-III and Type-IV respectively.

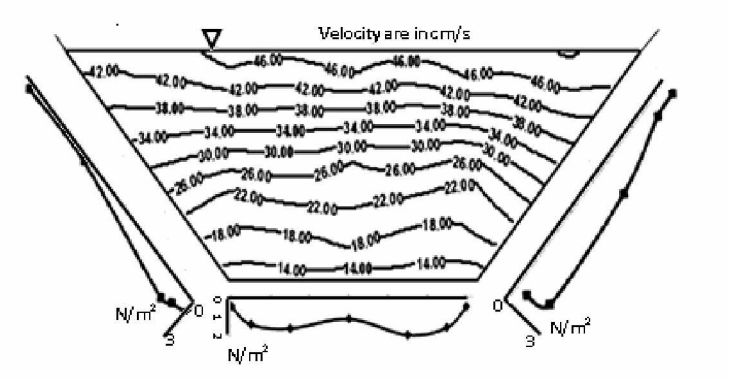

Fig. 4.5.1 Flow depth *h* = 5.2 cm (Type-II channel)

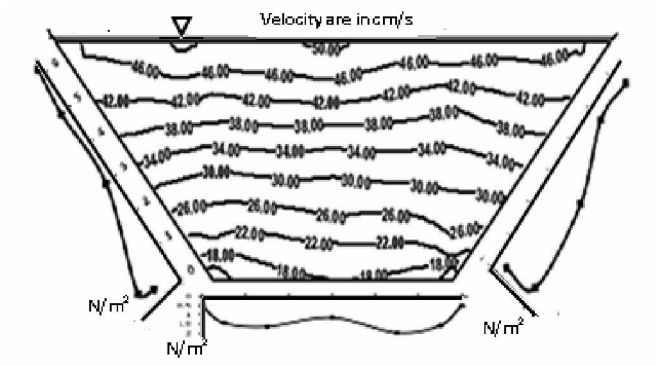

Fig. 4.5.2 Flow depth *h* = 6.4 cm (Type-II channel)

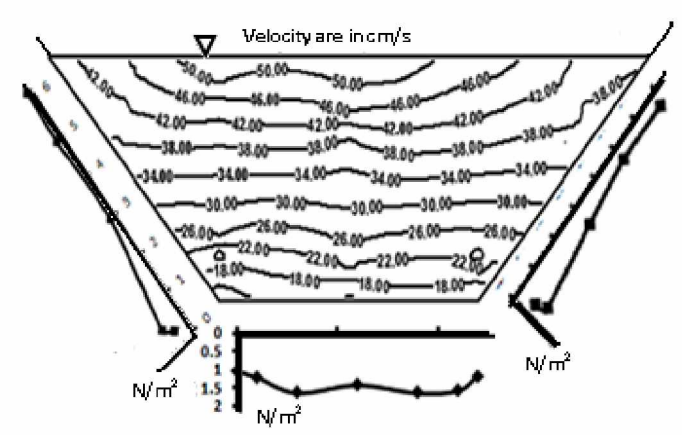

Fig. 4.5.3 Flow depth *h* = 7.0 cm (Type-II channel)

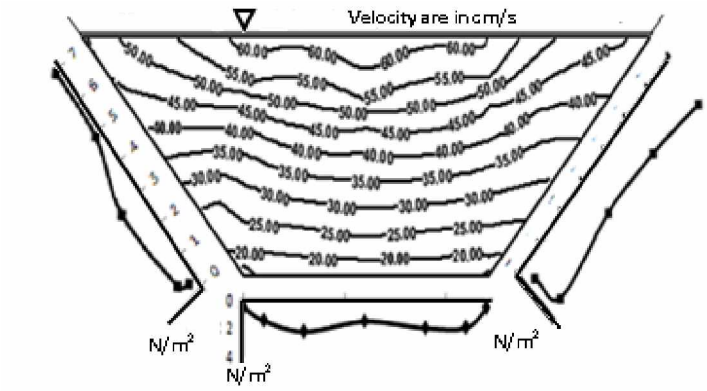

Fig. 4.5.4 Flow depth *h* = 7.4 cm (Type-II channel)

Figs. 4.5.1- 4.5.4 Contours Showing the Distribution of Tangential Velocity and Boundary Shear for Type-II Straight Channel

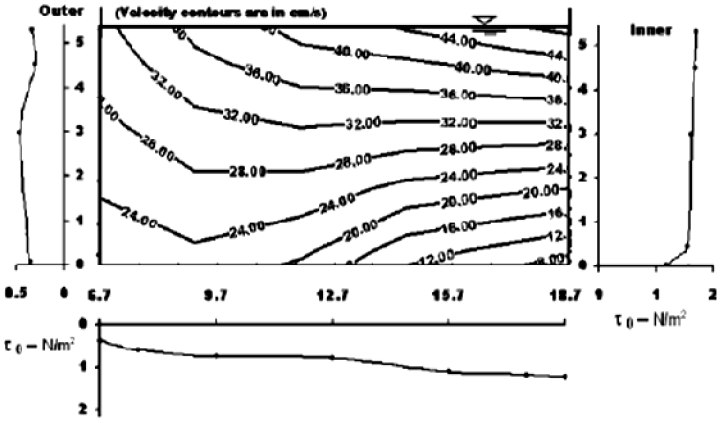

Fig. 4.6.1 Flow depth ` = 5.31cm (Type-III channel)

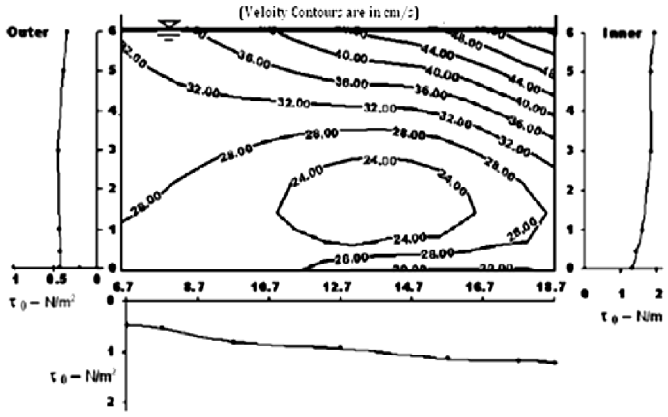

Fig. 4.6.2 Flow depth *h* = 6.08cm (Type-III channel)

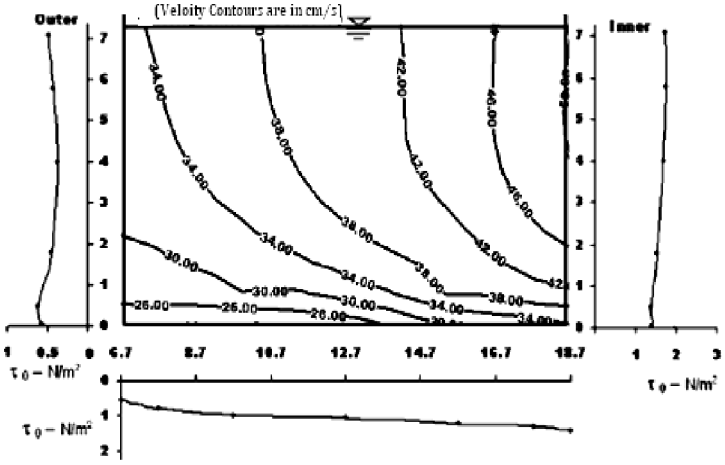

Fig. 4.6.3 Flow depth *h* = 7.11 cm (Type-III channel)

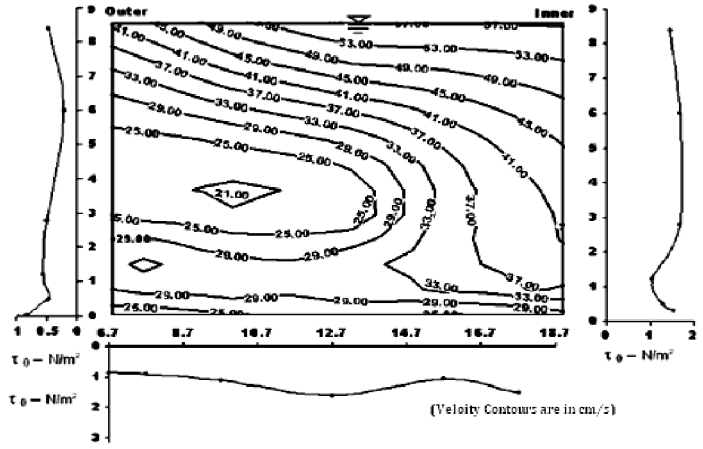

Fig. 4.6.4 Flow depth *h* = 8.55 cm (Type-III channel)

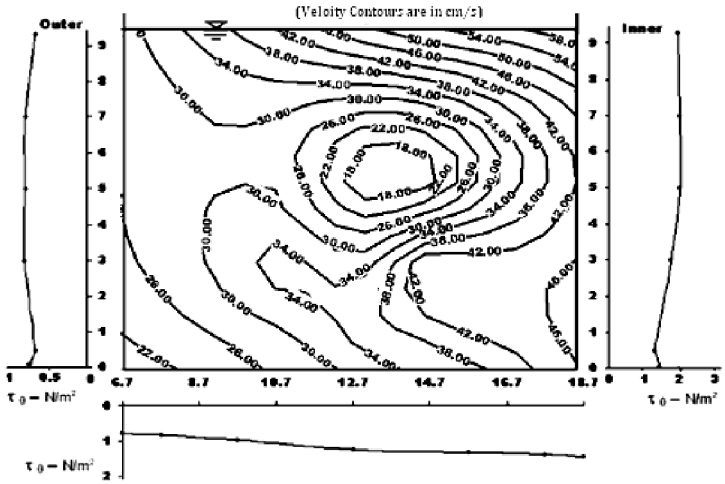

Fig. 4.6.5 Flow depth *h* = 9.34 cm (Type-III channel)

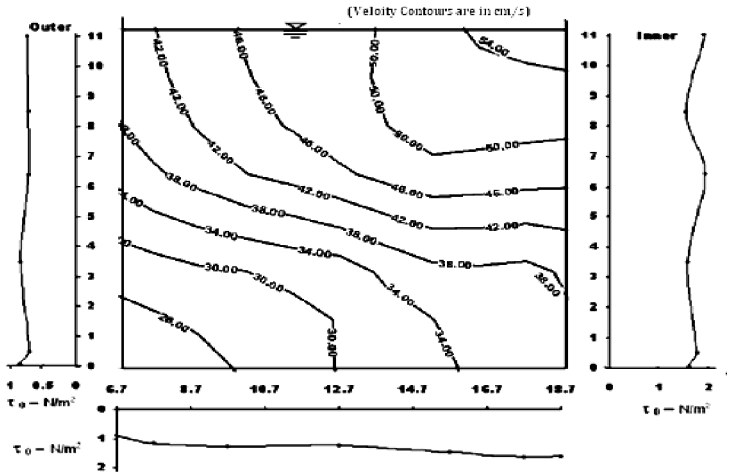

Fig. 4.6.6 Flow depth *h* = 11.01 cm (Type-III channel)

Figs. 4.6.1- 4.6.6 Contours Showing the Distribution of Tangential Velocity and Boundary Shear for Type-III Meandering Channel at Bend Apex (Section A-A)

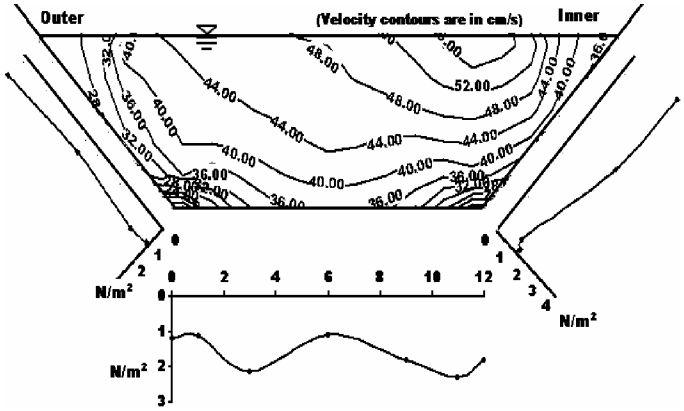

Fig. 4.7.1 Flow depth *h* = 5.3 cm (Type-IV channel)

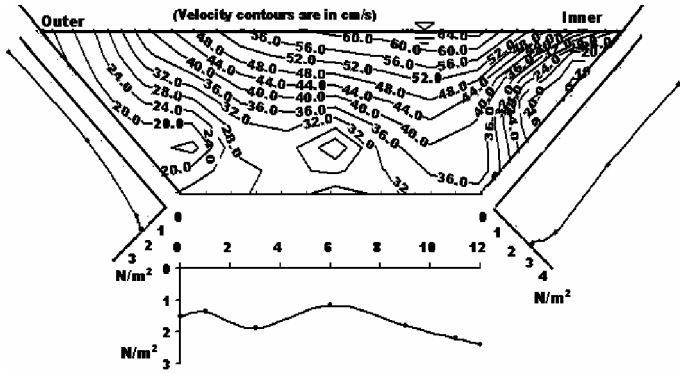

Fig. 4.7.2 Flow depth *h* = 5.62 cm (Type-IV channel)

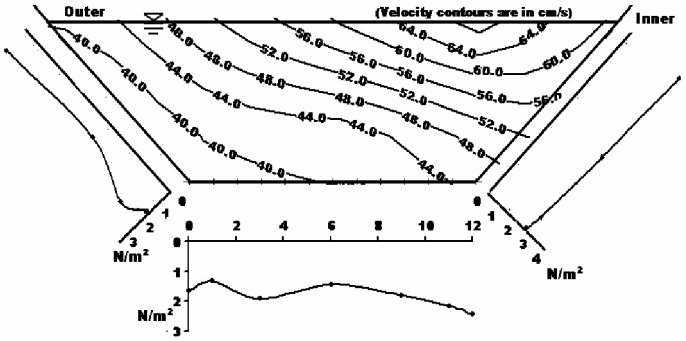

Fig. 4.7.3 Flow depth *h* = 5.93 cm (Type-IV)

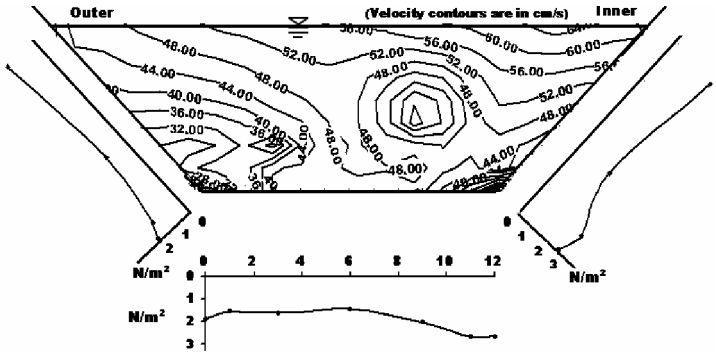

Fig. 4.7.4 Flow depth *h* = 6.18 cm (Type-IV channel)

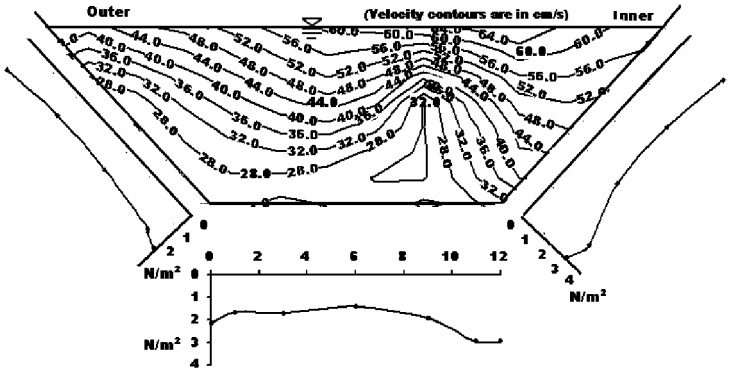

Fig. 4.7.5 Flow depth *h* = 6.71 cm (Type-IV channel)

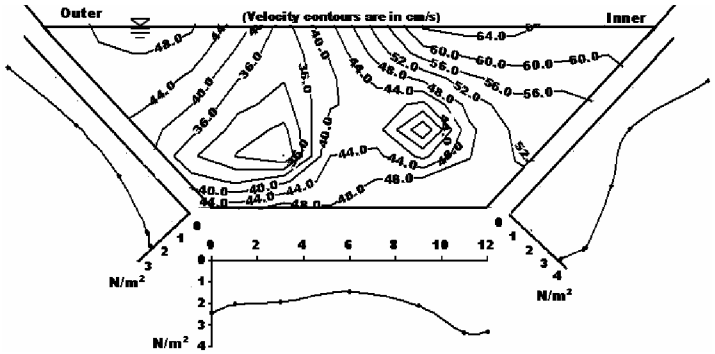

Fig. 4.7.6 Flow depth *h* = 7.33 cm (Type-IV channel)

Figs. 4.7.1 - 4.7.6 Contours Showing the Distribution of Tangential Velocity and Boundary Shear for Type-IV Meandering Channel at Bend Apex (Section AA)

4.4.1.Straight Channel

The Type-I straight channel and meandering channel Type-III are classified as deep main channel ($b/h<5$) where wall effects are felt throughout the section when compared to shallow channels. The distribution of tangential velocity in straight channels (e.g. Figs. 4.5.1 to 4.5.4) in contour form at any cross section is almost uniform in nature.

4.4.2.Meandering Channel

From the distribution of tangential velocity in meander channel sections in contour form (Figs. 4.6.1 to 4.6.6 and Figs. 4.7.1 to 4.7.6) at the locations AA the following features can be noted.

- The contours of tangential velocity distribution indicate that the velocity patterns are skewed with curvature. Higher velocity contours are found to concentrate gradually at the inner bank at the bend apex.

- Another feature is the location of the thread of maximum velocity is next to inner bank along the meander channel of experimental runs. For shallow meandering channels the thread of maximum velocity is located near the outer bank at the bend apex. It indicates that the effect of secondary circulation is predominant in shallow channels and is less effective in deep channels.

- From the contours of tangential velocity at these sections, it can be observed that the distribution of tangential velocity does not follow the power law or the logarithmic law. Under ideal conditions these theoretical velocity distribution laws gives the maximum velocity at the free water surface, where as the flow in any type of natural or laboratory channels do not show such a distribution.

- Sinuosity of the meander channel is found to affect the distribution of tangential velocity considerably. The results of channel Type-III and Type-IV (with sinuosity = 1.44 and 1.91 respectively) show irregular tangential velocity distribution. The magnitude and the concentration of velocity distribution are affected by the curvature of the meander channel. Similar reports are also seen for deep channels of Kar (1977), Das (1984), and Khatua (2008) the distribution of tangential velocity as erratic.

4.5. MEASUREMENTS OF BOUNDARY SHEAR STRESS

Wall shear stress is of great importance in fluid mechanics research, as it represents the local tangential force by the fluid on a surface in contact with it. There are several methods used to evaluate wall shear stress in an open channel. The velocity profile method is popularly used for experimental channels which are described below.

4.5.1. Velocity Profile Method

It is well established that for a regular prismatic channel under uniform flow conditions the sum of retarding boundary shear forces acting on the wetted perimeter must be equal to the resolved weight force along the direction of flow. Assuming the wall shear stress τ_0 to be constant over the entire boundary of the channel we can express τ_0 as

$$\tau_0 = \rho g R S \tag{4.1}$$

where, g = gravitational acceleration, ρ= density of flowing fluid, S = slope of the energy line, R = hydraulic radius of the channel cross section (A/P), A = area of channel cross section, and P = wetted perimeter of the channel section. From the mixing length theory, the shear stress for the turbulent flow is given as

$$\tau_0 = \rho k^2 h`^2 \left(\frac{du}{dh} \right)^2 \tag{4.2}$$

where, u = the velocity at location $h`$ from the wall, k = Von Karman's constant which has a value of approximately 0.40 for most of the flows. The shear stress τ_0 close to the boundary can be assumed to be equal to that at the boundary (τ_0), as is indeed shown to be reasonably true by measurements. Substituting, $\left(u_* = \sqrt{\frac{\tau_0}{\rho}} \right)$ in equation (4.2), integrating and taking $u = 0$ at $h` = h_o$ where, h_o is the distance from the channel bottom at which logarithmic law indicates zero velocity, the following equation results

$$\frac{u}{u_*} = \frac{1}{k} \ln\left(\frac{h`}{h_0} \right) = \frac{2.3}{k} \log\left( \frac{h`}{h_0} \right) = 5.75 \log\left(\frac{h`}{h_0} \right) \quad \text{Or} \quad u = 5.75\, u_* \log\left( \frac{h`}{h_0} \right) \tag{4.3}$$

Equation (4.3) is known as Prandtl-Karman law of velocity distribution and is generally found applicable over the entire depth of flow. In a curved channel, there is variation of the retarding shear force in the longitudinal and transverse direction and the variation is dependent on the location at the bend and the radius of curvature.

Nikuradse's experiment has enabled the evaluation $h`$ for different types of boundaries. For smooth boundary $h`= d`/107$, where as for rough boundary $h`=K_s/30$. Combining, with equation (4.3) we get,

For smooth boundary $$\frac{u}{u_*} = 5.75\log\left(\frac{hu}{v}\right) + 5.5\,8 \qquad (4.4a)$$

and for rough boundary $$\frac{u}{u_*} = 5.75\log\left(\frac{30h}{k_s}\right) = 5.75\log\left(\frac{h}{k_s}\right) + 8.5 \qquad (4.4b)$$

An indirect method to calculate the boundary shear stress is the graphical plotting of velocity distribution based on the work of Karman and Prandtl. Let u_1 and u_2 are the time averaged velocities measured at $h`_1$ and $h`_2$ heights respectively from the boundary. From the closely spaced velocity distribution observed at the vicinity of the channel bed and the wall we can take a difference of u and $h`$ between two points 1 and 2 close to each other. Substituting $u_1$, $h`_1$, u_2, and $h`_2$ in equation (4.4b), taking a finite difference and by substituting $u_* = \sqrt{\frac{\tau_0}{\rho}}$ we can write equation (4.4b) as

$$u_* = \frac{1}{5.75}\frac{u_2 - u_1}{\log_{10}(h'_2 / h'_1)} = \frac{M}{5.75} \qquad (4.4c)$$

Again by substituting $u_* = \sqrt{\frac{\tau_0}{\rho}}$ in equation (4.4b) we can rewrite it as

$$\tau_0 = \rho\left[\frac{M}{5.75}\right]^2 \qquad (4.4d)$$

where, $M = \frac{u_2 - u_1}{\log_{10}(h'_2 / h'_1)} = \frac{u_2 - u_1}{\log_{10}(h'_2) - \log_{10}(h'_1)}$ = the slope of the semi-log plot of velocity distributions near the channel bed and the wall.

Using the Micro-ADV, velocities readings close to boundary for each flow is recorded for boundary shear evaluation. Knowing the value of M (slope of the semi-logarithmic plot between distances from boundary h' against the corresponding velocity values) and using equation (4.4d), the local shear stress very close to the boundary are estimated.

4.6. DISTRIBUTION OF BOUNDARY SHEAR STRESS

Most of hydraulic formulae assume that the boundary shear stress distribution is uniform over the wetted perimeter. However, for meander channel geometry, there is a wide variation in the local shear stress distribution from point to point in the wetted perimeter. Therefore, there is a need to evaluate the shear stress carried by the channel boundary at various locations of meander path. Boundary shear stress measurements at one section of straight channel and at the bend apex of a meander path covering a number of points in the wetted perimeter have been obtained from the semi-log relationship of velocity distribution.

For each run of the experiment, shear stress distributions are found. The distribution of boundary shear along the channel perimeter for Type-II straight channel is shown in Figs. 4.5.1-4.5.4. Again, for meander channels of Type-III and Type-IV, the distribution of boundary shear along the channel perimeter at bend apex of the meander path is shown in Figs. 4.6.1-4.6.1 and Figs. 4.7.1-4.7.6. The total perimeter is marked and calculation of shear stress is carried out for both the walls and bed of the channel. The slope of the semi log-plot (*M*) close to the boundary at different points along the wetted perimeter of channels is calculated using equation (4.4d). Comparisons of mean shear obtained by the velocity distribution approach and energy gradient methods for straight and meander channels are presented in Table 4.2.

Table 4.2 Comparison of the Boundary Shear Results for Straight Channel and Meandering Channels at Bend Apex-AA

Channel Type	Run No	Flow Depth(m)	Discharge (m^3/s)	Cross Section Area (m^2)	Wetted Perimeter (m)	Overall shear Force by Energy Gradient Approach (N/m)	Overall Shear Force by Velocity Distribution Approach (N/m)
(1)	(2)	(3)	(4)	(5)	(6)	(9)	(10)
Straight Trapezoidal Channel **(Type-II,** Sinuosity =1**)**	ST1	0.052	0.00477	0.00894	0.267	0.290	0.310
	ST2	0.064	0.00696	0.01178	0.301	0.381	0.396
	ST3	0.070	0.00815	0.01330	0.318	0.431	0.459
	ST4	0.074	0.00896	0.01436	0.329	0.465	0.467
	ST5	0.078	0.00974	0.01536	0.340	0.497	0.502
Mildly Meandering Rectangular Channel **(Type-III,** Sinuosity =1.44)	MR6	0.0531	0.00236	0.00637	0.2262	0.194	0.203
	MR8	0.0608	0.00276	0.00730	0.2416	0.222	0.234
	MR10	0.0711	0.00334	0.00853	0.2622	0.260	0.273
	MR12	0.0855	0.00419	0.01026	0.2910	0.312	0.310
	MR13	0.0934	0.00466	0.01121	0.3068	0.362	0.371
	MR15	0.1101	0.00568	0.01321	0.3402	0.402	0.430
Highly Meandering Trapezoidal Channel **(Type-IV,** Sinuosity =1.91)	MT23	0.0530	0.00419	0.00917	0.2699	0.477	0.483
	MT24	0.0562	0.00486	0.00990	0.2789	0.515	0.544
	MT25	0.0593	0.00512	0.01063	0.2877	0.553	0.586
	MT26	0.0618	0.00552	0.01124	0.2948	0.584	0.610
	MT27	0.0671	0.00640	0.01255	0.3098	0.653	0.707
	MT28	0.0733	0.00755	0.01417	0.3273	0.737	0.794

For the experimental channels, the mean shear found from the velocity distribution approach agrees well with the mean value computed from energy gradient approach. The energy gradient states that the weight of water in the direction of flow in the channel is equal to the resistance offered by the channel. The following features can be noted from the figures of boundary shear distribution.

4.6.1. Straight Channel

- Symmetrical and uniform nature of boundary shear stress distribution is found for straight channel of Type-II when compared to the meandering channels of Type-III and Type-IV.
- The boundary shear at the channel junctions are generally found to be more than that compared to other points of the wetted perimeter.
- The overall mean value of boundary shear in the channel increases proportionately with the flow depth.
- Total shear carried by the wetted perimeter of the channel compares well with the energy gradient approach.

4.6.2. Meandering Channels

- On comparison of the results with straight uniform channel, it can be seen that there is asymmetrical nature of shear distribution especially where there is predominant curvature effect.
- The over all mean value of boundary shear stress obtained through the velocity distribution approach compares well with that obtained from energy gradient approach.
- Maximum value of wall shear occurs significantly below the free surface and is located at the inner walls.

4.7. ROUGHNESS COEFFICIENTS IN OPEN CHANNEL FLOW

Distribution of energy in a channel section is an important aspect that needs to be addressed properly. While using Manning's equation, selection of a suitable value of *n* is the single most important parameter for the proper estimation of velocity in an open channel. Major factors affecting Manning's roughness coefficient are the (i) surface roughness, (ii) vegetation, (iii) channel irregularity, (iv) channel alignment, (v) silting and scouring, (vi) shape and size of a channel, and (vii) stage-discharge relationship. Assuming the flow to be uniform and neglecting all non-friction losses, the energy gradient slope can be considered equal to the average longitudinal bed slope *S* of a channel. Under steady and uniform flow conditions, we use the equations proposed by Chezy, Darcy-Weisbach (1857), or Manning (1891) to compute the section mean velocity carried by a channel section proposed as

Manning's $$U=\frac{1}{n}R^{2/3}\sqrt{S} \qquad (4.5)$$

Chezy's equation $$U = C\sqrt{RS} \qquad (4.6)$$

Darcy-Weisbach's equation $$U=\sqrt{\frac{8gRS}{f}} \qquad (4.7)$$

where, A = the channel cross-sectional area, g = gravitational acceleration, R = the hydraulic mean radius of the channel section, f = the friction factor used, n = Manning's resistive coefficient, and C = Chezy's channel coefficient.

Sinuosity and slope have significant influences for the evaluation of channel discharge. The variation of resistance coefficients for the present experimental meandering channels are found to vary with depth, aspect ratio, slope and sinuosity and are all linked to the stage-discharge relationships.

Table 4.3 (a) Experimental Results for Straight Channels of Type-I and Type-II Showing *n, C* and *f* (Sinuosity=1)

(All Measurements in S.I. unit)

Channel Type	Run No	Discharge Q (m^3/sec)	Flow Depth h (m)	Channel Width b (m)	Cross Section Area (m^2)	Wetted Perimeter (m)	Average Velocity (Q/A) (m/sec)	$\sqrt{S/n}$	Manning`s Roughness *n*	Chezy`s *C*	Darcy Weisbach Friction Factor *f*
(1)	(2)	(3)	(4)	(5)	(6)	(7)	(8)	(11)	(10)	(12)	(13)
Type-I Straight Rectangular Channel Slope=0.0019	SR1	0.00106	0.030	0.12	0.0036	0.18	0.293	3.96	0.0110	47.389	0.0242
	SR2	0.00128	0.034	0.12	0.0041	0.19	0.310	3.97	0.0110	48.109	0.0235
	SR3	0.00215	0.050	0.12	0.0060	0.22	0.359	3.97	0.0110	49.987	0.0218
	SR4	0.00231	0.052	0.12	0.0063	0.22	0.367	3.98	0.0109	50.327	0.0215
	SR5	0.00290	0.062	0.12	0.0075	0.24	0.389	3.99	0.0109	51.143	0.0208
	SR6	0.00325	0.068	0.12	0.0082	0.26	0.398	3.96	0.0110	51.163	0.0208
	SR7	0.00412	0.082	0.12	0.0098	0.28	0.421	3.97	0.0110	51.950	0.0202
	SR8	0.00455	0.088	0.12	0.0106	0.30	0.430	3.96	0.0110	52.168	0.0200
	SR9	0.00506	0.096	0.12	0.0115	0.31	0.441	3.99	0.0109	52.748	0.0196
	SR10	0.00595	0.109	0.12	0.0131	0.34	0.454	3.97	0.0110	52.909	0.0194
	SR11	0.00631	0.115	0.12	0.0138	0.35	0.458	3.96	0.0110	52.953	0.0194
Type-II Straight Trapezoidal Channel Slope=0.0033	ST1	0.00477	0.052	0.12	0.0089	0.27	0.533	5.13	0.0110	50.692	0.0212
	ST2	0.00696	0.064	0.12	0.0118	0.30	0.591	5.13	0.0102	52.023	0.0201
	ST3	0.00815	0.070	0.12	0.0133	0.32	0.613	5.08	0.0112	52.140	0.0200
	ST4	0.00896	0.074	0.12	0.0144	0.33	0.624	5.04	0.0101	52.041	0.0201
	ST5	0.00974	0.078	0.12	0.0154	0.34	0.634	5.00	0.0111	51.903	0.0202

Table 4.3 (b) Experimental Results of Meandering Channel of Type-III Showing *n, C* and *f* (Sinuosity=1.44)

(All Measurements in S.I. unit)

Channel Type	Run No	Discharge Q (m^3/sec)	Flow Depth h (m)	Channel Width b (m)	Cross Section Area (m^2)	Wetted Perimeter (m)	Average Velocity (Q/A) (m/sec)	$\sqrt{S/n}$	Manning`s Roughness *n*	Chezy`s *C*	Darcy Weisbach Friction Factor *f*
(1)	(2)	(3)	(4)	(5)	(6)	(7)	(8)	(11)	(10)	(12)	(13)
Type-III Meandering Rectangular Channel Slope=0.0031	MR1	0.00032	0.013	0.12	0.0015	0.15	0.207	5.14	0.0108	43.279	0.0419
	MR2	0.00043	0.016	0.12	0.0019	0.15	0.229	5.11	0.0109	44.203	0.0401
	MR3	0.00135	0.034	0.12	0.0041	0.19	0.326	5.01	0.0111	47.561	0.0347
	MR4	0.00167	0.041	0.12	0.0049	0.20	0.343	4.93	0.0113	47.594	0.0346
	MR5	0.00220	0.050	0.12	0.0060	0.22	0.368	4.88	0.0114	48.099	0.0339
	MR6	0.00236	0.053	0.12	0.0064	0.23	0.370	4.79	0.0116	47.504	0.0347
	MR7	0.00262	0.058	0.12	0.0069	0.24	0.378	4.75	0.0117	47.433	0.0348
	MR8	0.00276	0.061	0.12	0.0073	0.24	0.378	4.68	0.0119	46.865	0.0357
	MR9	0.00295	0.064	0.12	0.0077	0.25	0.383	4.66	0.0120	46.897	0.0356
	MR10	0.00334	0.071	0.12	0.0085	0.26	0.391	4.61	0.0121	46.739	0.0359
	MR11	0.00370	0.077	0.12	0.0092	0.27	0.400	4.60	0.0121	46.966	0.0355
	MR12	0.00419	0.086	0.12	0.0103	0.29	0.408	4.56	0.0122	46.881	0.0357

Table 4.3 (c) Experimental Runs for Meandering Channel of Type-IV Showing *n*, *C* and *f* (Sinuosity=1.91)

(All Measurements in S.I. unit)

Channel Type	Run No	Discharge Q (m^3/sec)	Flow Depth h (m)	Channel Width b (m)	Cross Section Area (m^2)	Wetted Perimeter (m)	Average Velocity (Q/A) (m/sec)	$\sqrt{S/n}$	Manning`s Roughness *n*	Chezy`s *C*	Darcy Weisbach Friction Factor *f*
(2)	(1)	(3)	(4)	(5)	(6)	(7)	(8)	(9)	(10)	(11)	(12)
Type-IV Meandering Trapezoidal Channel Slope=0.003	MT1	0.00148	0.031	0.12	0.0047	0.21	0.316	5.47	0.0100	53.10	0.0278
	MT2	0.00261	0.045	0.12	0.0074	0.25	0.351	5.02	0.0109	51.09	0.0300
	MT3	0.00310	0.050	0.12	0.0085	0.26	0.364	4.94	0.0111	50.96	0.0302
	MT4	0.00372	0.056	0.12	0.0099	0.28	0.377	4.83	0.0113	50.57	0.0307
	MT5	0.00410	0.059	0.12	0.0106	0.29	0.388	4.84	0.0113	51.01	0.0301
	MT6	0.00456	0.063	0.12	0.0115	0.30	0.396	4.78	0.0115	50.78	0.0304
	MT7	0.00599	0.074	0.12	0.0144	0.33	0.418	4.66	0.0118	50.45	0.0308
Type-IV Meandering Trapezoidal Channel Slope=0.0042	MT8	0.00480	0.057	0.12	0.0101	0.28	0.476	6.04	0.0107	53.54	0.0273
	MT9	0.00533	0.061	0.12	0.0110	0.29	0.483	5.93	0.0109	52.98	0.0279
	MT10	0.00590	0.065	0.12	0.0120	0.30	0.491	5.84	0.0111	52.59	0.0284
	MT11	0.00721	0.072	0.12	0.0138	0.32	0.522	5.90	0.0110	53.81	0.0271
	MT12	0.00781	0.075	0.12	0.0146	0.33	0.534	5.92	0.0110	54.26	0.0266
	MT13	0.00864	0.078	0.12	0.0154	0.34	0.559	6.08	0.0107	56.00	0.0250
Type-IV Meandering Trapezoidal Channel Slope=0.0053	MT14	0.00029	0.011	0.12	0.0014	0.15	0.215	6.78	0.0107	42.57	0.0433
	MT15	0.00048	0.014	0.12	0.0019	0.16	0.250	6.58	0.0111	43.26	0.0419
	MT16	0.00099	0.022	0.12	0.0032	0.18	0.313	6.47	0.0113	45.18	0.0384
	MT17	0.00174	0.031	0.12	0.0047	0.21	0.368	6.34	0.0115	46.34	0.0365
	MT18	0.00205	0.034	0.12	0.0053	0.22	0.386	6.33	0.0115	46.81	0.0358
	MT19	0.00276	0.041	0.12	0.0066	0.24	0.418	6.26	0.0116	47.40	0.0349
	MT20	0.00322	0.046	0.12	0.0075	0.25	0.428	6.09	0.0120	46.70	0.0360
	MT21	0.00334	0.047	0.12	0.0077	0.25	0.431	6.07	0.0120	46.64	0.0360
	MT22	0.00370	0.049	0.12	0.0083	0.26	0.443	6.05	0.0120	46.89	0.0357
	MT23	0.00419	0.053	0.12	0.0092	0.27	0.457	6.02	0.0121	47.07	0.0354
	MT24	0.00466	0.056	0.12	0.0099	0.28	0.470	6.02	0.0121	47.37	0.0349
Type-IV Meandering Trapezoidal Channel Slope=0.008	MT28	0.00090	0.019	0.12	0.0026	0.17	0.342	7.71	0.0116	42.90	0.0426
	MT29	0.00142	0.025	0.12	0.0036	0.19	0.391	7.58	0.0118	43.78	0.0409
	MT30	0.00217	0.033	0.12	0.0050	0.21	0.437	7.38	0.0121	44.14	0.0402
	MT31	0.00486	0.051	0.12	0.0087	0.26	0.558	7.49	0.0119	47.43	0.0349
	MT32	0.00549	0.056	0.12	0.0097	0.28	0.564	7.26	0.0123	46.45	0.0363
	MT33	0.00677	0.062	0.12	0.0113	0.30	0.600	7.31	0.0122	47.41	0.0349
	MT34	0.00847	0.070	0.12	0.0133	0.32	0.637	7.31	0.0122	48.13	0.0338
Type-IV Meandering Trapezoidal Channel Slope=0.013	MT35	0.00236	0.031	0.12	0.0047	0.21	0.504	8.72	0.0131	40.65	0.0474
	MT36	0.00488	0.048	0.12	0.0080	0.25	0.613	8.53	0.0134	42.01	0.0444
	MT37	0.00541	0.051	0.12	0.0087	0.26	0.620	8.33	0.0137	41.39	0.0458
	MT38	0.00599	0.054	0.12	0.0094	0.27	0.638	8.32	0.0137	41.64	0.0452
	MT39	0.00718	0.060	0.12	0.0108	0.29	0.665	8.23	0.0138	41.74	0.0450
	MT40	0.00816	0.064	0.12	0.0118	0.30	0.693	8.31	0.0137	42.45	0.0435
	MT41	0.00948	0.070	0.12	0.0133	0.32	0.713	8.18	0.0139	42.24	0.0439
Type-IV Meandering Trapezoidal Channel Slope=0.015	MT42	0.00132	0.021	0.12	0.0030	0.18	0.445	9.50	0.0129	39.12	0.0512
	MT43	0.00274	0.033	0.12	0.0050	0.21	0.543	9.10	0.0135	39.83	0.0494
	MT44	0.00450	0.044	0.12	0.0072	0.24	0.623	9.02	0.0136	40.92	0.0468
	MT45	0.00488	0.046	0.12	0.0076	0.25	0.640	9.05	0.0135	41.30	0.0460
	MT46	0.00621	0.053	0.12	0.0092	0.27	0.677	8.92	0.0137	41.46	0.0456
	MT47	0.00811	0.062	0.12	0.0112	0.29	0.727	8.89	0.0138	42.08	0.0443
	MT48	0.00840	0.063	0.12	0.0115	0.30	0.728	8.80	0.0139	41.79	0.0449
Type-IV Meandering Trapezoidal Channel Slope=0.021	MT49	0.00129	0.019	0.12	0.0026	0.17	0.487	10.97	0.0132	37.67	0.0553
	MT50	0.00215	0.026	0.12	0.0038	0.19	0.566	10.76	0.0135	38.57	0.0527
	MT51	0.00335	0.034	0.12	0.0052	0.22	0.639	10.55	0.0137	39.15	0.0511
	MT52	0.00407	0.039	0.12	0.0062	0.23	0.656	10.10	0.0144	38.15	0.0539
	MT53	0.00545	0.046	0.12	0.0076	0.25	0.714	10.10	0.0143	38.96	0.0517
	MT54	0.00612	0.049	0.12	0.0083	0.26	0.739	10.13	0.0143	39.40	0.0505

4.7.1. Variation of Manning's *n* with Depth of Flow

The experimental results for Manning's *n* with depth of flow for channels investigated are plotted in Fig. 4.8. Manning's *n* is found to decrease with increase of aspect ratio (ratio of width of the channel to the depth of flow) indicating that meander channel consumes more energy as the depth of flow increases. So, with increase in aspect ratio Manning's *n* decreases. Manning's *n* also varies with aspect ratio for different slopes. For narrow channels the decrease in the value of *n* with depth is mainly due to the decrease of the resistance to flow and for wider channels the values of *n* increases with sinuosity and channel slope. For steeper slope Manning's *n* is less and for milder it is more. Again, for highly sinuous channels the values of *n* become large indicating that the energy loss is more for such channels.

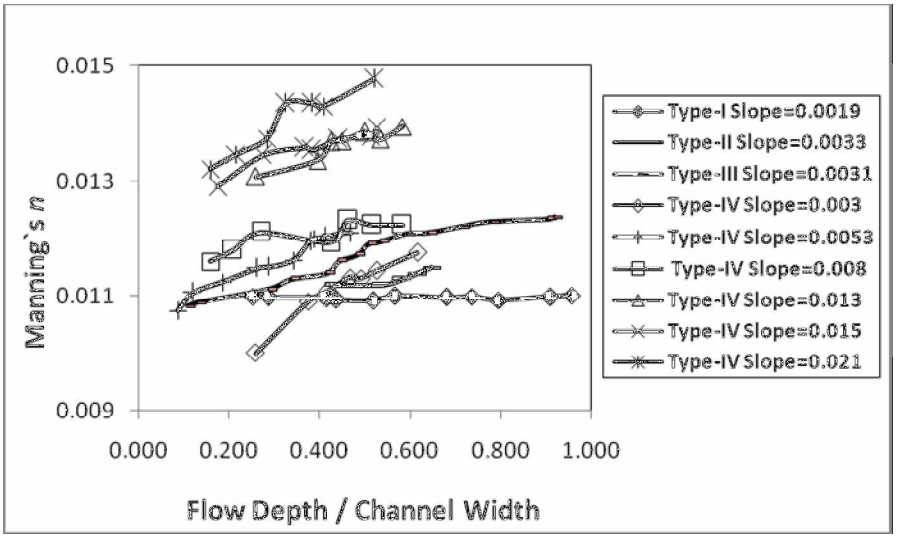

Fig. 4.8 Variation of Manning`s *n* with Flow Depth

4.7.2. Variation of Chezy`s *C* with Depth of Flow in Open Channel

The variation of Chezy's *C* with depth of flow for the channels investigated for different slopes is shown in Fig. 4.9. It can be seen from the figure that the meandering channels, exhibits a steady increase in the value of *C* with depth of flow. Chezy`s *C* is found to decrease with increase of aspect ratio indicating that the meander channel consumes more energy as the depth of flow increases. For a channel with increase in slope, the Chezy`s C is less for a particular stage.

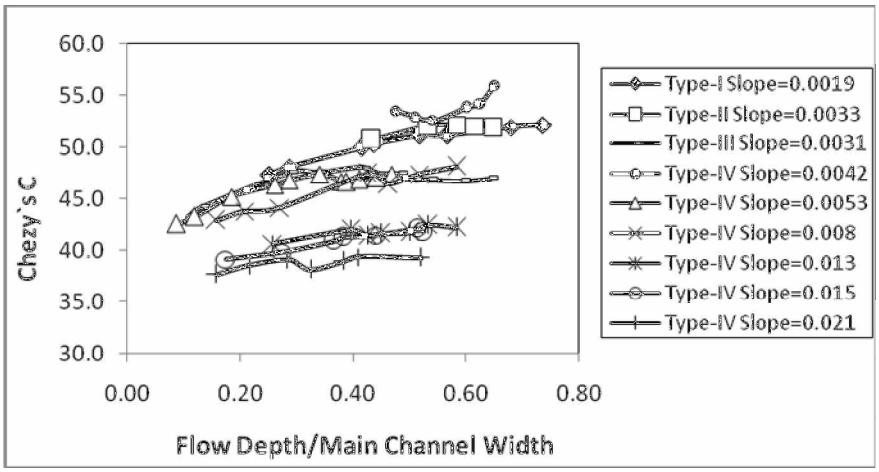

Fig. 4.9 Variation of Chezy`s *C* with Flow Depth

4.7.3. Variation of Darcy-Weisbach *f* with Depth of Flow in Open Channel

The variation of friction factor *f* with depth of flow for the straight and meandering channels are shown in Fig. 4.10. The behavioral trend of friction factor *f* is decreasing with flow depth.

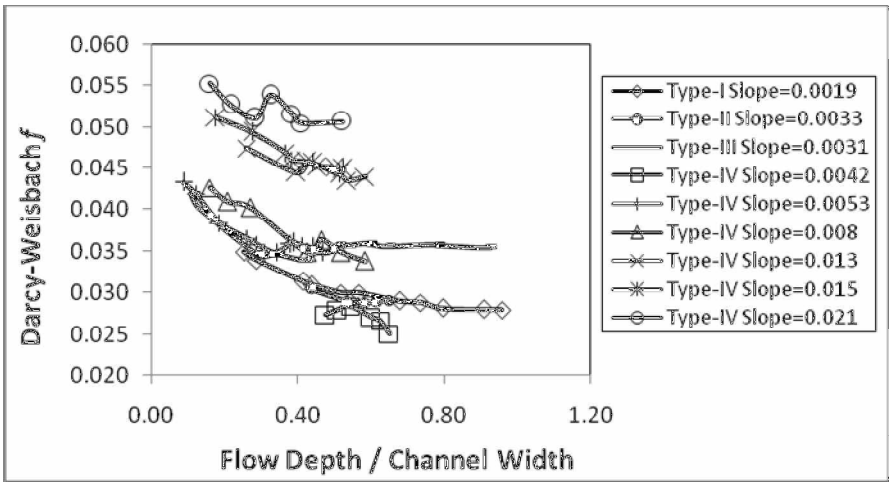

Fig. 4.10 Variation of Darcy - Weisbach *f* with Flow Depth

From the Figs. 4.8 and 4.10, it is seen that the roughness coefficients *n* and *f* are not behaving in similar manner for the experimental channels. The cause of this behavior may be due to the large variation of hydraulic radius (*R*) with depth of flow. By comparing equations 4.6 and 4.8, the relationship between the coefficients with hydraulic radius (*R*)

can be expressed as $f = \frac{8g}{R^{1/3}} n^2$. For the present study, dimensional analysis is done to evaluate the variation of roughness coefficients with depth of flow for meandering channels which is discussed in the next section. Some of the graphs have been omitted in the Figs. 4.8, 4.9 and 4.10 to maintain clarity of the graphs.

4.8. DIMENSIONAL ANALYSIS

Dimensional analysis offers a method for reducing complex physical problems to the simplest (i.e., most economical) form prior to obtaining a quantitative answer. Bridgman (1969) explains it thus: "The principal use of dimensional analysis is to deduce from a study of the dimensions of the variables in any physical system certain limitations on the form of any possible relationship between those variables. The method is of great generality and mathematical simplicity".

Accurate discharge assessment for meandering channel requires dimensional analysis. In quantitative analysis of physical events one seeks mathematical relationships between the numerical values of the physical quantities that describe the event.

A physical equation must be dimensionally homogeneous. Every correct physical equation—that is, every equation that expresses a physically significant relationship between numerical values of physical quantities—must be dimensionally homogeneous. Dimensional analysis reduces the number of variables that must be specified to describe an event.

4.8.1. Evaluation Of Roughness Coefficients

The important variables affecting the stage-discharge relationship are considered to be velocity U, hydraulic radius R, viscosity ν, gravitational acceleration g, bed slope S, sinuosity S_r, aspect ratio α, and it can be expressed functionally as,

$$\phi\{U, S, S_r, \alpha, g, R, \nu\} \qquad (4.8)$$

The dimensionless group used because of its similarity to the traditional roughness coefficient equations for one dimensional flow in a channel is expressed as

$$U = \frac{1}{n} R^{2/3} S^{1/2}$$

So,
$$\frac{UR}{\nu} = \frac{1}{n}\left(\frac{R^{10/3} S}{\nu^2}\right)^{1/2} \quad (4.9a)$$

Again, since $U = C R^{1/2} S^{1/2}$ and $U = \left(\frac{8g}{f} RS\right)^{1/2}$

=>
$$\frac{UR}{\nu} = \frac{C}{\nu} R^{3/2} S^{1/2} \quad (4.9b)$$

and
$$\frac{UR}{\nu} = \left(\frac{8}{f}\right)^{1/2}\left(\frac{gR^3 S}{\nu^2}\right)^{1/2} \quad (4.9c)$$

where, n = Manning's roughness co-efficient, C = Chezy`s roughness co-efficient and f = Darcy-Weisbach friction factor.

4.8.1.1. Derivation of Roughness Coefficients using Dimensional Analysis

Sinuosity (S_r) and is inversely related to the velocity therefore, it is in denominator. Eq. (4.8) may be rewritten in the following form as

$$\frac{UR}{\nu} = \phi\left[\frac{1}{S_r}, S, \alpha, \left(\frac{g.R^{10/3}}{\nu^2 m^{1/3}}\right)\right] \quad (4.10)$$

The dimensional group $\left(g.R^{10/3}/\nu^2 m^{1/3}\right)$ is used because of its similarity to the traditional Manning`s equation for one dimensional flow in a prismatic channel. As manning`s roughness coefficient is dimensionally non-homogenous, a length factor $m^{1/3}$ is considered to it to make it homogenous. After dimensional analysis, we obtain a relation between the parameters.

Now, $\left\{\frac{gR^{10/3}S^{1/2}}{\nu^2 m^{1/3}}\right\}$ vs. $\left\{\frac{URS_r}{\nu\alpha}\right\}$ is plotted using the new collected experimental data together with data from previously collected for meandering channel for different slopes, sinuosity, geometry etc in an attempt to find a simple relationship between the dimensionless groups for meandering channel shapes, under different hydraulic conditions.

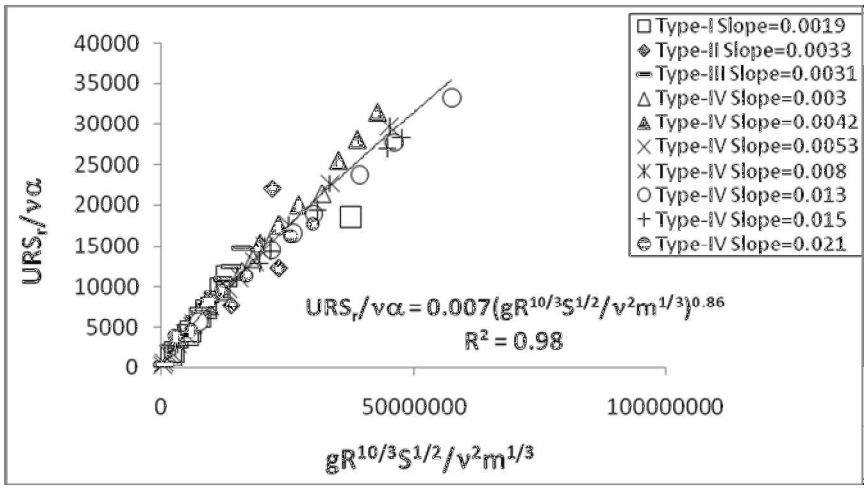

Fig. 4.11 Calibration Equation between $\left\{\frac{gR^{10/3}S^{1/2}}{\nu^2 m^{1/3}}\right\}$ and $\left\{\frac{URS_r}{\nu\alpha}\right\}$ for Manning`s *n*

After plotting between dimensionless parameters, the best possible combination is found to be given by the power equation having a regression correlation of 0.98 as,

$$\left\{\frac{URS_r}{\nu\alpha}\right\} = 7k\left\{\frac{gR^{10/3}S^{1/2}}{\nu^2 m^{1/3}}\right\}^{0.86} \tag{4.11}$$

The newly developed relationship for Manning`s *n* in a meandering channel is expressed as

Manning`s *n*
$$n = \frac{S_r \nu^{0.72} S^{0.07} m^{0.29}}{7k\alpha g^{0.86} R^{1.2}} \tag{4.12}$$

where, *k* is a constant of value 0.001found from the experiments.

Similarly, eq. (4.8) can also be rewritten for Chezy`s *C* and Darcy Weisbach *f* using dimensional analysis. Darcy Weisbach *f* is a dimensionally homogenous but Chezy`s *C* is dimensionally non-homogenous. So, the dimensional group $(g.R^3/\nu^2)$is used because of its similarity to the traditional Chezy`s equation for one dimensional flow in a prismatic channel. Both give similar equation which is expressed as

$$\frac{UR}{\nu} = \phi\left[\frac{1}{S_r}, S, \alpha, \left(\frac{gR^3}{\nu^2}\right)\right] \tag{4.13}$$

Then, $\left\{\frac{gR^3S^{1/2}}{\nu^2}\right\}$ vs. $\left\{\frac{URS_r}{\nu\alpha}\right\}$ is plotted using the new collected experimental data together with data from previously collected for meandering channel for different slopes etc, in an attempt to find a simple relationship between the dimensionless groups for meandering channel shapes, under different hydraulic conditions.

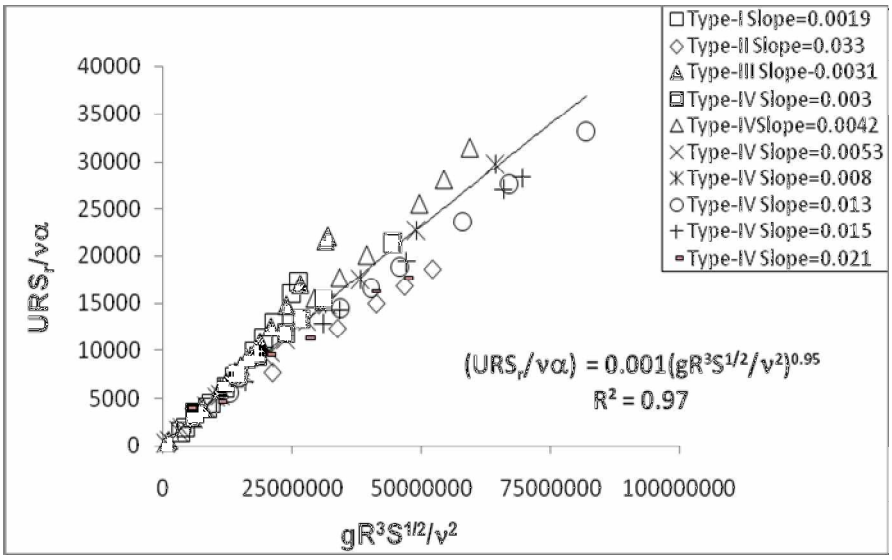

Fig. 4.12 Calibration Equation for between $\left\{\frac{gR^3S^{1/2}}{\nu^2}\right\}$ and $\left\{\frac{URS_r}{\nu\alpha}\right\}$ for Derivation of Chezy`s *C* and Darcy Weisbach *f*

After plotting between dimensionless parameters, the best possible condition is found to be given by the power equation having a regression correlation of 0.97 is,

$$\left\{\frac{URS_r}{\nu\alpha}\right\} = k \times \left\{\frac{gR^3S^{1/2}}{\nu^2}\right\}^{0.86} \tag{4.14}$$

Using he relation obtained from equation (4.14) and equation (4.9b), the newly developed relationship for Chezy`s *C* in a meandering channel is expressed as

Chezy`s C $$C = k \times \frac{g^{0.95} R^{1.35} \alpha}{S^{0.02} \nu^{0.9} S_r} \tag{4.15}$$

where *k* is a constant of value 0.001found from the experiments.

Again, from equation (4.14) and equation (4.9c), a relationship for Darcy Weisbach f is developed which is expressed as

Darcy-Weisbach f $$f = \frac{8\nu^{1.8} S_r^{2} S^{0.04}}{0.01^{2} \alpha^{2} R^{2.7} g^{0.9}} \quad (4.16)$$

Thus the newly developed equations of roughness coefficients as obtained from equations 4.12, 4.15 and 4.16 can be summarized as

Manning`s n $$n = \frac{S_r \nu^{0.72} S^{0.07} m^{0.29}}{7 k \alpha g^{0.86} R^{1.2}}$$

Chezy`s C $$C = k \times \frac{g^{0.95} R^{1.35} \alpha}{S^{0.02} \nu^{0.9} S_r}$$

Darcy Weisbach f $$f = \frac{8\nu^{1.8} S_r^{2} S^{0.04}}{0.01^{2} \alpha^{2} R^{2.7} g^{0.9}}$$

Here, k is a constant of value 0.001found from the experiments.

4.9. DISCHARGE ESTIMATION USING THE PRESENT APPROACH

For the given geometry of channels, the values of n, c and f are calculated using the equations (4.12), (4.15) and (4.16). Then, the corresponding discharge can be easily calculated. Graphs are plotted using the above mentioned equations, showing the variations of observed and calculated (modeled) discharge in Figs. 4.13(a), 4.13(b) and 4.13(c) for Manning`s $n$, Chezy`s C and Darcy Weisbach f, respectively.

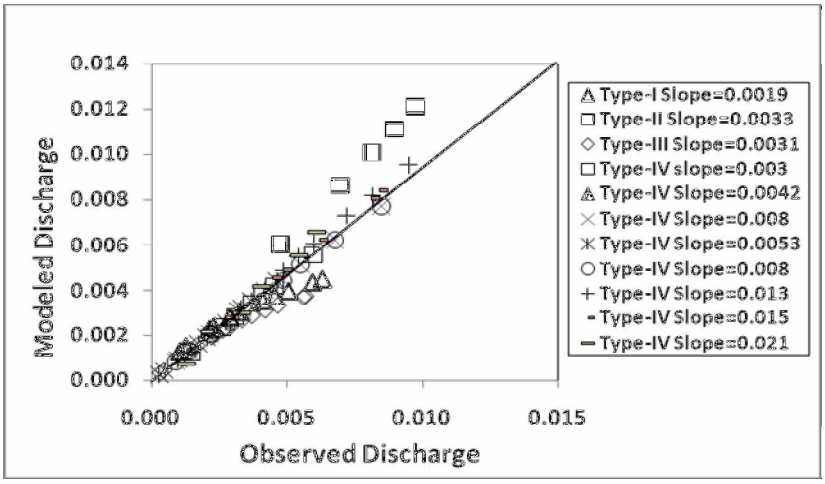

Fig. 4.13 (a) Variation of Observed and Modeled Discharge Using Manning`s *n*

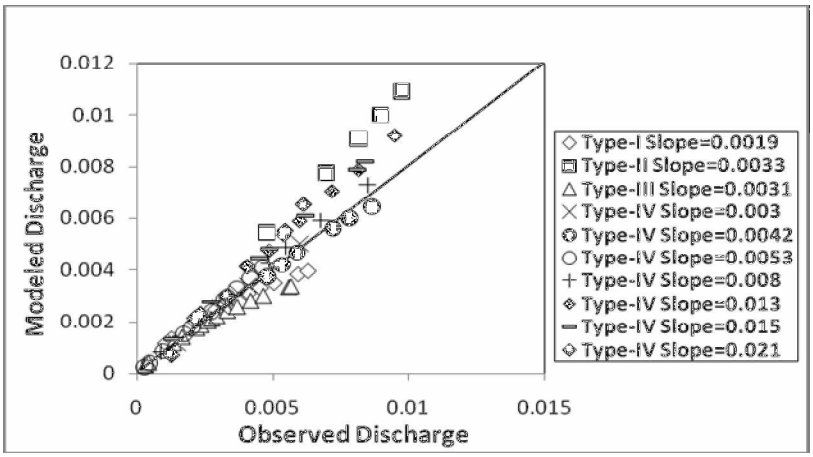

Fig. 4.13 (b) Variation of Observed and Modeled Discharge Using Chezy`s *C*

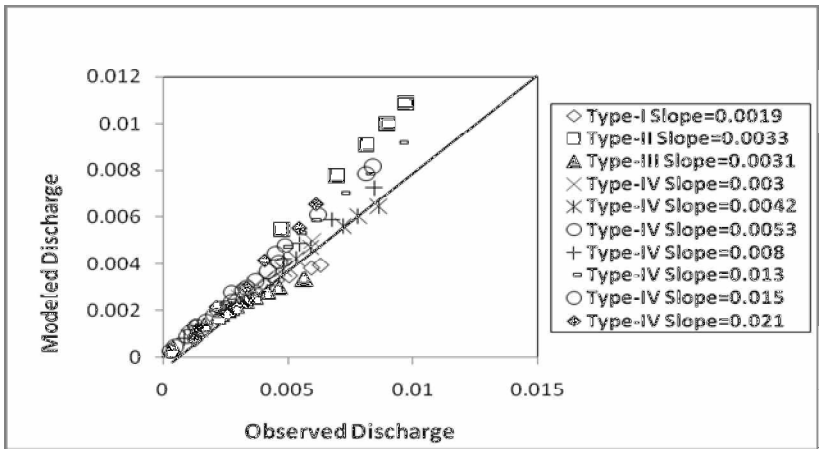

Fig. 4.13 (c) Variation of Observed and Modeled Discharge Using Darcy Weisbach *f*

From the figures 4.13 (a, b, c) it is clear that the present formulation gives better results. The calculated (modeled) discharge using the newly developed equations of manning`s *n*, Chezy`s *C* and Darcy-Weisbach *f* from equations 4.12, 4.15 and 4.16 respectively, is in good agreement with the observed value. The calculated discharge for the meandering channels of Type-III and Type-IV are more close to the observed value.

4.10. APPLICATION OF OTHER METHODS TO THE PRESENT CHANNEL

Some published approaches of discharge estimation for meandering flow are discussed and applied to the experimental data of the present very wide and highly sinuous channels to know their suitability for such geometry. The standard error of estimation of discharge by the present equation is compared well with some of the methods of other investigators which are shown in Fig. 4.14(a), 4.14(b) and 4.14(c) for *n*, *C* and *f*, respectively.

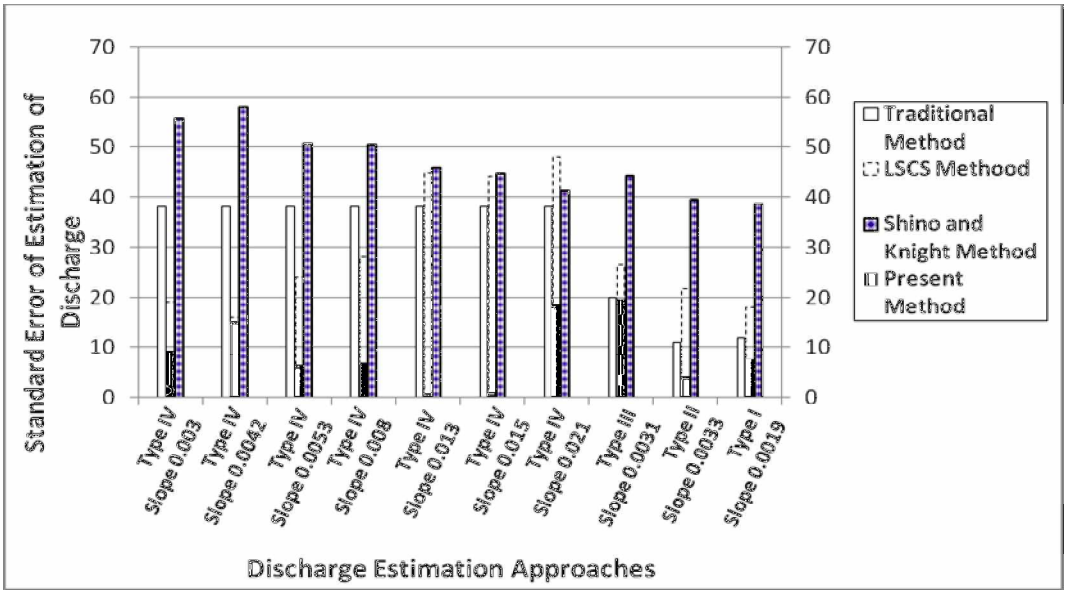

Fig. 4.14 (a) Standard Error of Estimation of Discharge using Proposed Manning`s Equation and other established Methods

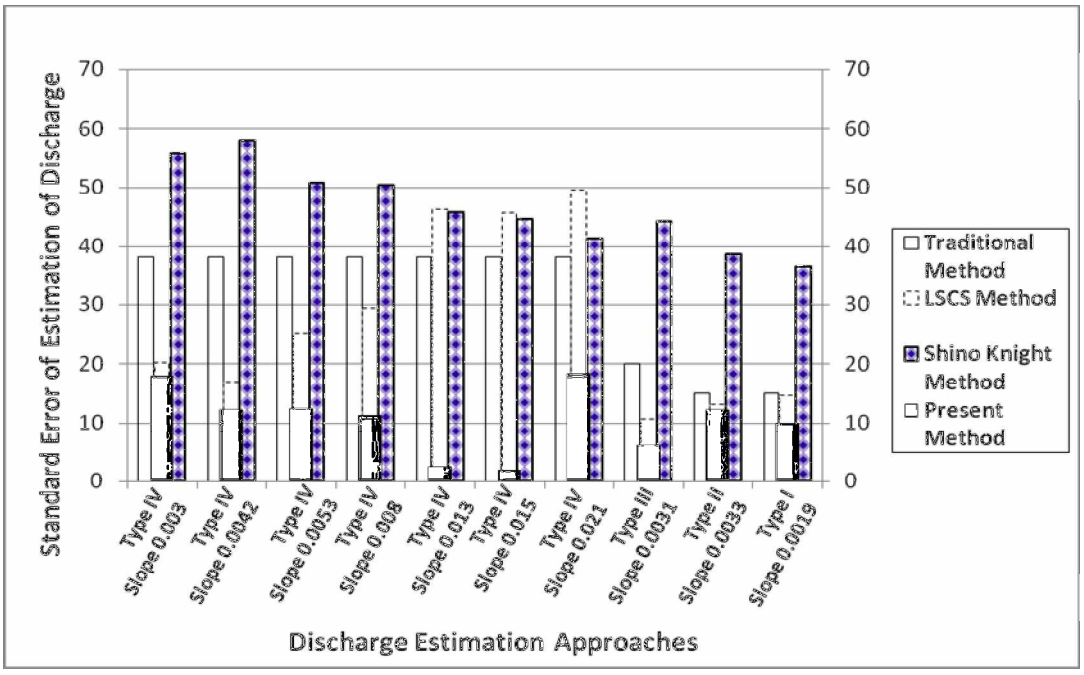

Fig. 4.14(b) Standard Error of Estimation of Discharge using Proposed Chezy`s Equation other established Methods

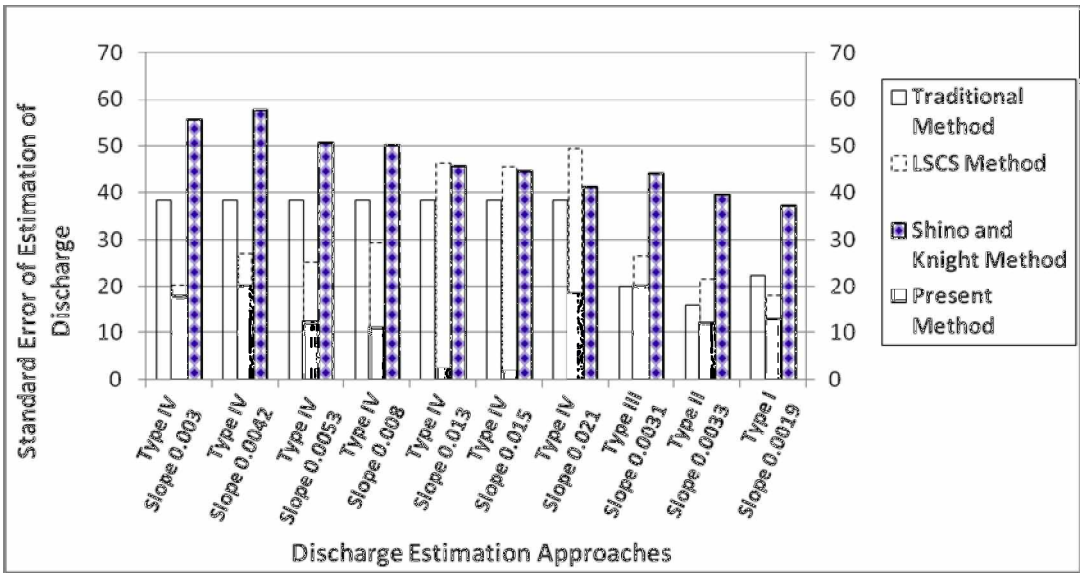

Fig. 4.14(c) Standard Error of Estimation of Discharge using Proposed Darcy Weisbach *f* and other established Methods

From Fig. 4.14 (a) the overall standard error of discharge from the proposed method using Manning`s *n* is 14.39 whereas, it is 30.04 for LSCS method, closely followed by the traditional method with standard error of 31.32 and the Shino Knight method with a value of 46.9. Similarly, from Fig. 4.14 (b) the overall standard error of discharge for the proposed method using Chezy`s *C* is 18.08 compared to 28.5 for LSCS method. In this case, the conventional method gives standard error of 31.32 followed by Shino and Knight method with standard error of 46.9. Further using Darcy Weisbach *f* for discharge calculation, the standard error for the present method is 18.07. This is in comparison to 20.79 for conventional method, 29.79 and 46.8 for LSCS and the Shino Knight method, respectively (Fig. 4.14 c). From the Figs. 4.14(a, b, c), it reveals that the proposed approach gives better discharge results as compared to other approaches for the present experimental channels.

4.11. BOUNDARY SHEAR DISTRIBUTION IN MEANDERING CHANNEL

Information regarding the nature of boundary shear stress distribution is needed to solve a variety of river hydraulics and engineering problems such as to give a basic understanding of the flow resistance relationship, to understand the mechanism of sediment transport, to design stable channels, revetments etc. The tractive force is commonly used to describe the average shear of the flow exerted on the wetted perimeter.

The complex three-dimensional flow structures in a channel leads to a complicated patterns of boundary shear stress distribution and becomes even more complicated when the channel is meandering. One line of approach to predict the distribution around the wetted perimeter of a given channel for a certain flow rate is from a theoretical approach, concerning a detailed knowledge of the distribution of numerous turbulence coefficients. The other one is to adopt an empirical approach, fitting equations to the data obtained. The first step of in deducing an empirical approach would be to obtain equations for the mean boundary shear stress or force on particular boundary elements. Then, it would be possible to fit equations for the local variations around the mean on a particular boundary element. This has been attempted many investigators as Knight (1981), Knight and Hamed (1984), Knight and Patel (1985), Patra (1999), Khatua (2008), Kean et al. (2009) etc.

The percentage of the total shear force carried by the walls ($\%SF_W$) is a useful parameter expressed as $\%SF_W = (100\ SF_W) / SF$. Similarly, the percentage of the total shear force carried by the bed, given as $\%SF_B = (100\ SF_B) / SF$, where $\%SF_W$ =Percentage of shear force which is carried by the walls, $\%SF_B$= percentage of shear force carried by the base and SF= total shear force.

Some of the works of previous investigators are like Ghosh and Roy (1970), Myers (1978) and Noutsopoulos and Hadjipanos (1982), etc in smooth rectangular channels, Patel (1984) and in smooth rectangular ducts in smooth trapezoidal channels with 45° side walls slope, and with uniformly roughened trapezoidal channels. They have used experimental data either for uniformly roughened or smooth trapezoidal channels by the use of duct and open channel flow data together. The $\%SF_W$ values show a systematic reduction with increase in aspect ratio ($\alpha = b/h$), typical of an exponential function first proposed by Knight (1981).

Knight *et.al* (1981, 1984) showed that for a straight channel the % of shear in wall $\%SF_W$ varied exponentially with the aspect ratio [i.e.$\alpha = b/h$)]. It can be expressed as

$$\%SF_w = e^m \tag{4.17}$$

By plotting separately to log-log scales and assuming a simpler linear relationship between $\%SF_w$ and ($\alpha = b/h$), we have

$$\log_{10}(\%\ SF_w) = 1.4026\ \log_{10}(\frac{b}{h} + 3) + 2.67 \tag{4.18}$$

Comparing equation 4.17 and 4.18 we can write

$$m = 2.30259\,[A_1 Log_{10}\left(\frac{b}{h} + A_2\right) + A_3] \quad \text{or} \quad m = -3.23\,Log_{10}(\alpha + 3) + 6.146 \qquad (4.19)$$

It proves that m is a function of the aspect ratio [i.e. $m = F(b/h) = F(\alpha)$].

Table 4.4(a) Summary of Experimental Results Showing Overall Shear Stress in Straight Channels of Type-I and II (Sinuosity=1)

Channel Type	Run No	Discharge Q (m^3/s)	Flow Depth h (m)	Channel Width (m)	Cross Section Area (m^2)	Wetted Perimeter (m)	Average Velocity (m/s)	Overall Mean Shear Stress (N/m^2)
(1)	(2)	(3)	(4)	(5)	(6)	(7)	(8)	(9)
Type-I Straight Rectangular Channel Slope=0.0019	SR1	0.00106	0.030	0.12	0.0036	0.18	0.293	0.37
	SR 2	0.00128	0.034	0.12	0.0041	0.19	0.310	0.41
	SR3	0.00215	0.050	0.12	0.0060	0.22	0.359	0.51
	SR4	0.00231	0.052	0.12	0.0063	0.22	0.367	0.52
	SR5	0.00290	0.062	0.12	0.0075	0.24	0.389	0.57
	SR6	0.00325	0.068	0.12	0.0082	0.26	0.398	0.59
	SR7	0.00412	0.082	0.12	0.0098	0.28	0.421	0.64
	SR8	0.00455	0.088	0.12	0.0106	0.30	0.430	0.67
	SR9	0.00506	0.096	0.12	0.0115	0.31	0.441	0.69
	SR10	0.00595	0.109	0.12	0.0131	0.34	0.454	0.72
	SR11	0.00631	0.115	0.12	0.0138	0.35	0.458	0.73
Type-II Straight Trapezoidal Channel Slope=0.0033	ST1	0.00477	0.052	0.12	0.0089	0.27	0.533	1.08
	ST2	0.00696	0.064	0.12	0.0118	0.30	0.591	1.27
	ST3	0.00815	0.070	0.12	0.0133	0.32	0.613	1.35
	ST4	0.00896	0.074	0.12	0.0144	0.33	0.624	1.41
	ST5	0.00974	0.078	0.12	0.0154	0.34	0.634	1.46

Table 4.4(b) Summary of Experimental Results Showing Overall Shear Stress in Meandering Channel of Type-III (Sinuosity=1.44)

Channel Type	Run No	Discharge Q (m^3/s)	Flow Depth h (m)	Channel Width (m)	Cross Section Area (m^2)	Wetted Perimeter (m)	Average Velocity (m/s)	Overall Mean Shear Stress (N/m^2)
(1)	(2)	(3)	(4)	(5)	(6)	(7)	(8)	(9)
Type-III Meandering Rectangular Channel Slope= 0.0031	MR1	0.00032	0.013	0.12	0.0015	0.15	0.207	0.32
	MR 2	0.00043	0.016	0.12	0.0019	0.15	0.229	0.38
	MR 3	0.00135	0.034	0.12	0.0041	0.19	0.326	0.66
	MR 4	0.00167	0.041	0.12	0.0049	0.20	0.343	0.74
	MR 5	0.00220	0.050	0.12	0.0060	0.22	0.368	0.83
	MR 6	0.00236	0.053	0.12	0.0064	0.23	0.370	0.86
	MR 7	0.00262	0.058	0.12	0.0069	0.24	0.378	0.90
	MR 8	0.00276	0.061	0.12	0.0073	0.24	0.378	0.92
	MR 9	0.00295	0.064	0.12	0.0077	0.25	0.383	0.94
	MR 10	0.00334	0.071	0.12	0.0085	0.26	0.391	0.99
	MR 11	0.00370	0.077	0.12	0.0092	0.27	0.400	1.03
	MR 12	0.00419	0.086	0.12	0.0103	0.29	0.408	1.07
	MR 13	0.00466	0.093	0.12	0.0112	0.31	0.415	1.11
	MR 14	0.00560	0.109	0.12	0.0130	0.34	0.429	1.18
	MR 15	0.00568	0.110	0.12	0.0132	0.34	0.430	1.18

Table 4.4(c) Summary of Experimental Results Showing Overall Shear Stress in Meandering Channel of Type-IV (Sinuosity=1.91)

Channel Type	Run No	Discharge Q (m^3/s)	Flow Depth h (m)	Channel Width (m)	Cross Section Area (m^2)	Wetted Perimeter (m)	Average Velocity (m/s)	Overall Mean Shear Stress (N/m^2)
(1)	(2)	(3)	(4)	(5)	(6)	(7)	(8)	(9)
Type-IV Meandering Trapezoidal Channel Slope=0.003	MT1	0.00148	0.031	0.12	0.0047	0.21	0.316	0.66
	MT2	0.00261	0.045	0.12	0.0074	0.25	0.351	0.88
	MT3	0.00310	0.050	0.12	0.0085	0.26	0.364	0.96
	MT4	0.00372	0.056	0.12	0.0099	0.28	0.377	1.04
	MT5	0.00410	0.059	0.12	0.0106	0.29	0.388	1.08
	MT6	0.00456	0.063	0.12	0.0115	0.30	0.396	1.14
	MT7	0.00599	0.074	0.12	0.0144	0.33	0.418	1.28
Type-IV Meandering Trapezoidal Channel Slope=0.0042	MT8	0.00480	0.057	0.12	0.0101	0.28	0.476	1.48
	MT9	0.00533	0.061	0.12	0.0110	0.29	0.483	1.56
	MT10	0.00590	0.065	0.12	0.0120	0.30	0.491	1.63
	MT11	0.00721	0.072	0.12	0.0138	0.32	0.522	1.76
	MT12	0.00781	0.075	0.12	0.0146	0.33	0.534	1.81
	MT13	0.00864	0.078	0.12	0.0154	0.34	0.559	1.87
Type-IV Meandering Trapezoidal Channel Slope=0.0053	MT15	0.00048	0.014	0.12	0.0019	0.16	0.250	0.63
	MT16	0.00099	0.022	0.12	0.0032	0.18	0.313	0.90
	MT17	0.00174	0.031	0.12	0.0047	0.21	0.368	1.18
	MT18	0.00205	0.034	0.12	0.0053	0.22	0.386	1.27
	MT19	0.00276	0.041	0.12	0.0066	0.24	0.418	1.45
	MT20	0.00322	0.046	0.12	0.0075	0.25	0.428	1.57
	MT21	0.00334	0.047	0.12	0.0077	0.25	0.431	1.60
	MT22	0.00370	0.049	0.12	0.0083	0.26	0.443	1.67
	MT23	0.00419	0.053	0.12	0.0092	0.27	0.457	1.77
	MT24	0.00466	0.056	0.12	0.0099	0.28	0.470	1.85
	MT25	0.00552	0.062	0.12	0.0112	0.29	0.491	1.98
	MT26	0.00640	0.067	0.12	0.0126	0.31	0.509	2.11
	MT27	0.00755	0.073	0.12	0.0142	0.33	0.533	2.25
Type-IV Meandering Trapezoidal Channel Slope=0.008	MT28	0.00090	0.019	0.12	0.0026	0.17	0.342	1.19
	MT29	0.00142	0.025	0.12	0.0036	0.19	0.391	1.49
	MT30	0.00217	0.033	0.12	0.0050	0.21	0.437	1.84
	MT31	0.00486	0.051	0.12	0.0087	0.26	0.558	2.59
	MT32	0.00549	0.056	0.12	0.0097	0.28	0.564	2.76
	MT33	0.00677	0.062	0.12	0.0113	0.30	0.600	3.00
	MT34	0.00847	0.070	0.12	0.0133	0.32	0.637	3.28
Type-IV Meandering Trapezoidal Channel Slope=0.013	MT35	0.00236	0.031	0.12	0.0047	0.21	0.504	2.87
	MT36	0.00488	0.048	0.12	0.0080	0.25	0.613	3.99
	MT37	0.00541	0.051	0.12	0.0087	0.26	0.620	4.21
	MT38	0.00599	0.054	0.12	0.0094	0.27	0.638	4.39
	MT39	0.00718	0.060	0.12	0.0108	0.29	0.665	4.75
	MT40	0.00816	0.064	0.12	0.0118	0.30	0.693	4.99
	MT41	0.00948	0.070	0.12	0.0133	0.32	0.713	5.33
Type-IV Meandering Trapezoidal Channel Slope=0.015	MT42	0.00132	0.021	0.12	0.0030	0.18	0.445	2.43
	MT43	0.00274	0.033	0.12	0.0050	0.21	0.543	3.48
	MT44	0.00450	0.044	0.12	0.0072	0.24	0.623	4.34
	MT45	0.00488	0.046	0.12	0.0076	0.25	0.640	4.49
	MT46	0.00621	0.053	0.12	0.0092	0.27	0.677	5.00
	MT47	0.00811	0.062	0.12	0.0112	0.29	0.727	5.59
	MT48	0.00840	0.063	0.12	0.0115	0.30	0.728	5.69
Type-IV Meandering Trapezoidal Channel Slope=0.021	MT49	0.00129	0.019	0.12	0.0026	0.17	0.487	3.13
	MT50	0.00215	0.026	0.12	0.0038	0.19	0.566	4.04
	MT51	0.00335	0.034	0.12	0.0052	0.22	0.639	4.99
	MT52	0.00407	0.039	0.12	0.0062	0.23	0.656	5.55
	MT53	0.00545	0.046	0.12	0.0076	0.25	0.714	6.29
	MT54	0.00612	0.049	0.12	0.0083	0.26	0.739	6.60
	MT55	0.00922	0.063	0.12	0.0114	0.30	0.809	7.92

The overall summary of the experiments runs concerning the distribution of shear force and boundary shear stress are presented in Table 4.4 (a) for Type-I and Type-II, Table 4.4 (b) for Type-III and Table 4.4 (c) for Type-IV channels respectively.

4.11.1. Analysis of Boundary Shear Results in Meandering Channels

For the present analysis, the published meandering channel data of Patra (1999) along with the current meandering channel data are used. Patra (1999) provided shear force data of two types of meandering channel having smooth and rough surfaces having sinuosity (S_r) 1.21 and 1.22 and aspect ratios varying from α =1.01 to 2.45. Now for the four types of meandering channels having sinuosity 1.21, 1.22, 1.44 and 1.91, the variation of wall shear with aspect ratio and sinuosity are shown in Fig. 4.15 (a, b) respectively.

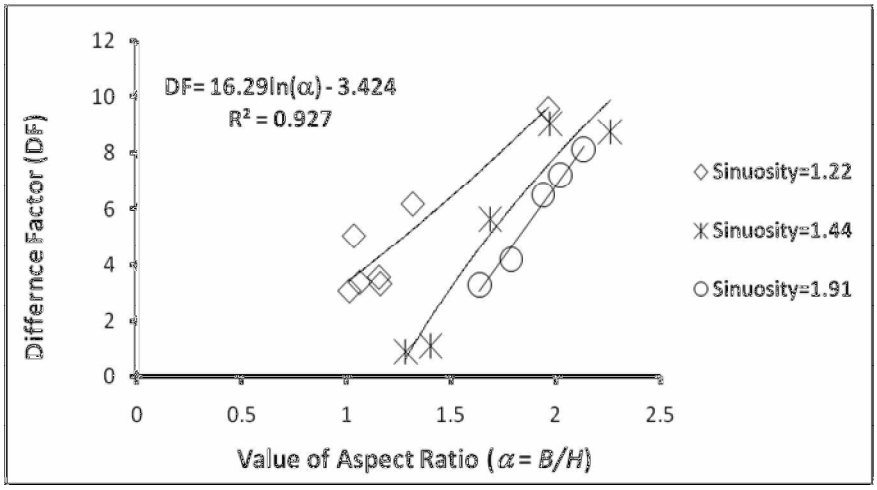

Fig. 4.15 (a) Variation of Percentage of Wall Shear with Aspect Ratio

In the Fig. 4.15(a), it is observed that the difference factor (DF) curves of the observed three channels remains almost parallel. The nature of variations of difference factor (DF) with respect to aspect ratio is same for all channels, irrespective of the difference in their sinuosity. Again, the plots in Fig 4.15 (b) show that the change in difference factor (DF) for channels having higher sinuosity is very small, irrespective of the change in geometry (aspect ratio) where as, there is a wide change in difference factor for channels of low sinuosity. The best fit relationship for the difference factor with aspect ratio is obtained from Fig. 4.15 (a) and with sinuosity is obtained from Fig 4.15 (b).

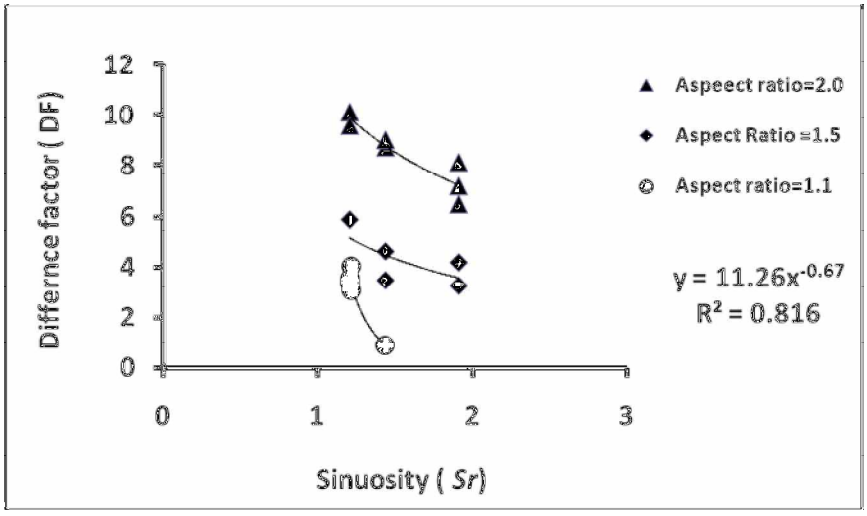

Fig. 4.15 (b) Variation of Percentage of Wall Shear with Sinuosity

For meandering channel the distribution of shear is complicated as compared to that of a straight channel. From Fig. 4.15 (a, b) it is clear that wall shear increases with channel aspect ratio ($b/h = \alpha$) and decreases with sinuosity (S_r), which are the most significant parameter influencing the flow mechanism in meandering channels.

The best fit functional relationships of the difference factor with the parameters obtained from the plots (Fig. 4.15 a, b) is given as

$$\text{Difference factor} = F_1(S_r^{-0.67}) \text{ and } F_2 \ln(30.692 \times \alpha) \tag{4.20}$$

Combining all the dependable parameters the difference factor is composited as

$$\text{Difference factor} = 2.15 S_r^{-0.67} Ln(30.692 \times \alpha) \tag{4.21}$$

Equation (4.17) is further modified to incorporate meandering effect and is written as

$$\%SF_W = e^m + 2.15 S_r^{-0.67} Ln(30.692 \times \alpha) \tag{4.22}$$

where, $m = -3.23 Log_{10}(\alpha + 3) + 6.146$

The percentage of wall shear is calculated for Type-III and Type-IV channels, and the two channels of Patra (1999) (S_r= 1.21 and 1.22) using (4.22) and the results are presented in Table 4.5 and Table 4.6, respectively. The calculated values are compared with the actual value and the percentages of error for SF_W for all the channels are given in Table 4.5 and Table 4.6.

Table 4.5 Results of Experimental Data for Boundary Shear Distribution in Type-III and Type-IV Meandering Channels

Expt. Runs	Sinuosity	Discharge (cm^3/sec)	Flow Depth h (cm)	α= b/h	Total shear stress (N/m^2)	SF1	SF2	SF3	% SF_w (Actual)	% SF_w (calculated from eq. 4.27)	% of error for % SF_w
(1)	(2)	(3)	(4)	(5)	(6)	(7)	(8)	(9)	(10)	(11)	(12)
MR6	1.44	2357	5.31	2.260	0.857	0.02	0.11	0.10	52.647	52.618	-0.057
MR8	1.44	2757	6.08	1.974	0.918	0.03	0.10	0.11	58.214	56.103	-3.627
MR10	1.44	3338	7.11	1.688	0.990	0.03	0.11	0.13	58.087	60.099	3.464
MR12	1.44	4191	8.55	1.404	1.072	0.04	0.19	0.23	58.352	64.691	10.863
MR13	1.44	4656	9.34	1.285	1.111	0.08	0.15	0.16	61.735	66.823	8.241
MT23	1.91	4656	5.62	2.135	1.257	0.10	0.24	0.20	55.165	52.864	-4.171
MT24	1.91	5122	5.93	2.024	1.286	0.13	0.25	0.21	57.264	54.262	-5.243
MT25	1.91	5515	6.18	1.942	1.308	0.14	0.25	0.23	59.420	55.335	-6.875
MT26	1.91	6396	6.71	1.788	1.352	0.17	0.30	0.24	57.187	57.465	0.486
MT27	1.91	7545	7.33	1.637	1.397	0.19	0.34	0.26	57.557	59.731	3.778

Table 4.6 Results of Experimental Data of Kar (1977) and Das (1984) (from Patra, 1999)

Expt. Runs/ Sinuosity	Discharge (cm^3/sec)	Flow Depth (cm)	Aspect Ratio α= b/h	Total shear stress (N/m^2)	By Integration Method			% SF_w (Actual)	% SF_w (calculated from eq. 4.27)	% of error for % SF_w
					SF1	SF2	SF3			
(1)	(2)	(3)	(4)	(5)	(6)	(7)	(8)	(9)	(10)	(11)
1.21(smooth)	750	4.08	2.451	0.882	4.90	10.00	5.71	51.475	51.434	-0.081
1.21(rough)	750	4.08	2.451	0.882	3.69	8.50	4.10	47.821	51.434	7.555
1.21(smooth)	1088	5.09	1.965	0.990	8.14	13.00	10.18	58.498	57.075	-2.434
1.21(rough)	1088	5.2	1.923	1.000	4.95	10.00	11.00	61.464	57.619	-6.256
1.21(smooth)	2350	7.59	1.318	1.183	12.14	20.00	22.77	63.579	66.992	5.367
1.21(rough)	2350	7.61	1.314	1.184	7.70	11.00	13.86	66.216	67.054	1.266
1.21(rough)	2960	8.6	1.163	1.241	9.46	13.00	16.34	66.495	69.906	5.131
1.21(smooth)	2960	8.65	1.156	1.243	15.57	21.00	26.82	66.869	70.039	4.740
1.21(smooth)	3300	9.4	1.064	1.281	16.92	22.00	31.96	68.962	71.906	4.269
1.22(rough)	1400	7.45	1.342	1.790	14.53	17.70	12.67	60.572	66.509	9.800
1.22(smooth)	1400	7.52	1.330	1.797	18.80	13.00	7.52	66.938	66.732	-0.307
1.22(smooth)	3000	9.85	1.015	1.985	24.63	19.00	18.72	69.522	72.893	4.849
1.22(rough)	3000	9.65	1.036	1.971	19.30	20.50	30.88	70.996	72.446	2.043

The variation of computed percentage of wall shear force of wetted perimeter, using equation (4.22), with the observed value of Type-III, Type-IV and that of Patra is shown in Fig. 4.16. The graph shows comparisons between the calculated and observed values. The calculated value is in good agreement with the observed value, irrespective of the variations in the aspect ratios.

Again, the variation of computed percentage of shear force error at the wall perimeter with the observed value of all these meandering channels are plotted in Fig. 4.17. The plot gives the percentage of error in predicting the SF_w distribution vs.

different flow depths (aspect ratio). From the figure it can be seen that the error in predicting the % *SFw* is very less. The value of average error is mostly in the range ±5.

The figures 4.16 and 4.17 show the adequacy of the developed equation.

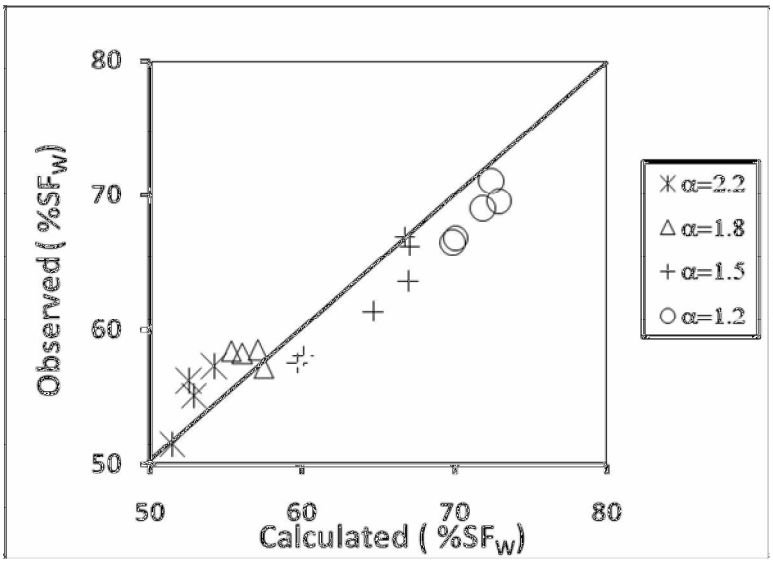

Fig. 4.16 Variation of Observed and Modeled Value of Wall Shear in Meandering Channel

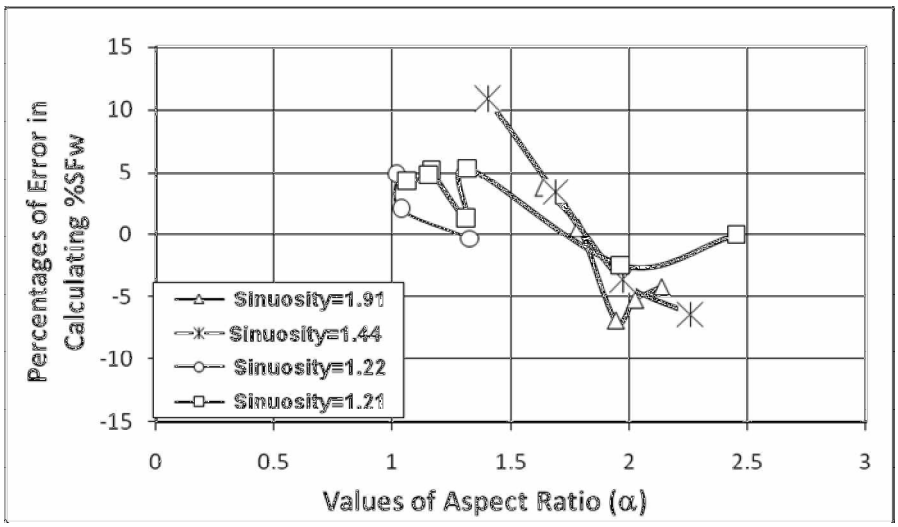

Fig. 4.17 Percentage of Error in Calculating %SF_W with Values of Aspect Ratios

CHAPTER 5

CONCLUSIONS

5.1. GENERAL

Experiments are carried out to examine the effect of channel sinuosity, and cross section geometry on the wall shear in a meandering channel. Point to point wall shear data of meandering channels by different aspect ratio and varying sinuosity is studied. The study is also extended to a meandering channel of higher sinuosity (S_r = 1.91). Based on analysis and discussions of the experimental investigations certain conclusions can be drawn.

The conclusions from the present work are as discussed below:

- The flow resistance in terms of Manning's *n*, Chezy's *C* and Darcy-Weisbach friction factors *f* changes with flow depth for a meandering channel. The resistance coefficient not only denotes the roughness characteristics of a channel but also the energy loss of the flow.

- It is an established fact that the influences of all the forces that resist the flow in an open channel are assumed to have been lumped to a single resistance coefficient in terms of *n*, *C* and *f*. The assumption of an average value of flow resistance coefficient in terms of Manning's *n* for all depths of flow results in significant errors in discharge estimation.

- Dimensional analysis has been carried out to predict the resistance coefficients in a meandering channel. These roughness coefficients are found to depend on the four dimensionless parameters namely, sinuosity, aspect ratio, longitudinal slope of the channel and Reynolds number of the flow.

- Using the proposed equations (4.12), (4.15) and (4.16) the stage discharge relationship in a meandering channel can be adequately predicted. The equation is found to give better discharge results as compared to the other established methods.

- Measurement of boundary shear from point to point along the wetted perimeter of meandering channels of different sinuosity and geometry are performed. The overall mean value of wall shear stress obtained through the velocity distribution approach compares well with that obtained from energy gradient approach.
- Comparing the results of wall shear stress distribution of meandering channel with straight channel, it can be seen that there is asymmetrical nature of shear distribution especially where there is predominant curvature effect. Maximum value of wall shear occurs significantly below the free surface and is located at the inner walls.
- The wall shear distribution in meandering channel is also found to be function of dimensionless parameters like aspect ratio and sinuosity. An equation (4.22) has been developed to predict the wall shear distribution in meandering channel. The proposed models give less error for the present meandering channel as well as for the meandering channels of other investigators.

5.2. SCOPE FOR FUTURE WORK

The present work leaves a wide scope for future investigators to explore many other aspects of meandering channel analysis. Evaluation of flow, energy loss aspects, and boundary shear stress distribution has been performed for the meandering and straight channels using limited data. The equations developed may be improved by incorporating more data from channels of different geometries and sinuosity. Further investigation is required to study the flow properties and develop models using numerical approaches. The channels here are rigid. Further investigation for the flow processes may also be carried out for mobile bed.

REFRENCES

REFERENCES

Acrement, G. J., Jr; and Schneider, V. R. (1989) ‘‘Guide for selecting Manning’s roughness coefficients for natural channels and flood plains’’ *U.S. Geological Survey Water-Supply paper* 2339, Federal Center, Colo.

Bridgman. P. W., (1969), “Dimensional Analysis”, in Encyclopaedia Britannica (Wm. Haley, Editor-in-Chief), Vol. 7, pp. 439-449: Encyclopaedia Britannica, Chicago.

Chang, H. H. (1983). ‘‘Energy expenditure in curved open channels” *Hydr. Engrg., ASCE*, 109(7), 1012–1022.

Chang, H. H. (1984). ‘‘Variation of flow resistance through curved channels’’, *Journal of Hydr. Engrg., ASCE*, 110(12), 1772–1782.

Chiu, C. L, Chiou, J. D. (1986). “Structure of 3-D flow in rectangular open-channels”. *Journal of Hydraulic. Eng*., 112(11), pg.1050–1068

Chow, Ven Te (1959), “Open-Channel Hydraulics” New York, McGraw- Hill Book Co.

Cowan, W. L., (1956). ‘‘Estimating Hydraulic roughness Coefficients.’’ *Agric. Engrg*, 37, 473-475.

Darcy, H. (1857) “Recherches Experimentales Relatives au Mouvement de L'Eau dans les Tuyaux” 2 volumes, Mallet-Bachelier, Paris. 268 pages and atlas. ("Experimental Research Relating to the Movement of Water in Pipes")

Das,A.K. (1984).‘‘A study of River Floodplain and Boundary Shear Stress Distribution in Meander Channels with One side Flood plains.’’ PhD Thesis Presented to the IIT, Kharagpur, India.

Dey S and Cheng N S (2005): “Reynolds stress in open channel flow with upward seepage”. *Journal of Engineering Mechanics, American Society of Civil Engineers (ASCE),* Vol. 131, No. 4, pp. 451-467.

Dey S and Lambert M F (2005): “Reynolds stress and bed shear in non-uniform unsteady open channel flow”. *Journal of Hydraulic Engineering, American Society of Civil Engineers (ASCE),* Vol. 131, No. 7, pp. 610-614.

Einstein, H. A (1942), “Formulas for the transportation of bed-load” *Trans. Am. Soc. Civ. Eng.*, 107, pg.561–597

Ervine, D. A., Willetts, B. B., Sellin, R. H. J., and Lorena, M. (1993). ‘‘Factors affecting conveyance in meandering compound flows.’’ *Journal of Hydr. Engg. ASCE*, 119(12), 1383–1399.

Ghosh, S. N., and Kar, S. K. (1975) ‘‘River flood plain interaction and distribution of boundary shear stress in a meander channel with flood plain.’’ *Proc. Inst. of Civ. Engrs.*, London, 59(2), 805–811.

Ghosh, S.N. and Roy, N. (1970) “Boundary shear distribution in open channel flow”. *Journal of Hydr. Div., ASCE* 96 (HY4), pg.967-994.

Greenhill, R.K. and Sellin, R.H.J., (1993), "Development of a Simple Method to Predict Discharge in Compound Meandering Channels", *Proc. Of Instn. Civil Engrs Wat., Merit and Energy*, 101, paper 10012, March, pp. 37-44.

“Guide for selecting roughness coefficient "*n*" values for channels”. (1963). *Soil Conservation Service, U.S. Dept. of Agric*., Washington, D.C.

Guo, J., and Julien, P. Y. (2005). ‘‘Boundary shear stress in smooth rectangular open channels.’’ *Proc., 13th Int. Association of Hydraulic Research, APD Congress*, Singapore, Vol. 1, 76–86.

Hu, C. H. (1985) “The effect of the width/depth ratio and side-wall roughness on velocity profile and resistance in rectangular open-channels” *MS thesis, Tsinghua Univ.*, Beijing for the Degree of Doctor of Philosophy.

"Hydraulic capacity of meandering channels in straight floodways." (1956). *Tech. Memorandum No. 2-429, U.S. Army Corps of Engineers*, Waterways Experiment Station, Vicksburg, Miss.

Inglis, C. C. (1947). “Meander and Their Bering on River Training.” *Proceedings of the Institution of Civil Engineers, Maritime and Waterways Engineering Div*., Meeting, 1947.

James, C. S. (1994). ‘‘Evaluation of methods for predicting bend loss in meandering channels.’’ *Journal of Hydraulics Engg*., *ASCE*, 120(2), 245–253.

James, C. S., and Wark, J. B. (1992). ‘‘Conveyance estimation for meandering channels.’’ *Rep. SR 329, HR Wallingford*, Wallingford, U.K., Dec.

Jana Sukanta (2007) “Stage-Discharge Relationship in Simple Meandering Channels”, Thesis Presented to the Indian Institute of Technology, Kharagpur, India, in partial fulfillments of the requirements for the Degree of Master of Technology.

Jarrett, R. D. (1984). ‘‘Hydraulics of high gradient streams’’ *Journal of Hydr. Engg*., *ASCE*, 110, 1519–1539.

Kar, S.K.,(1977),"A Study of Distribution of Boundary Shear in Meander Channel with and without Floodplain and River Floodplain Interaction", Thesis Presented to the Indian Institute of Technology, Kharagpur, at Kharagpur, in partial fulfillment of the requirements for the Degree of Doctor of Philosophy.

Kartha, V.C. and Leutheusser, H.J. (1970) "Distribution of tractive force in open channels". *Journal of Hydr. Div. ASCE* 96 (HY7), 1469-1483.

Kean, Jason W., Kuhnle, Roger A., Smith, J. Dungan, Alonso,Carlos V., and Langendoen, Eddy J. (2009) "Test of a Method to Calculate Near-Bank Velocity and Boundary Shear Stress". *Journal of Hydraulic Engineering*, Vol. 135, No. 7, July 1, 2009.

Khatua, K. K. (2008) "Interaction of flow and estimation of discharge in two stage meandering compound channels". Thesis Presented to the National Institute of Technology, Rourkela, in partial fulfillments of the requirements for the *Degree of Doctor of philosophy.*

Khatua, K. K., Patra, K.C. and Mahananda, G. (2009) "Numerical Evaluation of Boundary Shear Distribution in Meandering Channels". *Fifth M.I.T. Conference on Computational Fluid and Solid Mechanics — Focus: Advances in CFD.*

Knight, D. W., and Hamed, M. E. (1984). ''Boundary shear in symmetrical compound channels.'' *Journal of Hydr. Engrg., ASCE*, 110(10), 1412– 1430.

Knight, D. W., and MacDonald, J. A. (1979) "Open-channel flow with varying bed roughness" *Journal of Hydraulic. Div., Am. Soc. Civ. Eng*., 105(9), pg.1167–1183.

Knight, D. W., and Shiono, K. (1990). ''Turbulence measurements in a shear layer region of a compound channel.'' *Journal of Hydr. Res*., Delft, The Netherlands, 28(2), 175–194.

Knight, D.W. (1981). "Boundary Shear in Smooth and Rough Channels." Journal of Hydraulic Engineering, ASCE, Vol. 107, No.7, pp. 839-851.

Knight, D.W. (1989). "Hydraulics of Flood Channels In: Floods: Hydrological Sedimento-Logical and Geo-Morphological Implications." K. Beven (Ed.)Wiley, Chichester, 83 - 105

Knight, D.W. and Patel, H.S., (1985), "Boundary shear in smooth rectangular ducts". *Journal of Hydraulic Engineering,* ASCE, Vol. 111, No. 1, 29-47.

Knight, D.W., and Demetriou, J.D., (1983), "Flood Plain and Main Channel Flow Interaction". *Journal of Hyd. Engg., ASCE* Vo.109, No.8, pp-1073-1092.

Knight, D.W., Demetriou, J.D. and Hamed, ME. (1984) "Boundary shears in smooth rectangular channels" *Journal of Hydr. Engin. ASCE* 110, pg.405-422.

Knight,D.W.,Yuan,Y.M.,and Fares,Y.R..(1992). "Boundary shear in meandering channels." Proceedings of the Institution Symposium on Hydraulic research in nature and laboratory, Wuhan, China (1992) Paper No.11017, Vol. 118, Sept., pp. 151-159.

Lai Sai Hin, Nabil Bessaih, Law Puong Ling, Aminuddin Ab. Ghani, Nor Azazi Zakaria, Mahyau Seng (2008). "Discharge Estimation for Equatorial Natural Rivers with

Overbank Flow", *Intl. Journal of River Basin Management, IAHR, INBO & IAHS*, Vol. 6, No. 1 Pp. 13–21.

Leliavsky, S. (1955). "An Introduction to Fluvial Hydraulics."Constable, London.

Lundgren, H. and Jonsson, I.G (1964) "Shear and velocity distribution in shallow channels". *Journal of Hydr.Div., ASCE*, 90 (HY1), pg.1-21.

Manning R. (1891) "On the flow of water in open channels and pipes" Transactions of the Institution of Civil Engineers of Ireland, 20, 161-207.

Maria, A.A, and DaSilva A. F. (1999). "Friction Factor of Meandering Flows." *Journal of Hydraulic Engineerin, ASCE,* Vol.125, No.7, pp. 779-783.

Myers, W. R. C., and Elsawy, J. D. (1975). ''Boundary shear in channel with flood plain.'' *Journal of Hydr. Div., ASCE,* 101, 933–946.

Myers, W.R.C. (1978) "Momentum transfers in a compound channel". *Journal of Hyd. Res.*, 16(2), 139-150.

Nezu, I., and Nakagawa, H. (1993). "Turbulence in open-channel flows". *IAHR Monograph Series*, A. A. Balkema, Rotterdam, The Netherlands.

Noutsopoulos, G. C. and Hadjipanos, P. A. (1982) Discussion of "Boundary shear in smooth and rough channels", by D.W. Knight. *Journal of Hydr*. Div. ASCE 108 (HY6), 809-812.

Pang, B. (1998). ''River Flood Flow and Its Energy Loss.'' *Journal of Hydr. Engrg., ASCE*, 124(2), 228–231

Patel, H.S. (1984) "Boundary shear in rectangular and compound ducts." *PhD Thesis*. The University of Birmingham

Patra, K.C, and Kar, S. K. (2000), "Flow Interaction of Meandering River with Floodplains". *Journal of Hydr. Engrg., ASCE*, 126(8), 593–604.

Patra, K.C. (1999) " Flow interaction of Meandering River with Flood plains ", Thesis Presented to the Indian Institute of Technology, Kharagpur, at Kharagpur, in partial fulfillment of the requirements for the Degree of Doctor of philosophy.

Patra, K.C., and Khatua, K. K. (2006), "Energy Loss and Discharge Estimation in Two Stage Meandering and Straight Compound Channel", *EWRI of American Society of Civil Engineers* and IIT Kanpur, ASCE.

Rhodes, D. G., and Knight, D. W. (1994). ''Distribution of Shear Force on Boundary of Smooth Rectangular Duct.'' *Journal of Hydralic Engg.*, 120-7, 787– 807.

Rouse, H and S. Ince. (1957). “History of Hydraulics” Iowa Institute of Hydraulic Research, State Univ. of Iowa, Iowa City, IA.

Rozovskii, I. L. (1961). “Flow of water in bends of open channels” translated from Russian by the Israel program for scientific translations, Jerusalem, Israel

Sellin, R.H.J. (1964). “A Laboratory Investigation into the Interaction between Flow in the Channel of a River and that of its Flood Plain.” *La. Houille Blanche*, No.7, pp. 793-801.

Shiono, K., Al-Romaih, J.S., and Knight, D.W., (1999)."Stage-Discharge Assessment in Compound Meandering Channels", *Journal of Hydr.Engg. ASCE* vol.125, No.1. Pp.66-77.

Shiono, K., and Knight, D. W. (1991). ‘‘Turbulent open channel flows with variable depth across the channel.’’ Journal of Fluid Mech., Cambridge, U.K., 222, 617–646 [and 231 (Oct., 693)].

Thomson, W. (1876) “On the origin of windings of rivers in alluvial plains, with remarks on the flow of water round bends in pipes.” Proc. Royal Soc. London, 25, 5-8.

Toebes, G.H., and Sooky, A.A., (1967) "Hydraulics of Meandering Rivers with Flood Plains", Journal of the waterways and Harbor Div., Proc. of ASCE, Vol.93, No.WW2, May, pp. 213-236.

Wark, J.B., and James, C.S., (1994), "An Application of New Procedure for Estimating Discharge in Meandering Overbank Flows to Field Data", 2nd Intl. Conf. on River Flood Hydraulics 22-25 March, Published by John Wiley & Sons Ltd, pp.405-414.

Willetts, B. B., and Hardwick, R. (1993) ‘‘Stage Dependency for Overbank Flow in Meandering Channels.’’ Proc. Inst. of Civ. Engrs., Water, Maritime and Energy, London, 101 (March), 45–54.

Wormleaton, P. R., and Hadjipanos, P. (1985). ‘‘Flow distribution in compound channels.’’ Journal of Hydr. Div., ASCE, 111(2), 357–361.

Yang, S. Q. and McCorquodale, John A. (2004) “Determination of Boundary Shear Stress and Reynolds Shear Stress in Smooth Rectangular Channel Flows.” *Journal of Hydr. Engrg.*, Volume 130, Issue 5, pp. 458-462

Yang, S. Q., and Lim, S. Y. (1997) “Mechanism of energy transportation and turbulent flow in a 3D channel” Journal *of Hydraulic. Eng.*, 123(8), pg.684–692.

DISSEMINATION OF WORK

A: Published

1. Nayak, P.P., Khatua, K.K., Patra, K.C. (2009) "Evaluation of roughness coefficients in a meandering open channel flow". *7TH International R&D Conference on Development and Management of Water and Energy Resources* 4-6 February 2009, Bhubaneswar (Orissa), India.

2. Nayak, P.P., Khatua, K.K., Patra, K.C. (2009) "Variation of Resistance Coefficients in a Meandering Channel". *Proceedings of Advances in Environmental Engineering (AEE-09), 14-Nov-2009 to 15-Nov-2009, National Conference Advances in Environmental Engineering,* Department of Civil Engineering, National Institute of Technology, Rourkela, India.

3. Nayak, P.P., Khatua, K.K., Patra, K.C., Pradhan A.K. (2009) "Ground water prospecting by soil resistivity meter - A case study". *Proceeding of Water Resources Management in 21st century*, NITRAAB 2009.

4. Khatua, K.K., Patra, K.C., Nayak, P.P., Sahu, M. (2010) "Wall Shear Distribution in Meandering Channel". *Institute of Engineers India (IEI),* February, 2010. (Obtained gold medal for the best paper)

B: Accepted for Publication

1. K.K.Khatua, K.C.Patra, N. Sahoo, Nayak, P. P. (2010) Evaluation of boundary shear Distribution in a Meandering Channel". *The ninth International Conference on Hydro-Science and Engineering (ICHE 2010)*, 2-5 August, 2010

2. Nayak, P.P., Khatua, K.K., Patra, K.C., (2010) "Roughness evaluation for meandering channels" *International conferences in Advances in Fluid Mechanics, AFM-2010,*Portugal, Lisbon, September,2010.

C: Communicated

1. Sahu, M., Nayak, P.P., Khatua, K.K. (2010) "Meandering effect for Evaluation of roughness coefficients in open channel flow" *Tenth International Conference on Modeling, Monitoring and Management of Water Pollution, WATER POLLUTION 2010,* Wessex Institute of Technology, Bucharest, Romania.

BRIEF BIODATA OF THE AUTHOR

NAME	: PINAKI PARASANNA NAYAK
FATHER'S NAME	: Mr. AMIYA KUMAR NAYAK
MOTHER'S NAME	: Mrs. JYOTSNAMAYEE NAYAK
DATE OF BIRTH	: 02-03-1983
NATIONALITY	: INDIAN
PRESENT ADDRESS	: M.TECH (RES.), DEPT. OF CIVIL ENGINEERING, NATIONAL INSTITUTE OF TECHNOLOGY, ROURKELA - 769008
PERMANENT ADDRESS	: D/O Mr. A. K. NAYAK, PLOT No. 573, SAHIDNAGAR, BHUBANESWAR – 751007
EDUCATIONAL QUALIFICATIONS	: B.TECH, CIVIL ENGINEERING, 2006 (WITH Hons.) +2 SCIENCE, 2001 H. S. C., 1999